Nucleic acid sensing in CD4 T cells during HIV-1 and other viral infections

Marvin Holz

ORCID ID:

0000-0003-4290-7009

from Bocholt, Germany

Submitted in total fulfilment of the requirements of the joint degree of Doctor of Philosophy (PhD)

of the Medical Faculty

The Rheinische Friedrich-Wilhelms-Universität Bonn

And

The Department of Microbiology and Immunology

The University of Melbourne

Bonn/Melbourne, 2021

Performed and approved by the Medical Faculty of The Rheinische Friedrich-Wilhelms-Universität Bonn and The University of Melbourne

1. Examiner: Prof. Dr. Gunther Hartmann, The Medical Faculty, The Rheinische Friedrich-Wilhelms-Universität Bonn

2. Examiner: Prof. Sharon Lewin, PhD, The Department of Infectious Diseases, The University of Melbourne

Date of submission: 21.03.2021

Date of oral examination: 04.10.2021

Institute of Clinical Chemistry and Clinical Pharmacology, Director:
Professor Dr. med. Gunther Hartmann

Table of Content

ABBREVIATIONS

#	
° C	Degree Celsius
%	Per cent
(-)ssRNA	Negative-sense ssRNA
3p-RNA	Triphosphorylated RNA
A	
A	Ampere
ADAR1	Adenosine deaminase RNA-specific
AIDS	Acquired immune deficiency syndrome
AIM2	Absent in melanoma 2
AMP	Adenosine monophosphate
ANOVA	Analysis of variance
APC	Antigen presenting cell
APC	Allophycocyanin
APOBEC	apolipoprotein B mRNA editing enzyme catalytic polypeptide-like
APS	Ammonium persulfate
ART	Antiretroviral therapy
ATP	Adenosine triphosphate
B	
BAX	BCL-2 associated X protein
BCA	Bicinchoninic acid
BG	Background
BM	Bone marrow
bp	Basepair
BSA	Bovine serum albumine
BST2	Bone marrow stromal antigen 2
C	
CA	Capsid protein
CARD	caspase activation and recruitment domain
CCR5	C-C chemokine receptor type 5
CD	Cluster of differentiation
cDNA	Complement DNA
cGAMP	Cyclic GMP-AMP
cGAS	Cyclic GMP-AMP synthase
CLR	C-type lectin receptor

CMV	Cytomegalovirus
CO_2	Carbon dioxide
CRISPR	Clustered regularly interspaced short palindromic repeats
crRNA	Trans-activating RNA
CTD	C-terminal RNA-binding domain
CTL	Cytotoxic T cell
Ctrl	Control
CXCL10	Chemokine ligand 10 (IP-10)
CXCR4	C-X-C chemokine receptor type 4

D

Da	Dalton
DC	Dendritic cell
DDX58	DExD/H-Box Helicase 58
DMEM	Dulbelco's Modified Eagle's medium
DNA	Deoxyribonucleic acid
dNTP	Deoxynucleoside triphosphate
dsDNA	Double-stranded DNA
dsRNA	Double-stranded RNA
DTT	Dithiothreitol
DV	Darunavir

E

E. coli	*Escherichia coli*
ECAR	Extracellular acidification rate
EDTA	Ethylendiaminetetraacetic acid
eGFP	Enhanced green fluorescent protein
EIF2AK2	Eukaryotic translation initiation factor 2 alpha kinase 2 gene
eIF2α	Eukaryotic translation initiation factor 2A protein
ELISA	Enzme-linked immunosorbent assay
env	Envelope
ESCRT	Endosomal sorting complexes required for transport

F

FACS	Fluorescence-activated cell sorting
FBS	Foetal bovine serum
f.c.	Final concentration
FDA	Food and drug administration
FITC	Fluorescein isothiocyanate
Fluc	Firefly luciferase
FP	Fusion peptide

FT	Flow through

G

g	Gram
gag	Group-specific antigen
GFP	Green fluorescent protein
Gluc	Gaussia Luciferase
GM-CSF	Granulocyte-macrophage colony-stimulating factor
GMP	Guanosine monophosphate
GO:BP	Gene ontology biological process
GO:MF	Gene ontology term molecular function
Gp120	Glycoprotein 120
Gp160	Glycoprotein 160
Gp41	Glycoprotein 41
gRNA	Genomic RNA
GTP	Guanosine triphosphate
GvHD	Graft versus host disease

H

h	Hour(s)
HAU	Hemagglutination units
HCl	Hydrochloric acid
HDAC	Histone deacetylase
HDACi	Histone deacetylase inhibitors
HEK293	Human embryonic kidney 293 cells
HeLa	Henrietta Lacks cell line
HF	High Fidelity
His-tag	Histidine protein tag
HIV	Human immunodeficiency virus
HLA-DR	Human leukocyte antigen DR isotope
HMG/Y	High-mobility group protein I
HP	HiPerFect
HRP	Horseradish peroxidase

I

IFI16	IFN gamma-inducible protein 16
IFIH1	Interferon induced with helicase C domain 1
IFIT	interferon-induced protein with tetratricopeptide repeats
IFITM	Interferon induced transmembrane protein
IFN	Interferon
IFNα	Interferon alpha

IFNAR	Interferon alpha/beta receptor
IFNγ	Interferon gamma
IKK	Inhibitor of nuclear factor kappa-B kinase
IL	Interleukin
IN	integrase
IPTG	Isopropyl β-d-1-thiogalactopyranoside
IRES	Internal ribosome entry site
IRF	Interferon regulatory factor
ISG	Interferon stimulated gene
IVT4	In vitro transcript 4

K

kb	Kilobase
KO	Knockout

L

L	Litre
L2K	Lipofectamine 2000
LB	Luria-Bertani broth
LC	Langerhans cell
LN	Liquid nitrogen
LPG2	Laboratory of genetics and physiology 2
LRR	Leucine rich repeat
LT1	TransIT-LT1
LTR	Long terminal repeat
LTX	Lipofectamine LTX
Lys	Lysine

M

µ	Micro
M	Molarity
MA	Matrix protein
MAVS	Mitochondrial antiviral-signalling protein
MCLR	Mannose-binding C-type lectin receptor
MDA5	Melanoma differentiation-associated gene 5
MES	2-(N-morpholino)ethanesulfonic acid
MF	MACSfectin
MHCI	Major histocompatibility complex I
MHCII	Major histocompatibility complex II
min	Minute(s)
miRNA	Micro RNA

mRNA	Messenger RNA
MX	MX dynamin like GTPase
MYD88	Myeloid differentiation primary response protein 88

N

n	Nano
NaCl	Sodium chloride
NaOH	Sodium hydroxide
NC	Nulceocapsid
NFkB	Nuclear factor kappa-light-chain-enhancer of activated B cells
Ni-NTA	Nickel-nitrilotriacetic acid
NK	Natural killer cell
NKT	Natural killer T cell
NLR	NOD-LRR-containing receptor
NLRP3	NLR family pyrin domain containing 3
NNRTI	Non-nucleoside reverse transcriptase inhibitor
NOD	Nucleotide-binding oligomerisation domain
NRTI	Nucleoside reverse transcriptase inhibitor

O

OAS1	2´-5´-oligoadenylate synthetase 1
OCR	Oxygen consumption rate
OD	Optical density
OWM	Old world monkey
OxPhos	Oxidative phosphrylation

P

poly(I:C)	Polyinosinic:polycytidylic acid
PAGE	polyacrylamide gel electrophoresis
PAMP	Pathogen-associated molecular pattern
PBMC	Peripheral blood mononuclear cells
PBS	Phosphate buffered saline
PBST	Phosphate buffered saline with Tween-20
PCR	Polymerase chain reaction
pDC	Plasmacytoid dendritic cell
PE	Phycoerythrin
PFA	Paraformaldehyde
PGE-2	Prostaglandin E2
pH	Power of hydrogen
PI	Protease inhibitor

PIC	Pre-integration complex
PKC	Protein kinase C
PKR	Protein kinase R
PLWH	People living with HIV
PMA	Phorbol 12-myristate 13-acetate
pNPP	Para-Nitrophenylphosphate
pol	DNA-polymerase
pp65	CMV phosphoprotein 65
PQBP1	Polyglutamine bidning protein 1
PR	HIV-1 protease
PrEP	Pre-Exposure Prophylaxis
PRR	Pattern recognition receptor

Q

QA/QC	Quality assurance / quality control

R

R5	CCR5-tropic strain of HIV
rCD4	Resting memory CD4 T cell
rcf	Relative centrifugal force
REAC	Reactome pathway database
RELA	RELA proto-oncogene
RIG-I	Retinoic acid inducible gene 1
RIPA	Radioimmunoprecipitation assay
RLR	RIG-I like receptor
RM	RIG-I / MDA5 deficient
RNA	Ribonucleic acid
RNP	Ribonucleoprotein
rpm	Revolutions per minute
RRE	Rev responsive element
RT	Reverse transcriptase
RT	Room temperature
RT/RH	Reverse transcriptase / Rnase H

S

SD	Standard deviation
SDS	Sodium dodecyl sulphate
SEC	Super elongation complex
SeV	Sendai virus
SFA	ScreenFectA
SIV	Simian immunodeficiency virus

SN	Supernatant
SOC	Super optimal broth with catabolic repression
SP	Spacer peptide
ssDNA	Single-stranded DNA
ssRNA	Single-stranded RNA
STAT	Signal transducer and activator of transcription
STING	Stimulator of IFN genes
SU	Surface glycoprotein

T

TAR	Trans-activation response element
Tat	Trans-activating regulatory protein
TBK1	TANK-binding kinase 1
TCID50	Median tissue culture infectious dose
T_{CM}	Central memory t cell
TCR	T cell receptor
T_{EM}	Effector memory t cell
TEMED	Tetramethylethylenediamine
Tfh	Follicular CD4+ T helper cell
TGFβ	Transforming growth factor beta
TGN	Trans-Golgi network
Th	CD4 t helper cell
THP-1	THP-1 cell line
TLR	Toll like receptor
TM	Transmembrane glycoprotein 41
TMM	Trimmed mean of M values
TNFα	Tumour necrosis factor alpha
TRAF	Tumour necrosis factor associated factor
TRBP	TAR RNA-binding protein
Treg	Regulatory t cell
TRIF	TIR-domain-containing adaptor-inducing interferon-β
TRIM	Tripartite motif-containing protein
Tris	Trisaminomethane
tRNA	Transfer RNA

U

U	Units
UTR	Untranslated region

V

V	Volt

v/v	Volume per volume

W

WT	Wildtype

X

X4	CXCR4-tropic strain of HIV

LIST OF TABLES

List of figures

ABSTRACT

Viruses are small intracellular parasites and use the host cell's biosynthesis machinery to replicate and spread. Therefore, viral particles incorporate structures that are similar to the ones that naturally occur within host cells. A major mechanism to identify viral entry and replication within an infected cell is the recognition of viral nucleic acids. Sensors of the innate immune system can detect foreign nucleic acids by their unusual subcellular localisation or modification or both. Once innate immune sensors are activated, they induce distinct signalling cascades which modulate cellular responses to invading pathogens like viruses. In this thesis, we studied the role of RNA sensors RIG-I (retinoic acid-inducible gene 1) and MDA5 (melanoma differentiation-associated protein 5) in CD4 T cells during infections with SeV (Sendai virus) or HIV-1 (Human Immunodeficiency virus 1).

HIV-1 is the causative agent for the acquired immunodeficiency syndrome (AIDS). Globally, more than 30 million people are living with HIV-1 and hundreds of thousands of people are newly infected every year. Today, HIV-1 infection is a chronic and manageable disease. The progression to AIDS is prevented by ART (antiretroviral therapy) which inhibits viral replication but is unable to clear the latent viral reservoir – inactive HIV-1 proviruses within long-lived subsets of immune cells. These latent viruses are not detected by innate and adaptive immunity. Furthermore, HIV-1 manipulates cellular restriction factors and sensors of viral infection to evade immune recognition. This highlights the demand for new approaches to restore innate immune sensing during latency reversal to allow the specific killing of infected cells to the clearance of the latent reservoir.

We first studied the RIG-I signalling pathway in human CD4 T cells, the main reservoir for HIV-1 infection *in vivo*. Using SeV, a specific activator of RIG-I, and a cell-based type-I interferon reporter assay we showed that the RIG-I signalling pathway was functional in activated CD4 T cells. In resting CD4 T cells, we did not detect the release of type-I IFNs and used next generation sequencing (NGS) to verify the expression of members of the RIG-I signalling pathway. A typical

type-I IFN signature was observed in resting CD4 T cells following the stimulation of RIG-I with SeV. These data also showed the downregulation of pathways relevant for T cell activation. We next evaluated how the activation of the RIG-I signalling pathway affects the biology of CD4 T cells. RIG-I activation diminished proliferation, metabolic activity and release of effector cytokine IFNγ in CD4 T cells.

RIG-I and MDA5 are potential sensors for HIV-1 and their role during HIV-1 infection is not fully understood to date. We discovered that HIV-1 protease (PR) directly degrades RIG-I and MDA5 independently of other cellular factors. We showed this by co-expression of HIV-1 PR and RIG-I or MDA5 in HEK293T cells and in an in vitro assay using purified recombinant HIV-1 PR and RIG-I or MDA5 proteins. The degradation of RIG-I and MDA5 by HIV-1 PR sequestrated the sensing of stimulatory RNAs in an *in vitro* reporter assay. These data indicate that the degradation of RIG-I and MDA5 is a potential immune evasion mechanism for HIV-1 which could be exploited in novel HIV-1 cure approaches. Furthermore, we generated RIG-I and MDA5 knockouts in primary human CD4 T cells and Jurkat cells and performed initial characterisations of those cell lines. Knockout cell lines will be useful in future studies on the role of RIG-I and MDA5 during HIV-1 infection.

Preface

This work was carried out in the PC2 laboratory, University Hospital Bonn, at the Institute for Clinical Chemistry and Clinical Pharmacology, Bonn, Germany and in the PC2 and PC3 laboratories, The University of Melbourne, at the Peter Doherty Institute for Infection and Immunity, Melbourne, Australia, under the supervision of Prof. Martin Schlee, Prof. Sharon Lewin and Prof. Damian Purcell.

The contributions to this thesis by the following individuals are as follows:

Dr Juliane Daßler-Plenker and Mr Bastian Putschli (The University Hospital Bonn) provided the exosomes that were used in CD4 T cell stimulation assays.

The Next Generation Sequencing Core Facility (The University of Bonn) performed the final RNA library preparation and sequencing of the CD4 T cell samples on the HiSeq 2500 V4 platform.

Ms Vanessa Schmitt and Mr Mario Lauterbach (The University Hospital Bonn) assisted in the preparation, performance and analysis of the CD4 T cell metabolic assay using the Seahorse platform.

ACKNOWLEDGEMENTS

Numerous people inside and outside of the lab made this project possible, a journey of four and a half years through three labs located on two continents, powered by a great set of brains and hearts.

This collaboration was formed as part of the Bonn & Melbourne Research and Graduate School Immunosciences. Special thanks to everyone involved in setting up and maintaining this excellent research platform.

This project was guided by Professor Martin Schlee, Professor Sharon Lewin and Professor Damian Purcell – the triforce of knowledge. Each of them contributed with an enormous amount of expertise in innate immunity, viral infectious diseases and host pathogens interactions. Thank you for being exceptionally approachable throughout the project, for the many ideas and lively discussions and for the great opportunity to undertake this research project under your supervision. Thank you, Professor Martin Schlee, for offering me this research position in the first place, for the ongoing funding of big parts of the project even when my year abroad turned into two and then three years and for making the best ideas better. Thank you, Professor Sharon Lewin, for your mentorship and the many exciting and challenging discussions. I am still very impressed by your quick comprehension of new concepts that are thrown your way, taking them apart and identifying flaws and opportunities at lightspeed. Thank you, Professor Damian Purcell, for letting me work in your lab for most of my PhD, for being supportive no matter what I asked for and for giving honest and constructive advise when science didn’t go my way.

Thank you to the past and present members of the Schlee Lab. Ann Kristin, Steven, Saskia and Alex made my start in Bonn so easy. Christina organised the bureaucratic shipment of cells and reagents between Germany and Australia. Heike, for keeping the supplies coming – in Bonn and Melbourne. Thais, for the input on the NGS data.

Thank you to the past and present members of the Purcell lab. Charlene, for the PC3 training, Georges and Leigh, for their smart ideas and extended discussions about my project. My fellow PhD students Ash and Natalia - sharing is caring. Paula, for being my bridge over troubled water, for the laughter and joy and everything else inside and outside of the lab – you are truly a great friend!

Thank you to the past and present members of the Lewin Lab. Rachel, for the PC3 training and helping hands to produce tons of infectious virus. Members of the immunomodulation group, for critical discussions and guidance. Jenny, for the input on HIV latency models.

Thank you to my thesis committees in Bonn and Melbourne for spending some of your precious time to evaluate this thesis.

Special thanks goes to my family. Meinen Eltern, meinem Bruder und meinen Großeltern. Für die unschätzbare Unterstützung in allen Lebenslagen, während des Studiums und des PhDs. Diese Arbeit ist eine Gemeinschaftsleistung, die ohne euch nicht möglich gewesen wäre. Vielen Dank!

Special thanks goes to my partner. Querido Vicente, gracias por estar a mi lado durante esta etapa compleja de mi vida. Gracias por tu apoyo, por brindarme tu oido, por tus consejos y por tu amor.

Thank you to my friends near and far. For your support, when things did not go as planned in the lab and for helping me regain my energy and strength when my batteries were drained. I have been a bad friend for the last couple of years – I hope you will accept my apology and I will try to make up for it! Special thanks to Laith, you’re my best friend. Even though you ultimately shipped me to Australia by supporting me to apply for this position!

I crossed paths with so many more people, which are not named. Thank you for being my companions on this exciting journey!

1. Literature Review

1. Introduction

Viruses can be detected by sensors of the innate immune system. Once activated, these sensors induce a broad antiviral response within infected and neighbouring cells to counteract viral replication and spread. The activation of innate immune sensors leads to the induction of cell-autonomous defence mechanisms and initiates adaptive immune responses.

CD4 T cells are the main target for infection with the Human Immunodeficiency Virus 1 (HIV-1). Once established, HIV-1 infection is persistent and leads to immune dysregulation if left untreated. The knowledge on viral nucleic acid sensing in CD4 T cells and HIV-1 immune evasion strategies is incomplete and will be addressed in this thesis.

1.1 Innate and Adaptive Immunity

The innate immune system is the so-called *first line of defence* against pathogens like bacteria, fungi, parasites and viruses. It comprises physical barriers (epithelia), the complement system, phagocytic and antigen-presenting cells (APCs) as well as pattern recognition receptors (PRRs) (reviewed in Gasteiger et al., 2017).

The innate immune response is immediate and induces different defence mechanisms in infected and neighbouring cells. These mechanisms include programmed cell death of infected cells, the release of cytokines and chemokines and the attraction of cells of innate and adaptive immunity (reviewed in Stögerer and Stäger, 2020). Cells involved in innate immune responses are dendritic cells (DCs), macrophages, monocytes and natural killer (NK) cells, among others (reviewed in Marshall et al., 2018). APCs possess the ability to recognise and phagocytise extracellular pathogens. Internalised proteins are processed and presented as short peptides in combination with major histocompatibility complex II (MHCII) on the cell surface, which can elicit an adaptive immune response (Hamilos, 1989). T cells can recognise antigens presented by MHCI and MHCII molecules, while B cells directly bind to their antigen. Antigen-specific activation of B and T cells induces a process of cell differentiation, clonal selection and

expansion to finetune the adaptive immune response (reviewed in Cyster and Allen, 2019 and Kumar et al., 2018). All nucleated cells of the human body present MHCI molecules on their cell surface (reviewed in Montealegre and van Endert, 2019). These proteins are loaded with short peptides, representing all proteins within a cell, including pathogen-derived proteins that occur during intracellular replication. Cytotoxic T cells, also called CD8 T cells, can detect non-self peptides in combination with MHCI proteins and directly kill infected cells and release large amounts of interferon gamma (IFNγ). In contrast, CD4 T cells are restricted by MHCII:peptide complexes and acquire different effector functions (reviewed in Kedzierska and Koutsakos, 2020, see chapter 1.1.4 T cells). The innate immune system is not only fundamental to initiate and orchestrate most parts of adaptive immunity, but also to contain infections until adaptive immunity sets in, which usually takes several days (reviewed in Iwasaki and Medzhitov, 2015).

1.1.1 Pattern Recognition Receptors

PRRs are cytosolic or membrane-bound receptors, present in different compartments of the body. They recognise pathogen-associated molecular patterns (PAMPs) in molecules like carbohydrates, lipids, nucleic acids and proteins derived from bacteria, viruses and other pathogens. PAMPs are invariable among whole classes of pathogens and recognisable as non-self. They comprise motifs in molecules that are essential for the survival of the pathogen and are evolutionary conserved (Asiamah et al., 2019). Activation of PRRs induce the expression of chemokines and cytokines, induce apoptosis and other cell death pathways and provide co-stimulatory signals to adaptive immunity (reviewed in Amarante-Mendes et al., 2018). This thesis explores the innate immune recognition of viral nucleic acids and their effects on viral replication and host cell functions. PRRs and other immune receptors relevant in the context of nucleic acid-sensing will be discussed in more detail in the following sections.

1.1.2 DNA Sensing Receptors

Foreign nuclear acids are recognised as non-self if their localisation or chemical modification differs from nucleic acid species that are typically present in the host. DNA sensing receptors are found in the nucleus as well as in the cytoplasmic and endosomal compartments of the cell. This section will discuss endosomal and cytosolic DNA receptors.

Although many DNA receptors have been described, three DNA receptors are commonly thought to be responsible for the majority of DNA-induced immune responses: Absent in melanoma 2 (AIM2), toll-like receptor 9 (TLR9) and cyclic GMP-AMP synthase (cGAS), Figure 1.1.

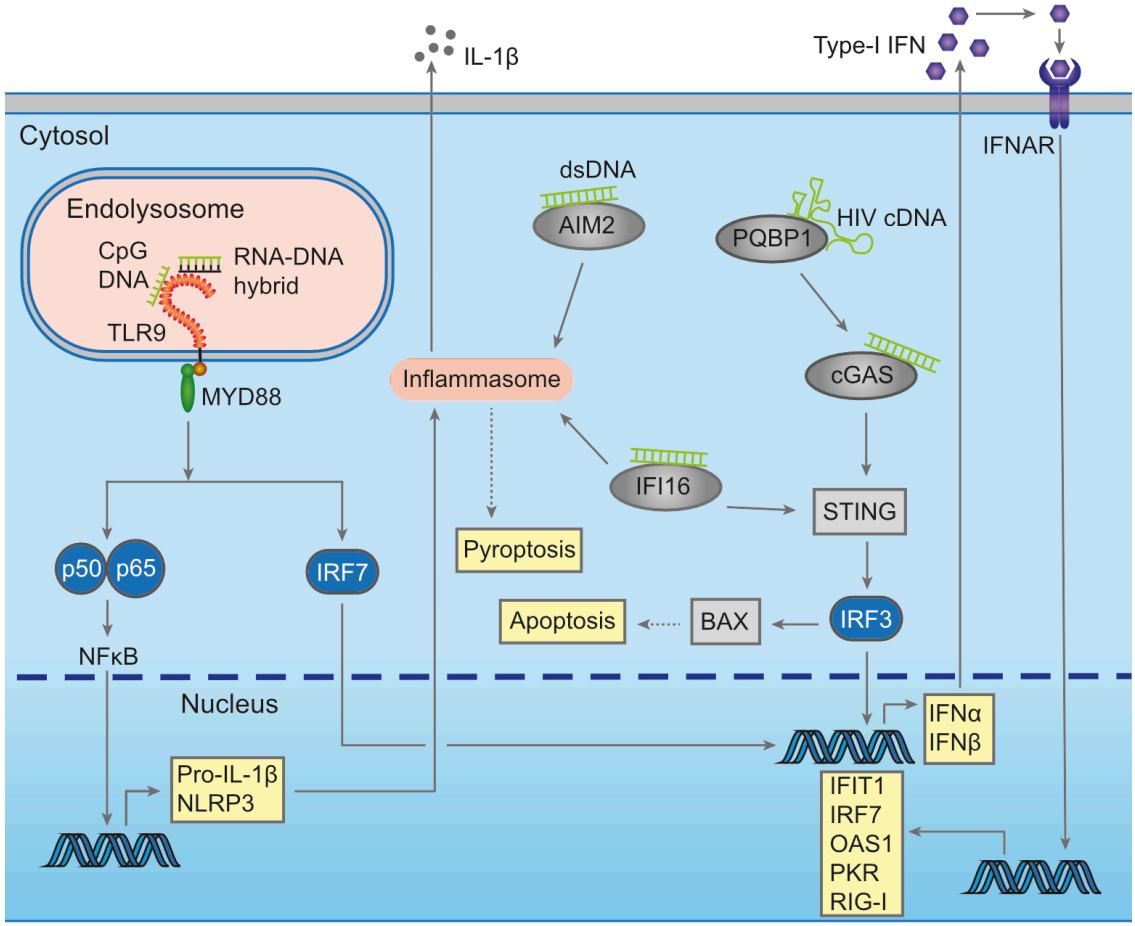

Figure 1.1: DNA-sensing immune receptors. Toll-like receptor 9 (TLR9) senses RNA-DNA hybrids and CpG-DNA in the endolysosomal compartment. The downstream signalling cascade involves myeloid differentiation primary response protein 88 (MYD88), interferon regulatory factor 7 (IRF7) and nuclear factor kappa B (NFκB). IRF7 induces the expression of interferon (IFN), while

NFκB induces pro-interleukin-1 beta (pro-IL-1β) and inflammasome associated factor NOD-, LRR- and pyrin domain-containing protein 3 (NLRP3). Cytosolic receptors absent in melanoma 2 (AIM2), cyclic GMP-AMP synthetase (cGAS) and IFN gamma-inducible protein 16 (IFI16) recognise dsDNA. AIM2 activation induces the assembly of the AIM2 inflammasome with active caspase-1 that cleaves and activates pro-IL-1β and induces pyroptosis. Ligand binding by cGAS and probably IFI16 triggers stimulator of IFN genes (STING) dependent IRF3 activation, which induces IFN expression and mediates apoptosis via BCL-2 associated X protein (BAX). Polyglutamine binding protein 1 (PQBP1) enhances cGAS dependent recognition of retroviral cDNA transcripts (e.g. HIV-1). Type-I IFN expression induces an antiviral response via the interferon-α/β receptor (IFNAR). Interferon stimulated genes (ISGs) like retinoic acid-inducible gene 1 (RIG-I), interferon-induced protein with tetratricopeptide repeats 1 (IFIT1), 2´-5´-oligoadenylate synthetase 1 (OAS1), protein kinase R (PKR) and IRF7 are upregulated. They possess direct antiviral activity or are involved in innate nucleic acid sensing pathways. (Figure adapted from Schlee and Hartmann, 2016).

AIM2 recognises double-stranded DNA (dsDNA) in the cytosol and induces the assembly of the AIM2 inflammasome, which mediates caspase-1 dependent processing of pro-interleukin-1 beta (pro-IL-1β) and pro-IL-18 (Bürckstümmer et al., 2009; Hornung et al., 2009). TLR9 is a membrane-bound receptor, expressed in the endoplasmic reticulum and translocated to the endosome. TLR9 is activated by engagement with bacterial or viral hypomethylated CpG-dsDNA (reviewed in Schlee and Hartmann, 2016). Downstream signalling through myeloid differentiation primary response protein 88 (MYD88) induces the activation of interferon regulatory factor 7 (IRF7) and nuclear factor kappa B (NFκB)-dependent expression of type-I interferons (IFNs) and inflammatory cytokines (reviewed in Schlee and Hartmann, 2016). cGAS is another important cytosolic DNA sensor. It plays a crucial role in the innate immune response to cytosolic and nuclear DNA viruses. cGas can bind to any DNA, self and non-self, and longer DNA (>45 bp) induces a stronger stimulation of the pathway than shorter DNA (20 bp) molecules (Li et al., 2013). The ability of cGAS to sense self-DNA assists in the indirect recognition of RNA viruses (Dengue virus and Zika virus) that cause the release of mitochondrial DNA into the cytoplasm of infected cells (reviewed in Coldbeck-Shackley et al., 2020). cGAS processes guanosine triphosphate (GTP) and adenosine triphosphate (ATP) to form the second messenger cyclic guanosine monophosphate-adenosine monophosphate (cGAMP). The latter activates adaptor protein stimulator of interferon genes

(STING), an endoplasmic reticulum-resident transmembrane protein. Subsequently, STING is translocated to the Golgi and interacts with cytosolic TANK-binding kinase 1 (TBK1). Downstream signalling involves IRF3 and nuclear factor kappa B (NFκB) and induces a broad antiviral type-I IFN-dominated transcriptional programme. Besides, activation of the cGAS-STING pathway can also affect other cellular processes like autophagy and apoptosis (reviewed in Motwani et al., 2019). Involvement of cytosolic DNA sensor gamma-interferon-inducible protein 16 (IFI16) in the cGAS-STING pathway has been described, in which cGAS and IFI16 are both necessary for the optimal activation of STING (Almine et al., 2017). DNA sensor polyglutamine binding protein 1 (PQBP1) functions as a co-receptor of cGAS: PQBP1 binds to unintegrated HIV-1 and other retroviral cDNAs and forms a signalling complex with cGAS. PBQP1 appears to play a role for efficient immune responses against early retroviral infection events, but not for other cGAS-dependent responses to cytosolic DNAs (Yoh et al., 2015).

1.1.3 RNA Sensing Receptors

While the presence of DNA is usually restricted to the nucleus and mitochondria, RNA is more abundant throughout the cell, and its translocation between different compartments is a fundamental requirement for gene expression (reviewed in Williams et al., 2018). Detection of foreign RNA species by most RNA sensing receptors relies on the localisation of RNAs as well as on chemical modifications or the structure of nucleic acid molecules, Figure 1.2.

PRRs of the toll-like-receptor family (TLR3, TLR7, TLR8) as well as three members of the retinoic acid-inducible gene-1-like receptor (RLR) family (retinoic acid-inducible gene-1 (RIG-I), melanoma differentiation-associated protein 5 (MDA5), laboratory of genetics and physiology 2 (LPG2)) are involved in RNA-mediated immune activation. While the mentioned RNA sensing TLRs are expressed as membrane-bound proteins within the endosomal compartment of the cell, RLRs are present as soluble receptors in the cytosol. TLR7 and TLR8 show affinities to polyU and GU-rich nucleic acid sequences, which are present

in viral, bacterial and host RNA species (reviewed in Schlee and Hartmann, 2016). The engagement of TLR7 and TLR8 drives distinct pathways involved in cell differentiation and activation of monocytes and dendritic cells (Larange et al., 2009; de Marcken et al., 2019).

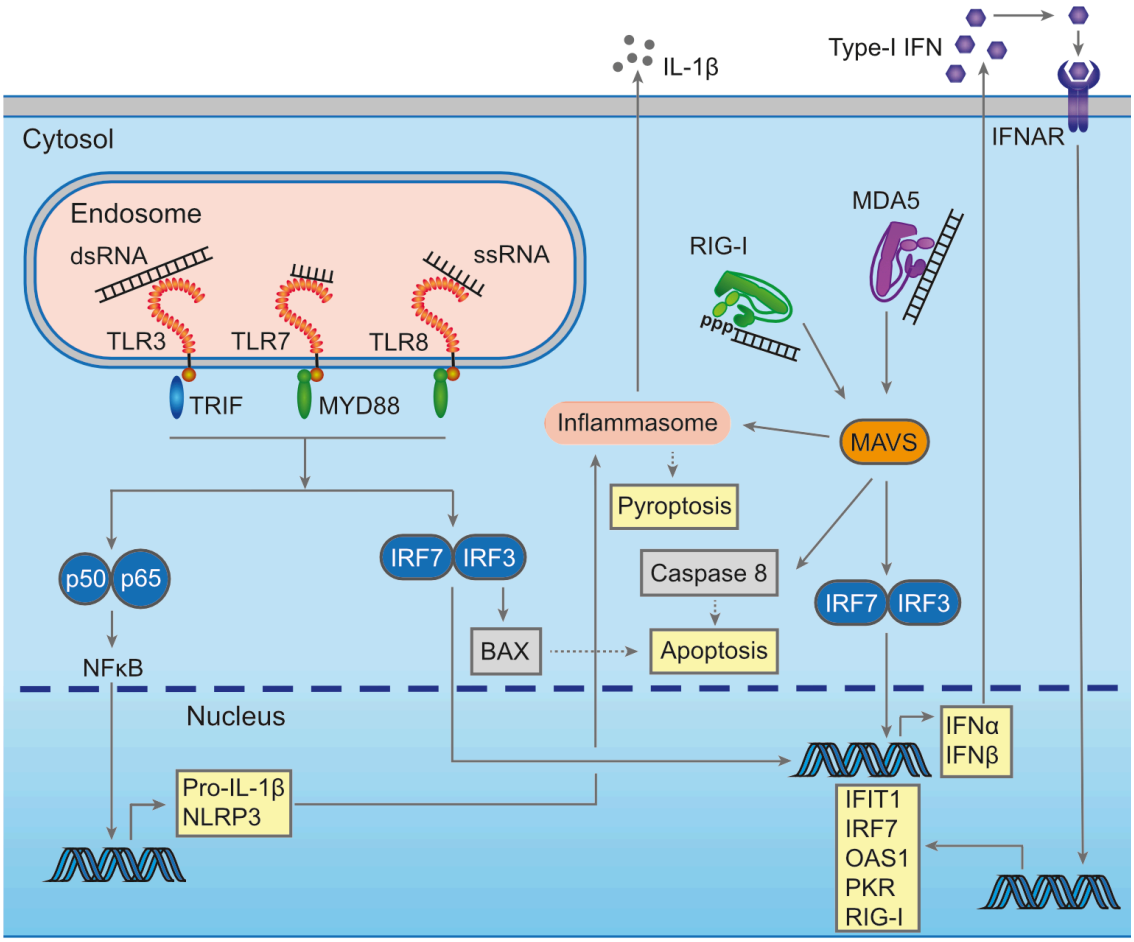

Figure 1.2: RNA-sensing immune receptors. Toll-like receptor (TLR) 3, TLR7 and TLR8 sense RNA in the endosomal compartment. TLR3 senses long, double-stranded (ds) RNA, TLR7 senses single-stranded (ss) RNA and dsRNA and TLR8 senses only ssRNA. Downstream signalling involves myeloid differentiation primary re-sponse protein 88 (MYD88) or TIR domain-containing adaptor protein inducing IFNβ (TRIF), interferon regulatory factor (IRF) 3 and IRF7 as well as nuclear factor kappa B (NFκB). IRF3/IRF7 induce, besides other cytokines and chemokines, type-I interferon (IFN), while NFκB induces pro-interleukin-1 beta (pro-IL-1β) and inflammasome associated factor NOD-, LRR- and pyrin domain-containing protein 3 (NLRP3). Retinoic acid-inducible gene I (RIG-I) and melanoma differentiation-associated gene 5 (MDA5) detect dsRNA in the cytosol. Both signal via mitochondrial associated antiviral signalling protein (MAVS) to induce IRF3/IRF7 dependent IFN synthesis. Type-I IFN expression mediates an antiviral response via the interferon-α/β receptor (IFNAR). Interferon stimulated genes (ISGs) can possess direct antiviral activity (interferon-induced

protein with tetratricopeptide repeats 1 (IFIT1), 2´-5´-oligoadenylate synthetase 1 (OAS1), protein kinase R (PKR) or are involved in innate nucleic acid pathways (RIG-I) or downstream signalling/transcription (IRF7). Also, MAVS and IRF3 stimulate apoptosis via BCL-2 associated X protein (BAX) or caspase-8 and are involved in the stimulation of the inflammasome. It is involved in pro-IL-1β processing and the induction of pyroptosis. (Figure adapted from Schlee and Hartmann, 2016).

TLR3 is a sensor for viral dsRNA and UV-damaged noncoding self-RNA (Alexopoulou et al., 2001; Bernard et al., 2012). While TLR7 and TLR8 signal though MYD88, TLR3 associates with signalling adaptor TIR-domain-containing adaptor-inducing interferon-β (TRIF) (Verstak et al., 2013). Pathway activation induces interferon regulatory factors (IRFs) and NFκB regulated transcription of proinflammatory cytokines and type-I IFNs, as previously described. Soluble receptors RIG-I and MDA5 share the same domain organisation: two N-terminal caspase activation and recruitment domains (CARDs), a DexD/H-box helicase domain (hel-1, hel-2 and hel-2i), and a C-terminal RNA-binding domain (CTD). The domains are separated by two flexible hinge regions (Rawling and Pyle, 2014), Figure 1.3A.

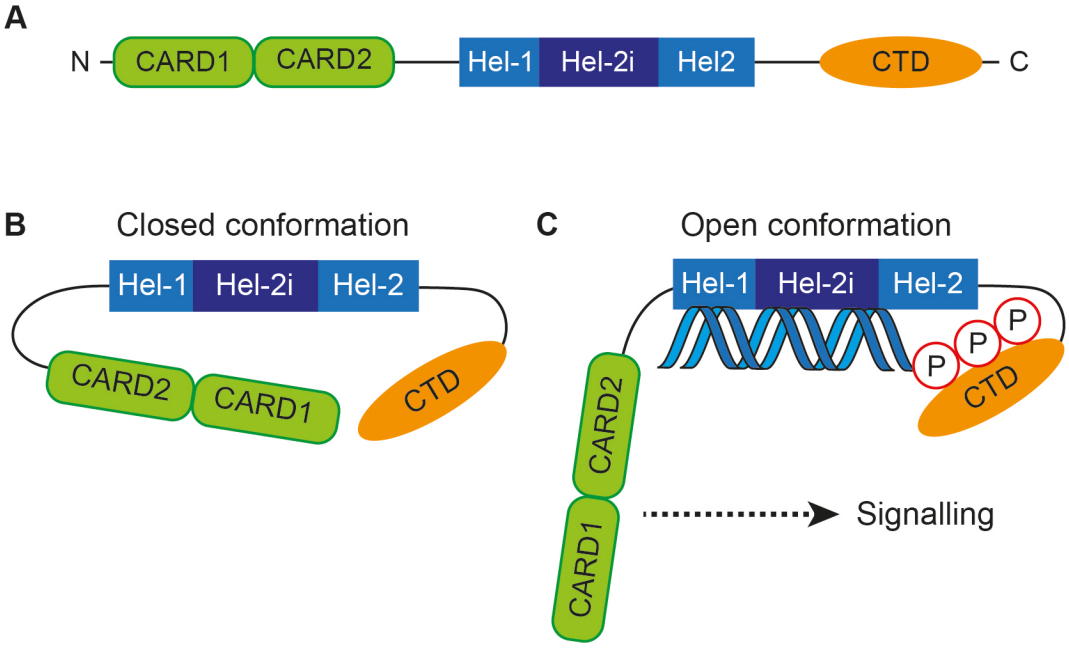

Figure 1.3: RIG-I-like receptor domain organisation. A: Retinoic acid-inducible gene-1 (RIG-I) and melanoma differentiation-associated protein 5 (MDA5) share the same domain organisation. A flexible hinge region connects two N-terminal caspase activation and recruitment domains (CARDs) with a DexD/H-box helicase domain, which is separated into hel-1, hel-2 and hel-2i. Another flexible

hinge region leads to the RNA binding C-terminal domain (CTD). Both receptors exist in two major conformations: the auto-inhibited state in the absence of a specific ligand (B) and the open conformation during RNA recognition, which releases the two CARDs and allows for downstream signalling (C, shows ligand recognition by RIG-I). (Figure adapted from Abdullah and Atif, 2017; Uchikawa et al., 2016).

Both receptors show specificity towards distinct RNA species. RIG-I recognises short blunt-ended double stranded (dsRNA) molecules with a 5´-triphosphate or diphosphate. MDA5 is activated by long dsRNA molecules or long single stranded (ssRNA) molecules with internal base pairing (Berke and Modis, 2012; Goubau et al., 2014; Hornung et al., 2006; Schlee et al., 2009; Schmidt et al., 2009; Wu et al., 2013). Conformational changes upon ligand recognition enable engagement of the CARDs with mitochondrial antiviral-signalling protein (MAVS), Figure 1.3B/C.

The signal is transduced via TBK1 / I-kappa-B kinase epsilon (IKKε) and the phosphorylation of transcription factors IRF3 and IRF7, which induce the expression of type-I IFNs (Beckham et al., 2013; Berke and Modis, 2012). RIG-I and MDA5 are both interferon-stimulated genes (ISGs), creating a positive feedback loop upon stimulation (Kang et al., 2002; L. Xu et al., 2017).

Type-I IFN can induce cell-autonomous effector proteins like adenosine deaminase RNA-specific (ADAR1), interferon-induced protein with tetratricopeptide repeats 1 (IFIT1), 2´-5´-oligoadenylate synthetase 1 (OAS1) and protein kinase R (PKR), which posses RNA binding and direct antiviral capabilities (reviewed in Schlee and Hartmann, 2016). It is important to note that the expression of PRRs is cell type-specific and that many cell lines show defects in one or more innate immune signalling pathways (East and Isacke, 2002; Muzio et al., 2000; Rausell et al., 2016). The expression of PRRs in CD4 T cells is outlined in section 1.1.4.3.

1.1.4 T cells

T cells are fundamental for the adaptive immune response. They are involved in the establishment and orchestration of immune responses and form immunologic memory. They recognise antigens derived from pathogens, tumours and the environment through a specialised T cell receptor (TCR). At the same time self-tolerance is maintained through a complex selection process during T cell maturation (reviewed in Kumar et al., 2018). All T cell progenitors arise from the bone marrow (BM) and undergo selection and maturation in the thymus before they migrate to tissues throughout the body. The majority of T cells reside in lymphoid tissues like BM, lymph nodes and the spleen, but are found in smaller numbers in nearly every organ and tissue (reviewed in Kumar et al., 2018).

It has been estimated that the human T cell compartment consists of about 10^{12} T-cells with a TCR repertoire of more than 100 million different sequences. These sequences mediate specificity against virtually every antigen (Qi et al., 2014). T cells emigrate from the thymus as naïve T cells with the capacity to be activated upon antigen recognition and have an estimated lifespan of 6-10 years (den Braber et al., 2012; Garcia et al., 1999; Wang et al., 2001). Antigen-specific activation leads to the differentiation into various short-lived effector subsets (further discussed in section 1.1.4.2). Apoptosis causes a rapid contraction of the effector population once the antigen is cleared from the body and only a small fraction of T cells differentiate into long-lived memory subsets (reviewed in Zhan et al., 2017). The longevity of these cells was verified in different settings, including the following. Yellow fever virus-specific memory CD8 T cells were detectable more than 25 years after vaccination with a live-attenuated virus vaccine (Fuertes Marraco et al., 2015) and a replication-incompetent HIV-1 provirus was contained in a pool of CD4 effector memory T cells for over 17 years (Imamichi et al., 2014). While these long life spans guarantee long-term immunological memory, they also bear the potential to harbour possibly harmful infections like HIV-1 for a long time.

1.1.4.1 T Cell Metabolism

T cells undergo extensive metabolic changes depending on their activation status. While naïve and memory T cells use oxidative phosphorylation (OxPhos) as their primary energy source, activated T cells switch their metabolic program and rely predominantly on aerobic glycolysis (reviewed in MacIver et al., 2013). The usage of glycolysis in the presence of sufficient oxygen levels can also be found in cancer cells and is known as the Warburg effect (Luengo et al., 2020). Resting CD4 T cells show minimal nutrient uptake, ATP production and biosynthesis activity and once they become activated their metabolism changes rapidly (reviewed in Balyan et al., 2020). Anabolic pathways are upregulated, and aerobic glycolysis becomes the main energy source. Subsequently, cells increase in size and begin to proliferate. A fraction of activated T cells return to a resting state and reverse the metabolic program once the antigen is cleared. Of note, resting T cells are not resting in a classical sense; they migrate through lymphoid tissues and provide constant immune surveillance (reviewed in Balyan et al., 2020). Metabolic changes are a prerequisite for T cell activation and effector functions, and the effects of nucleic acid sensor stimulation on T cell activation and metabolism will be addressed in this thesis.

1.1.4.2 CD4 T Cell Differentiation

CD4 T cells are activated by their specific antigen, presented as a peptide:MHCII complex by APCs. Their microenvironment determines the fate of naïve CD4 T cells. They can differentiate into various types depending on the cytokine milieu and mediate distinct effector functions (reviewed in Kedzierska and Koutsakos, 2020). The cytokine milieu is modulated in dependence of the pathogen (intracellular/extracellular, virus, bacteria, fungi, etc.) and prompts the differentiation of CD4 T cell subsets specialised to assist in the clearance of a specific class of pathogen, Figure 1.4.

The classic CD4 T cell subtypes include T helper 1 (Th1) and Th2 cells, which induce immune responses against intracellular pathogens like viruses and bacteria, and extracellular parasites like helminths, respectively (reviewed in Zhu

and Zhu, 2020). Subsequent studies identified other CD4 T cell subtypes including Th9, Th17, follicular helper T cells (Tfh), cytotoxic CD4 T cells (CTL) and regulatory T cells (Treg) (reviewed in Golubovskaya and Wu, 2016 and Pennock et al., 2013). Tregs limit the extent of the immune response and control immune tolerance, while all other previously mentioned CD4 T cell classes amplify the immune response.

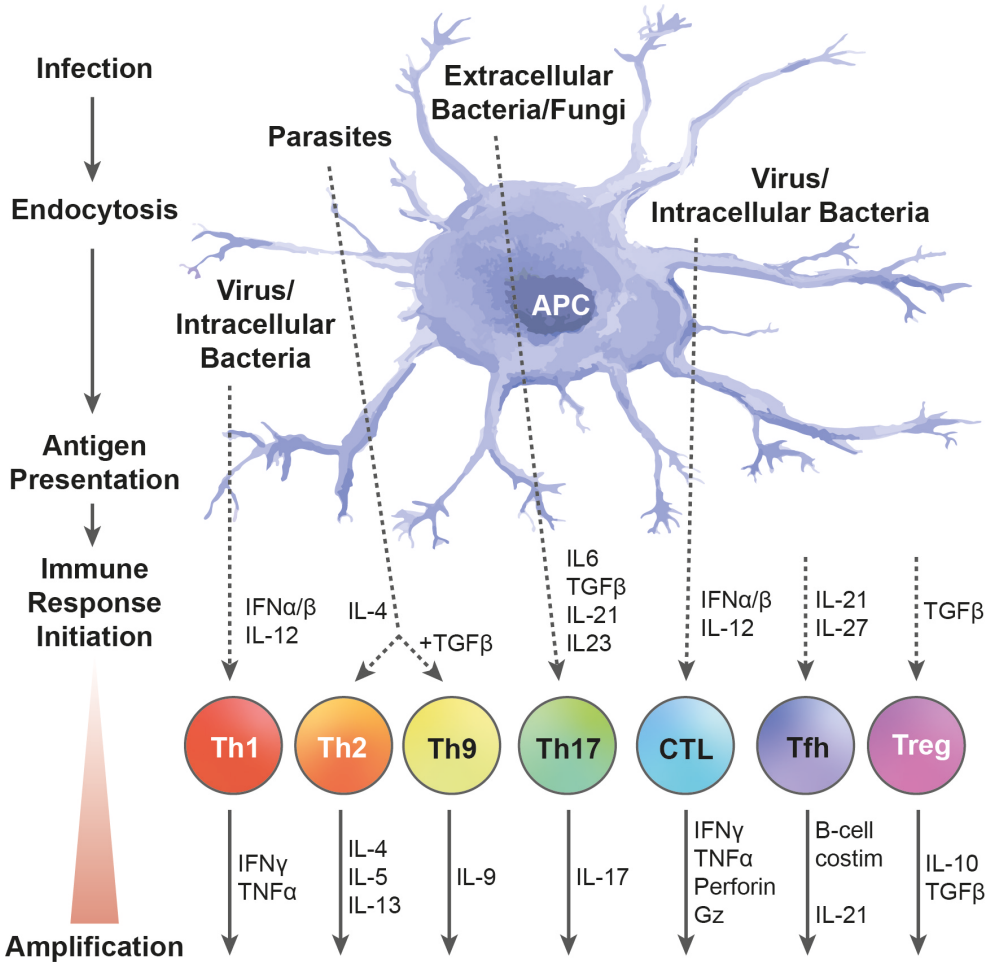

Figure 1.4: Differentiation of CD4 T cells and their effector functions. Antigen-presenting cells (APCs) recognise and process a spectrum of pathogens. Subsequently, CD4 T cells are activated by engagement with their specific antigen, which is presented as a peptide:MHCII complex by APCs (not shown). Cytokines in the microenvironment reflect the initial immune response to the causing pathogen and drive different transcriptional programs in CD4 T cells. They allow for a pathogen-specific amplification of the immune response in order to control and clear the infection. Differentiated CD4 T cells produce various cytokines, which feed back into the cytokine milieu, activating or suppressing other immune cells or promoting the expression of cell-autonomous defence mechanisms in neighbouring cells. Cytotoxic T cell (CTL), granzyme B (Gz), interferon (IFN), interleukin (IL), T follicular helper cell (Tfh), T helper cell (Th),

transcription growth factor beta (TGFβ), tumor necrosis factor alpha (TNFα), regulatory T cell (Treg). (Figure adapted from Pennock et al., 2013).

Intracellular pathogens like viruses induce and increase type-I IFNs and IL-12 production, which upregulate transcription factor T-bet in activated CD4 T cells. Th1 differentiation is driven by T-bet and induces the expression of large amounts of IFNγ and tumour necrosis factor alpha (TNFα), which assist in the clearing of intracellular pathogens (Hernandez-Pando and Rook, 1994; Mullen, 2001).

Cytotoxic CD4 T cells (CD4 CTLs) are a small and emerging subtype of the CD4 T cell population. Detection and cytotoxic killing of virus-infected cells is a crucial feature of cytotoxic CD8 T and NK cells. CD4 CTLs were once believed to be an *in vitro* artefact, but subsequent studies have identified them *in vivo*. They can release perforin and granzyme B and mediate direct killing of virus-infected cells. They are activated via MHCII receptors, which is remarkable in the context of viral escape from CD8 CTLs by downregulation of MHCI receptors (Juno et al., 2017; Takeuchi and Saito, 2017).

Effector T cell numbers increase exponentially during an adaptive immune response and decline rapidly once the antigen is cleared. Only 5-10 % of antigen-specific CD4 T cells survive and differentiate into long-lived memory cells (Gasper et al., 2014). The two main types of memory cells are central memory (T_{CM}) and effector-memory (T_{EM}) cells. T_{CM} have a high proliferative potential after reactivation, while T_{EM} show a lower potential for proliferation, but a rapid release of effector cytokines (reviewed in Pennock et al., 2013).

1.1.4.3 PRRs in CD4 T cells and their role in T cell immunity

The cytokine milieu plays an important role in determining T cell fates, as outlined in the previous section. Other important regulators of the biology of T cells are innate immune sensors. They can provide co-stimulatory signals that modulate cell survival, proliferation and the release of effector cytokines (Reynolds et al., 2010; Wang et al., 2007).

PRRs are differentially expressed, and not all of them are found in CD4 T cells. Resting pan-T cells (CD4/CD8 positive) express only low levels of TLR1-3 and TLR6/8/9 mRNA (Hornung et al., 2002). A subsequent study analysed TLR expression levels in highly purified CD4 T cells and Jurkat cells. They found TLR1-3 and TLR5 messenger RNA (mRNA) to be expressed at high levels and TLR4/7/9 mRNA to be expressed at low levels in CD4 T cells. TLR expression differed in Jurkat cells, and only TLR3 and TLR5 mRNAs were present at high levels, with TLR1/2/7/9 being expressed at low levels. In addition to different TLRs, CD4 T cells express *DDX58* (RIG-I), *IFIH1* (MDA5), cGAS, *EIF2AK2* (PKR) and interferon gamma inducible gene 16 (IFI16), among others (Elsner et al., 2020; Li et al., 2016; Monroe et al., 2014; Nagai et al., 1997; Proteinatlas, 2020; Uhlen et al., 2017; Vermeire et al., 2016).

The stimulation of TLR2, TLR5 or TLR7 significantly increased IFNγ production and cell proliferation of CD4 T cells *in vitro.* The effect on proliferation was more prominent in T_{EM} than in naïve CD4 T cells (Caron et al., 2005). Another study with CD4 T cells derived from mice showed that TLR3 and TLR9 stimulation promotes survival of activated cells, without affecting proliferation kinetics (Gelman et al., 2004).

Activation of the cGAS-STING pathway in murine T cells was found to induce a type-I IFN response and cell death (Larkin et al., 2017). In contrast, RIG-I showed more differential functions beyond its role as an innate immune receptor. A myeloproliferative disorder was observed in mice with a disrupted RIG-I gene (Zhang et al., 2008) and RIG-I-deficient mice showed defects in interferon responses and T cell activation during influenza infection (Kandasamy et al., 2016). It became evident that not only T cell activation but also T cell differentiation may be affected by RIG-I. Treg generation was impaired in RIG-I deficient mice, resulting in an imbalance of Treg and Th17 cells and the occurrence of colitis, an inflammatory disease of the colon (Yang et al., 2017). These finings might have implications during HIV-1 infection, as RIG-I is

degraded by a mechanism involving HIV-1 protease (Solis et al., 2011), with potential effects on T cell differentiation.

1.2 The Human Immunodeficiency Virus

1.2.1 The HIV pandemic and AIDS

Since the onset of the HIV pandemic (including HIV-1 and HIV-2), more than 32 million people have died from Acquired Immunodeficiency Syndrome (AIDS)-related illnesses, and between 32.7 million to 44.0 million people were living with HIV in 2018 (UNAIDS, 2019). Two HIV types exist, HIV-1 and HIV-2, two related viruses with 35-55 % amino acid and 55 % nucleotide sequence identity (reviewed in Esbjörnsson et al., 2019). HIV-1 has a higher prevalence and pathogenicity than HIV-2 (Esbjörnsson et al., 2019). This thesis and the following review focus on HIV-1, the term HIV is used for statements that are relevant for HIV-1 and HIV-2.

Transmission occurs from human to human through contact with certain body fluids from an HIV infected person who has a detectable viral load (Bavinton and Rodger, 2020; Levy, 1993). Upon infection, HIV disseminates quickly throughout the body and predominantly replicates in CD4 T cells. The acute phase of the infection is recognisable by high levels of viremia and decreasing CD4 T cells counts in the blood, Figure 1.5.

A few weeks following primary infection, viremia drops and CD4 T cell counts recover. A balance between viral replication and immune control is established and indicative for the beginning of the chronic phase of the infection, which can last for many years. The ongoing chronic infection eventually progresses to AIDS. Viral replication is no longer effectively controlled and CD4 T cell counts rapidly decline while the viral load increases. The resulting immunodeficiency makes patients more susceptible to secondary infections and other AIDS-related illnesses, ultimately leading to the death of the infected individual (reviewed in Deeks et al., 2015).

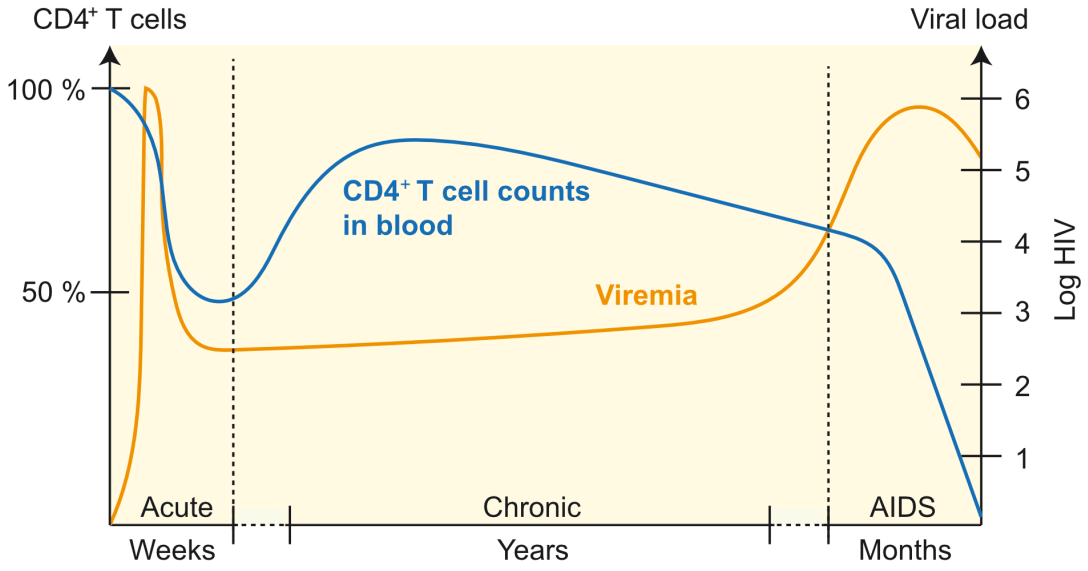

Figure 1.5: Course of untreated HIV-1 infection. The exponential increase of viremia occurs during the early stages of the acute phase of infection. Cytotoxic effects of viral replication and immune recognition of infected cells causes a decrease of CD4 T cells. After several weeks, the infection is controlled by the immune system and CD4 T cell numbers recover, followed by an asymptomatic phase, which can last for several years. Eventually, viremia increases and CD4 T cells counts decrease, initiating the progression to AIDS (Figure adapted from Grossman et al., 2006).

1.2.2 Controlling HIV and prevention of AIDS

Today, more than forty antiretroviral drugs and drug combinations are available for the treatment of HIV, effectively controlling viral replication and preventing the progression to AIDS (AIDSinfo, 2020). Modern antiretroviral therapy (ART) is highly effective and induces a rapid decrease in viral load (Hoenigl et al., 2016). After nearly four decades of extensive research on HIV, medicine is still lacking a treatment to cure the infection. A rapid viral rebound (2-8 weeks after treatment interruption) occurs even in individuals who received treatment for a prolonged period (Pannus et al., 2020), Figure 1.6.

ART targets different steps of the viral lifecycle and the drugs can be divided into seven different classes: Nucleoside reverse transcriptase inhibitors (NRTIs) and non-nucleoside reverse transcriptase inhibitors (NNRTIs) interfere with the

process of reverse transcription; protease inhibitors (PIs) block proteolytic maturation of viral particles and render them non-infectious; integration inhibitors prevent integration of the provirus into the host genome; fusion inhibitors, CCR5 antagonists and post-attachment inhibitors block viral entry (AIDSinfo, 2020; Kemnic and Gulick, 2020).

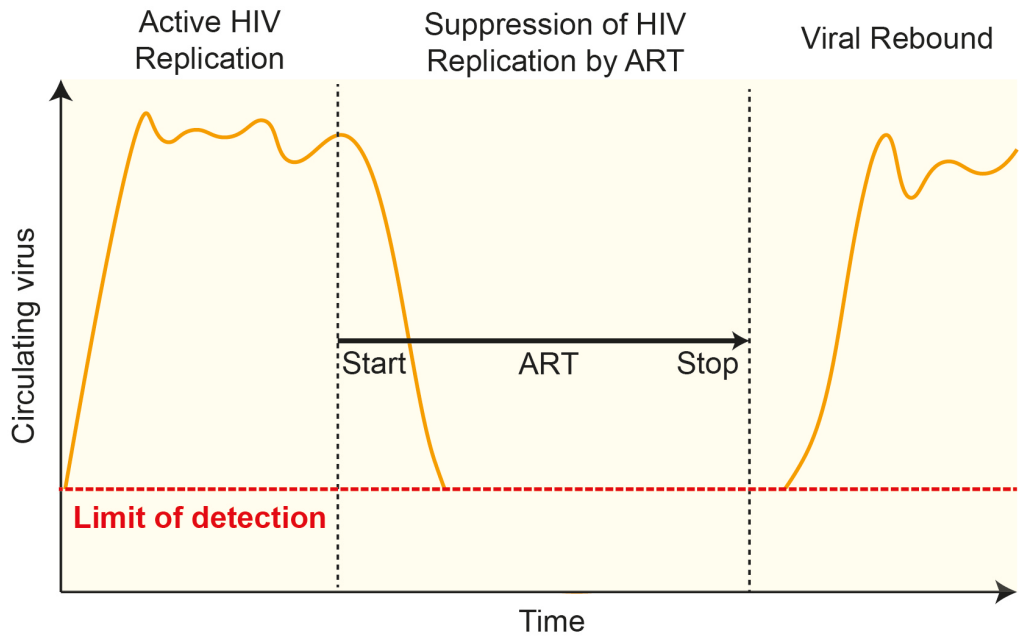

Figure 1.6: Dynamics of plasma viremia in the setting of antiretroviral therapy and treatment interruption. Exponentially increasing plasma viremia can be detected during a phase of active HIV replication. Administration of ART induces the suppression of viral replication below the limit of detection. A rapid viral rebound occurs shortly after treatment interruption. (Figure adapted from Kulpa and Chomont, 2015).

While ART is becoming widely accessible, one third of people living with HIV (PLWH) do not receive any ART regimen, resulting in the ongoing spread of the virus with an estimated 1.7 million new cases worldwide in 2018 (UNAIDS, 2019). A cure for HIV is of high importance despite the effectiveness of ART. Modern ART regimens are normally safe, but can have side effects in some individuals and many PLWH are affected by stigmatisation and discrimination (Tran et al., 2019; Venter et al., 2019). A cure for HIV would improve transmission control and ease the pressure on public-health systems (reviewed in Ndung'u et al., 2019).

1.2.3 The HIV-1 genome and its gene products

The HIV-1 genome is made up of two identical copies of a 9.2 kb long, positive-sense, ssRNA molecule (reviewed in Shi et al., 2021) and is organised in nine genes (Clever and Parslow, 1997). The viral genes can be divided into three classes: structural proteins (*gag*, *pol* and *env*), essential regulatory elements (*tat* and *rev*) and accessory regulatory proteins (*nef*, *vpr*, *vif* and *vpu*) (Frankel and Young, 1998). Coding regions are flanked by long terminal repeat (LTR) sequences. They assist in the integration of the viral genome and regulation of viral gene expression (Khan et al., 1991; Shah et al., 2014). A complex system of RNA splicing and post-translational processing gives rise to fifteen viral proteins, Figure 1.7.

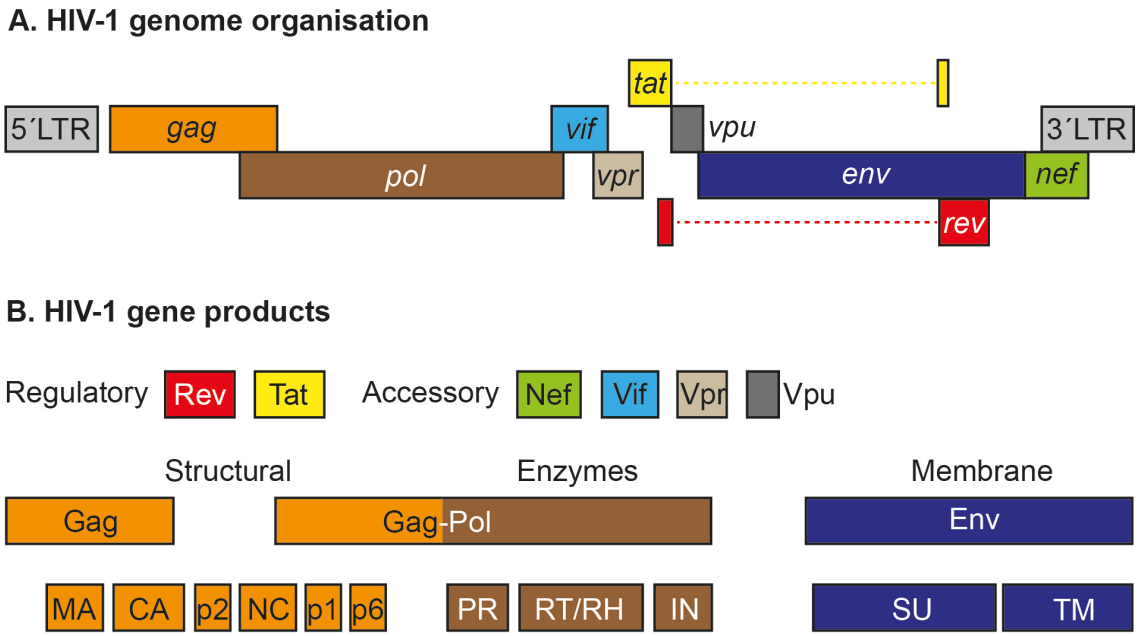

Figure 1.7: HIV-1 genome organisation and gene products. A: The HIV-1 genome is organised in nine viral genes, and expression involves mRNA splicing events for some of the genes. The coding region is flanked by long terminal repeats (LTRs), which assist in viral integration and regulation of viral gene expression. B: Multiply spliced viral mRNA gives rise to early viral proteins Nef, Tat and Rev. Singly spliced viral mRNA allows expression of *env*, *tat*, *vif*, *vpr* and *vpu*. Unspliced viral mRNA encodes Gag and Gag-Pol proteins. Precursor proteins Gag, Gag-Pol and Env are proteolytically processed to matrix protein (MA), capsid protein (CA), spacer protein 1 and 2 (p2, p1), nucleocapsid protein (NC), protease (PR), reverse transcriptase / RNase H (RT/RH), glycoprotein 120 (SU) and glycoprotein 41 (TM). (Figure adapted from Peterlin and Trono, 2003; Stoltzfus, 2009).

The transcribed viral genome harbours multiple splice sites, which allow for multiply spliced, singly spliced and unspliced mRNA species. During the early stage of viral replication multiply spliced mRNA gives rise to regulatory proteins trans-activating regulatory protein (Tat), Rev and Nef (Kim et al., 1989; Klotman et al., 1991). Tat enhances the transcription of the viral genome (Parada and Roeder, 1996; Zhu et al., 1997). Rev protein binds to the Rev Responsive Element (RRE) in single spliced and unspliced transcripts and facilitates the export from the nucleus to the cytoplasm (Hadzopoulou-Cladaras et al., 1989), enabling the translation of structural, accessory and envelope proteins (Tazi et al., 2010).

Envelope (*env*) is transcribed from a singly spliced mRNA species and encodes glycoprotein 160 (Gp160), which is processed to envelope glycoprotein 120 (Gp120, SU) and glycoprotein 41 (Gp41, TM) catalysed by host proteases including protease furin (Arrigo et al., 1990; Hallenberger et al., 1992; Willey et al., 1988).

Group-specific antigen (*gag*) and *DNA polymerase* (*pol*) are transcribed from the unspliced viral mRNA. Precursor protein Gag is processed to matrix protein (MA, P17), capsid protein (CA, P24), spacer peptide 1 (SP1, P2), spacer peptide 2 (SP2, P1), nucleocapsid protein (NC, P7) and P6 protein by viral protease (Könnyű et al., 2013). *Pol* is translated as the Gag-Pol precursor protein. A -1 bp ribosomal frameshift during translation allows the expression of the Gag-Pol fusion protein in about 5 % of the translations (Jacks et al., 1988; Shehu-Xhilaga et al., 2001; Wilson et al., 1988). The Gag-Pol precursor protein gives rise to viral enzymes reverse transcriptase (RT), RNase H, integrase (IN) and protease (PR) (Könnyű et al., 2013), as well as to the Gag precursor derived proteins (see above).

1.2.4 The HIV-1 particle – structure and formation

HIV-1 propagation relies on particles that can leave the producer cells to spread and infect other susceptible cells. HIV-1 is an enveloped virus, and its envelope

is derived from the host's cell membrane (reviewed in Podkalicka and Bassereau, 2019). An estimated seven to fourteen molecules of trimeric envelope glycoproteins, which are heterodimers of the transmembrane glycoprotein (Gp41, TM) and surface glycoprotein (Gp120, SU) are presented on the surface of each virion (Chertova et al., 2002). MA protein is associated with the inner layer of the envelope. The central icosahedral capsid encapsulates a non-covalently linked genomic RNA (gRNA) dimer (Xiao et al., 2019). The viral genome is coated with NC proteins which assist in viral RNA packaging and reverse transcription during early infection (reviewed in Thomas and Gorelick, 2008). Several copies of mature viral enzymes RT (heterodimer) and IN (tetramer) are associated with the viral gRNA (Esposito and Craigie, 1999; Wang et al., 1994). Further proteins present in the viral particle are PR, P1, P2 and accessory proteins Vif, Vpr and Nef, Figure 1.8.

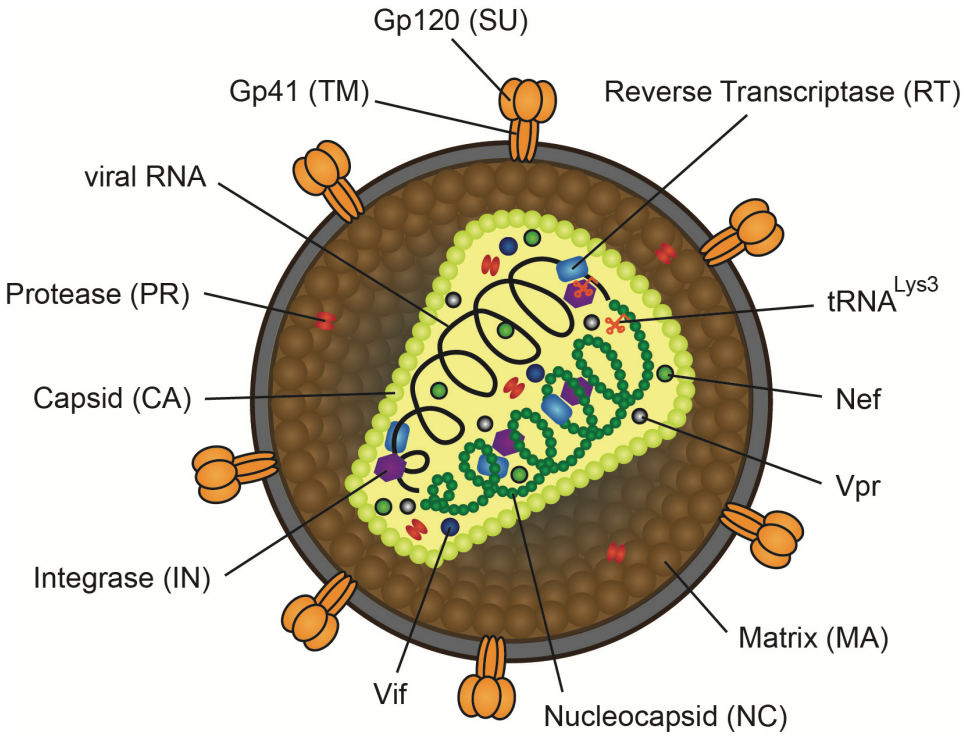

Figure 1.8: Organisation of the HIV-1 virion. The envelope encloses an icosahedral capsid (CA) which encapsulates two copies of the ssRNA genome. Viral RNA is coated with nucleocapsid protein (NC) and associated with reverse transcriptase (RT) and integrase (IN). Protease (PR) and accessory proteins Vif, Vpr and Nef are also present in the viral particle. $tRNA^{Lys}$ is selectively packaged into the particle. The envelope is derived from the plasma membrane of the host cell. It is associated with matrix protein (MA) on the inside and exposes several molecules of trimeric envelope glycoproteins, which are heterodimers of the

transmembrane glycoprotein (Gp41, TM) and surface glycoprotein (Gp120, SU), on the outside. (Figure adapted from Frankel and Young, 1998; Steckbeck et al., 2013).

The formation of infective HIV-1 virions can be divided into three major steps: the *assembly* of the viral particle in proximity to the host's cell membrane; *budding* (release) of the viral particle and *maturation*, wherein proteolytic processing and structural rearrangement of viral proteins renders the particles infectious (Sundquist and Krausslich, 2012).

After translation, viral proteins assemble at the plasma membrane: Gp160 protein is processed and trafficked through the Golgi and trans-Golgi-network (TGN) and oligomerised Gp120 and Gp41 proteins are presented on the cell's surface (Stein and Engleman, 1990). Gag polyproteins fold into auto-inhibited structures and polymerise at the plasma membrane, but not in the cytosol (Kutluay and Bieniasz, 2010).

Four domains of the Gag polyprotein are involved in early steps of particle formation. A highly basic region of N-terminal MA domain interacts with the plasma membrane and assists in RNA binding. The NC domain specifically selects viral unspliced gRNA by binding the packaging signal (Ψ), which is mainly located in the 5`-untranslated region (UTR). Also, MA-MA, CA-CA and NC-NC interactions have been described during particle formation (Berkowitz et al., 1995; Chukkapalli et al., 2010; Kroupa et al., 2020; Mariani et al., 2014; Zhang and Barklis, 1995). Pol polyprotein is incorporated as Gag-Pol precursor (Cen et al., 2004).

HIV-1 selectively packages transfer RNA^{Lys} into the viral particle, which acts as a primer for reverse transcription during the next replicative cycle (Isel et al., 1996; Lanchy et al., 1998; Mak et al., 1994). Budding is mediated by the C-terminal P6 domain of Gag, which recruits the endosomal sorting complexes required for transport machinery (ESCRT) to facilitate particle release (Garrus et al., 2001). The immature particle is organised in different radial layers of viral proteins, with

the MA domain bound to the envelope and the P6 domain facing to the inside of the particle (Fuller et al., 1997).

Maturation occurs while or shortly after budding of the particle and is initiated by HIV-1 protease, which is part of the Gag-Pol precursor protein. HIV-1 protease is autocatalytic and gains enzymatic activity by assembling to homodimers. It cleaves Gag and Gag-Pol precursor proteins at eleven different sites to release MA, CA, P2, NC, P1, P6, RT and IN proteins (Torrecilla et al., 2014). Sequential proteolytic cleavage induces the rearrangement of viral proteins and gRNA into mature and infectious HIV-1 virions (Wiegers et al., 1998).

1.2.5 The HIV-1 replication cycle

The HIV-1 replicative cycle can be divided into different steps, Figure 1.9, and begins with the infection of susceptible cells, predominantly CD4 T cells that express one or both of the HIV-1 entry co-receptors CCR5 or CXCR4 (Deeks et al., 2015). Reports about other cell types that can be infected by HIV-1 in vivo and in vitro include macrophages, monocytes and DCs, even though viral entry and replication in those cell types are reduced compared to activated CD4 T cells (Cavrois et al., 2006; Kedzierska and Crowe, 2002; Pion et al., 2006).

The first step during HIV-1 replication is the delivery of the viral core to the cytoplasm of the host cell. This process is initiated by binding of Gp120 on the viral particle to the viral entry receptor CD4 on the surface of the target cell (Maddon et al., 1986; McDougal et al., 1986). Binding leads to conformational changes within Gp120 and allows for subsequent binding of HIV-1 co-receptor CCR5 or CXCR4 (Kwong et al., 1998; Raja et al., 2003).

Engagement of the co-receptor exposes the fusion peptide (FP) portion of Gp41, which inserts either in an α-helical or β-sheet confirmation into the lipid bilayer of the target cell (Lai and Freed, 2014). Membrane fusion allows the entry of the viral core into the cytoplasm of the target cell (reviewed in Wilen et al., 2012).

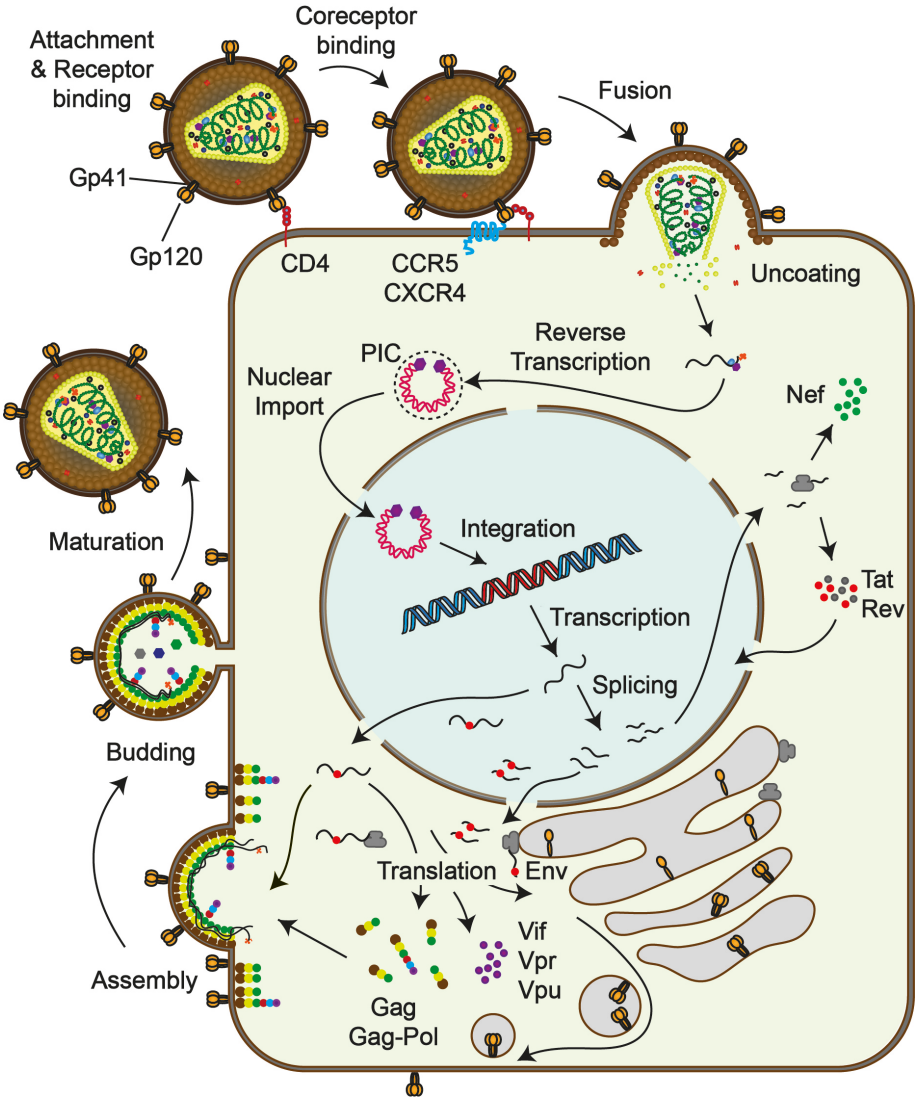

Figure 1.9: The HIV-1 replication cycle. Attachment of HIV-1 to its target cell allows the binding of Gp120 to entry receptor CD4. Conformational changes of Gp120 mediate engagement of HIV-1 co-receptor CCR5 or CXCR4 with gp41, which initiates fusion of the viral envelope and cell membrane. Organised disassembly of the viral core begins after it reached the cytoplasm. Viral genomic RNA is released, and viral reverse transcriptase (RT) produces the double-stranded proviral DNA. The pre-integration complex (PIC) assembles and is transported into the nucleus. Viral integrase catalyses the integration of the proviral DNA into the host genome. Transcription of the provirus and subsequent mRNA splicing gives rise to Tat, Rev and Nef proteins. Tat induces a positive feedback loop by enhancing transcription. Presence of Rev facilitates nuclear export of singly and unspliced mRNA species, which give rise to Vpr, Vif, Vpu and precursor proteins Env, Gag and Gag-pol. Env is processed in the endoplasmic reticulum and trans-Golgi network and presented as trimeric heterodimers on the cell surface. Assembly of the viral particle occurs at the plasma membrane. Maturation of the viral particle is mediated by viral protease while or after budding. Enzymatic processing and rearrangement give rise to infectious, mature HIV-1 virions. (Figure adapted from Ferguson et al., 2002).

Efficient disassembly of the viral core is a prerequisite for the subsequent transcription of the viral RNA into complement DNA (cDNA) (Forshey et al., 2002). Reverse transcription is dependent on $tRNA^{Lys3}$, which is associated with the viral gRNA and functions as a primer for RT (Isel et al., 1996; Lanchy et al., 1998).

The newly formed RNA-DNA duplex is a substrate for RNase H, which degrades the RNA template. DNA polymerase activity of RT synthesises the sense strand from the antisense cDNA to form the proviral dsDNA genome (Hu and Hughes, 2012). The 9.8 kb proviral genome associates with IN, MA, Vpr, RT, and host cell-derived high-mobility group protein (HMG/Y) to form the pre-integration complex (PIC).

PIC has an affinity to cellular karyopherin alpha, which facilitates nuclear import across the intact nuclear membrane (Miller et al., 1997; Popov, 1998). IN catalyses the integration of the proviral dsDNA into the host cell genome. Two 3' nucleotides (d(C-A)) are cleaved from each proviral DNA strand, and the free 3'-hydroxyls assist in restriction of the chromosomal DNA. The free 5'-phosphates are then joined with the proviral DNA (Engelman and Cherepanov, 2012; Esposito and Craigie, 1999).

Following the integration of the viral genome, the virus can either stay in an inactive (latent) state, which will be discussed in the next section, or proceed to late steps of the replication cycle. Late replicative steps include the expression of viral genes, the assembly, budding and maturation of infective particles, which has been outlined in the previous sections.

1.2.6 HIV-1 latency – establishment, maintenance and reversal

Once HIV-1 integrated into the genome of the host cell, new virions can be produced. However, under certain circumstances the viral life cycle comes to a halt and viral genes are no longer expressed. The state of reversible non-productive infection is called latency. Establishment, maintenance and reversal

of latency is dependent on several factors, which will be further discussed in this section.

Usually CD4 T cells die shortly after *de-novo* HIV-1 infection due to cytotoxic effects during productive infection or innate immune responses during abortive infections (reviewed in Doitsh and Greene, 2016). Rarely, an infected cell survives and differentiates into a long-lived memory CD4 T cell in which epigenetic and metabolic changes promote the formation of transcriptionally inactive integrated virus (Kumar et al., 2015; Palmer et al., 2018). HIV-1 can stay in a latent state during the whole lifetime of an infected cell and those latent proviruses make up the viral reservoir and are the main obstacle for an HIV-1 cure (Buzon et al., 2014). Latent viruses are eventually reactivated once cellular factors change. The early phase of proviral gene expression is dependent on cellular factors, for example, the presence of transcription factors and epigenetic modifications of histones and DNA (Hakre et al., 2011; Kumar et al., 2015; Nabel and Baltimore, 1987). A prime example for naturally occurring latency reversal is the activation of resting memory CD4 T cells during an adaptive immune response. T cell activation leads to the upregulation of transcription factors NFκB and Sp1. The resulting changes in cell metabolism and anabolic pathways can then promote progression of the HIV-1 replicative cycle (Amie et al., 2013; Böhnlein et al., 1988; Pearce et al., 2013; Perkins et al., 1993; Tong-Starksen et al., 1987; Valle-Casuso et al., 2019).

While cellular factors NFκB and Sp1 directly bind the viral promoter to induce viral gene expression, the transcriptional elongation is very inefficient at this stage, and only a few molecules of full-length transcripts are completed. RNA splicing gives rise to viral regulatory factors Tat and Rev. Tat induces a positive feedback loop by recruiting the super elongation complex (SEC) to the LTR, which promotes a more efficient transcription (Frankel and Young, 1998; He et al., 2010; Kao et al., 1987; Marciniak and Sharp, 1991; Sobhian et al., 2010).

Aside from the induction of cellular transcription factors, CD4 T cell activation causes wide epigenetic and metabolic changes in these cells, as discussed previously. These changes create an environment in which viral gene expression is most efficient (reviewed in Pan et al., 2013).

Increasing knowledge on how HIV-1 latency is established and maintained allowed the manipulation of underlying mechanisms and to reverse latency *in vitro, ex vivo* and *in vivo* (Jiang et al., 2015; Rasmussen et al., 2014; Spina et al., 2013). Compounds used for this purpose are called latency-reversing agents (LRAs), and include histone deacetylase inhibitors (HDACi) and protein kinase C (PKC) agonists, among others. Coordinated and effective latency reversal is of importance to an HIV-1 cure attempt called *shock and kill*, which will be discussed later in this review.

1.2.7 HIV-1 persistence and the viral reservoir

The size of the viral reservoir has been studied extensively. It was estimated that the frequency of latently infected cells is about one cell per million resting CD4 T cells, with an overall size of the reservoir being less than ten million cells (Chun et al., 1997; Silicano, 2010). Interestingly most HIV-1 proviruses are defective (up to 98 %), due to a missing proofreading function of the viral reverse transcriptase (Bruner et al., 2016; Roberts et al., 1988). Latently infected cells are refractory to drugs interfering with the viral life cycle and are not recognised and killed by the immune system (G. Zhang et al., 2019).

To date, long-lived resting memory CD4 T cells (rCD4) are the only reservoir in humans for which experimentally demonstrated evidence exists that it harbours long-term replication-competent proviruses *in vivo* (Churchill et al., 2016; Eisele and Siliciano, 2012). Upon reactivation these cells can produce new virions and spread the infection as described in the previous section. Clonal expansion driven by antigen-mediated, homeostatic and integration site proliferation shapes and replenishes the viral reservoir *in vivo* (reviewed in Liu et al., 2020).

Ongoing discussions to what extent other cell types and tissues contribute to the viral reservoir are dependent on how the terms latency and reservoir are defined (Churchill et al., 2016). In contrast, a reservoir can be defined as long-lived cells that harbour a copy of a latent (as defined above) and replication-competent virus for a prolonged period (Siliciano and Greene, 2011).

There are two forms of HIV-1 latency, pre-integration and post-integration latency. Pre-integration latency describes the persistence of unintegrated HIV-1 DNA. Integration may still occur at a later time point within days of infection (Hakre et al., 2012).

Macrophages and DCs are sometimes considered to be part of the HIV-1 reservoir as they can harbour infective HIV-1 particles and spread the infection over several days (Geijtenbeek et al., 2000; Yu et al., 2008). If the short-term persistence of HIV-1 in those cells qualifies as a latent reservoir has been discussed ambiguously in the literature (Churchill et al., 2016).

1.2.8 HIV-1 and the Immune System

Exponential replication of viral particles during the early phase of HIV-1 infection elicits a strong response of the innate immune system: a broad repertoire of pro-inflammatory cytokines (cytokine storm), chemokines and type-I IFNs are released and attract and activate innate and adaptive immune cells (reviewed in Kazer et al., 2020). A significant reduction in CD4 T cell numbers in the blood and gastrointestinal tract occurs, caused by direct viral cytotoxic effects, but also by apoptosis and cell-mediated killing - indicative for an efficient innate immune activation (Brenchley et al., 2004). Despite the robust and immediate response, the immune system is not able to clear the infection.

The early immune response against HIV-1 infection involves NK cells, DCs, monocytes, macrophages, natural killer T (NKT) cells, infected CD4 T cells, among others. These cells release large amounts of cytokines and chemokines (IFNs, CXC chemokine ligand 10 (CXCL10), TNFα, IFNγ, IL- 1β, IL10, IL12, IL15, IL18, IL22) (reviewed in Kazer et al., 2020).

HIV-1 infects immune cells that are usually involved in innate and adaptive immune responses against pathogens like bacteria and viruses, including HIV-1 (Mogensen et al., 2010). Ongoing viral replication leads to an exponential increase of plasma viremia and decrease of CD4 T cell counts in the blood and gastrointestinal tract during the acute phase of HIV-1 infection (Brenchley et al., 2004).

The pressure of the adaptive immune response selects for escape mutants and drives viral diversification (Price et al., 1997). Viremia declines naturally over a period of several weeks if untreated and is rapidly reduced once ART commences (Ananworanich et al., 2017; Perelson et al., 1996; Wei et al., 1995). Central memory and naïve CD4 T cells are not profoundly affected during the acute phase of the infection due to the lack of CCR5 expression, allowing for recovery of CD4 T cell levels in the blood (Grossman et al., 2006). A phase with stable viremia (viral set point) and CD4 T cell counts follows and can last for years before the onset of AIDS (Buchbinder et al., 1994).

Further, it has been shown, that HIV-1 infection causes ongoing lymphoid tissue fibrosis and depletion of naïve T cells and that prolonged ART with suppression of plasma viremia failed to reverse these effects (Sanchez et al., 2015).

1.2.8.1 Evasion of Cellular Restriction Factors by HIV-1

HIV-1 uses a wide range of viral and host components to evade restriction factors and innate immune sensing, summarised in Table 1.1. Proteins of the apolipoprotein B mRNA editing enzyme catalytic polypeptide-like 3 (APOBEC3) protein family (specifically APOBEC3G and APOBEC3F) can induce significant inhibition of HIV-1 replication (Sheehy et al., 2003; Zheng et al., 2004). APOBEC3G binds to NC and viral genomic RNA during the process of reverse transcription. Deamination of cytidine to uridine in the newly synthesised cDNA strand can induce the degradation of the viral genome. The provirus is usually highly mutated and gives rise to defective mRNA if integration still occurs

(Mangeat et al., 2003). HIV-1 circumvents this cellular restriction factor through its accessory protein Vif, which induces the proteasomal degradation of APOBEC3G (Sheehy et al., 2003).

Another well-known restriction factor for retroviral replication is tripartite motif-containing protein 5 (TRIM5α). The protein can inhibit reverse transcription by binding to the core of incoming viral particles. While the expression of simian TRIM5α renders old world monkey (OWM) and human cells resistant against HIV-1 infection, the human analogue shows weak HIV-1 restriction (Nakayama and Shioda, 2012). Human TRIM5α alleles are some of the strongest selected alleles in the human linage, with TRIM5α being among the major restriction factors of cross-species transmission of simian immunodeficiency virus (SIV) (Sawyer et al., 2005; Sharp and Hahn, 2011). HIV-1 may resemble a naturally selected pool of viruses able to evade human TRIM5α (Malim and Emerman, 2008). Selective pressure can reverse this effect when cytotoxic CD8 T cell escape mutants against CA protein arise. In essence, those HIV-1 mutants showed to be up to ten times more sensitive to TRIM5α than wildtype viruses (Battivelli et al., 2011).

Bone marrow stromal antigen 2 (*BST2*) is an interferon-stimulated gene, encoding for tetherin, a membrane-bound glycoprotein. Tetherin can retain viral HIV-1 particles on the cell surface and thereby restrict viral budding. Viral accessory protein Vpu compromises this effect by inducing the degradation of tetherin (Douglas et al., 2009; Iwabu et al., 2009; Neil et al., 2007; Venkatesh and Bieniasz, 2013). Vpu also targets newly synthesised CD4 proteins in the endoplasmic reticulum for degradation (Magadán et al., 2010). Nef mediates a similar function and targets CD4 receptors for internalisation and lysosomal degradation, allowing for efficient budding and Env integration into the viral particle (Lindwasser et al., 2007; Schaefer et al., 2008). Nef was also found to prevent Gag-polyprotein and Vif degradation by HDAC6 (Marrero-Hernández et al., 2019).

HIV-1 does not only target the previously mentioned cellular restriction factors of viral replication but also PRR mediated antiviral responses. Envelope protein Gp120 renders plasmacytoid dendritic cells (pDCs) unresponsive to TLR9 signalling through a mechanism involving CD4 and mannose-binding C-type lectin receptors (MCLRs), causing suppression of IFNα, IL-6 and TNFα synthesis upon CpG-oligonucleotide challenge. This effect demonstrated to have even broader consequences as subsequent B cell and NK cell activation by pDCs was impaired *in vitro* (Chung et al., 2012; Martinelli et al., 2007).

PKR and its downstream signalling are targeted through different mechanisms by HIV-1. The trans-activation response sequence (TAR) within the viral genomic RNA is recognised by PKR. Low concentrations of TAR RNA have a stimulatory effect on PKR, while high TAT RNA concentrations inhibit PKR activation (Gunnery et al., 1990; Maitra et al., 1994). This mechanism may prevent PKR-dependent recognition of viral RNA during late stages of the viral lifecycle. PKR activity is sensed by Tat during the early stages of the viral lifecycle. Tat is a substrate for PKR and phosphorylated Tat binds TAR RNA faster and stronger than the unphosphorylated Tat. More efficient binding leads to more efficient transcription and expression of viral genes (Endo-Munoz et al., 2005). High levels of Tat can inhibit PKR signalling in three different ways: 1) Tat competes with the natural substrate of PKR, eukaryotic translation initiation factor 2A (eIF2α), thereby decreasing the effectiveness of signal transduction. 2) Tat binds TAT RNA and shields it against PKR. 3) Tat binds directly to PKR and inhibits its autophosphorylation and activation (Brand et al., 1997; Cai et al., 2000; Clerzius et al., 2011). In conclusion, low level PKR activation seems to be beneficial for viral replication at early stages of viral replication and PKR signalling is effectively abrogated at later time points.

Another important protein is HIV-1 PR. It is not only crucial for the maturation of viral particles, but also for immune evasion. Several cellular proteins are substrates for HIV-1 protease, and it was reported that viral protease is involved in sequestration of the RIG-I signalling pathway (Impens et al., 2012; Solis et al.,

2011). The underlying mechanism is not fully understood and will be addressed in this thesis.

Signal transducer and activator of transcription (STAT) 1 and STAT3 are necessary for the signal transduction after receptor-ligand-binding (e.g. IFNα and type-I IFN receptor) (reviewed in Tsai et al., 2019). Viral proteins Nef and Vpu have been described to block the phosphorylation and thereby the activation of STAT1 (Nguyen et al., 2018) and viral protein Vif was found to mediate the degradation of STAT1 and STAT3, but not STAT2 (Gargan et al., 2018).

Table 1.1: HIV-1 components and their cellular targets.

Viral component	**Cellular target**	**Effect**	**References**
Gp120	MCLRs and CD4	Immune evasion by abrogation of TLR9 signalling in pDCs; impaired B and NK cell activation.	Chung et al., 2012; Martinelli et al., 2007
Nef	CD4	Efficient budding by preventing retention of viral particles.	Lindwasser et al., 2007; Schaefer et al., 2008)
	HDAC6	Counteracts HDAC6 mediated degradation of Gag-polyprotein and Vif.	Marrero-Hernández et al., 2019
	STAT1	Blockage of the antiviral effects of type-I IFNs.	Nguyen et al., 2018

Viral component	**Cellular target**	**Effect**	**References**
Protease	RIG-I	Immune evasion by abrogating of RIG-I signalling.	Solis et al., 2011
TAR RNA	PKR	Immune evasion by inhibition of PKR at high concentrations.	Gunnery et al., 1990
Tat	PKR	Immune evasion by inhibition of PKR auto-phosphorylation; competes with eIF2α as a substrate for PKR.	Brand et al., 1997; Cai et al., 2000
Vif	APOBEC3G STAT1/3	Immune escape by degradation of APOBEC3G; progression of reverse transcription and integration. Blockage of the antiviral effects of type-I IFNs.	Sheehy et al., 2003 Gargan et al., 2018
Vpu	Tetherin, CD4 STAT1	Efficient budding by preventing retention of viral particles. Blockage of the antiviral effects of type-I IFNs.	Douglas et al., 2009; Lindwasser et al., 2007 Nguyen et al., 2018

1.2.9 A cure for HIV-1

After cessation of ART, HIV-1 rapidly rebounds in about 2-3 weeks. The source of viral rebound is not fully understood but is thought to predominantly arise from long lived and proliferating latently infected cells. Two cure strategies have been proposed, both aiming for removing the need for long term ART. The first one is the sterilising cure strategy, which attempts to eliminate all replication-competent proviruses from the body, resulting in complete clearance of the viral reservoir. The second strategy aims for a functional cure, or what is now commonly called remission, through reduction (not elimination of infected cells) as well as induction of a sustained and more effective immune response, which can control viral replication in the absence of ART (reviewed in Deeks et al., 2016; and Xu et al., 2017).

There are only two cases of long-term remission of HIV-1, referred to as the *Berlin patient* and the *London patient*. The circumstances of these cases are extraordinary: Both patients suffered from acute myeloid leukemia, underwent full-body irradiation and received allogenic haemopoietic stem-cell transplants that did not express HIV-1 coreceptor CCR5 (CCR5Δ32). Both patients developed mild forms of graft versus host disease (GvHD), and it remains unclear if GvHD is a necessary component of achieving HIV-1 remission off ART (R. K. Gupta et al., 2020; Hütter et al., 2009; Zou et al., 2013). Both patients were monitored extensively following transplantation. Low levels of HIV-1 DNA, RNA and declining amounts of antibodies against Env were found in different tissue samples of the Berlin patient (Hütter et al., 2009; Yukl et al., 2013). Replication competent virus was not detected, no sequence confirmation was provided and calculated viral levels were far below what was found in ART-treated patients. As full length and replication competent virus could not be identified, the patient was considered cured (Yukl et al., 2013).

Similar findings have been reported for the London patient: low-level HIV-1 DNA and declining antibodies against Env protein over 27 months after stopping ART. Mathematical modelling found the probability of a life-long remission to be 98 %

(R. K. Gupta et al., 2020). Even though this treatment regimen is not applicable for a population-wide use, it shows that an HIV-1 cure is achievable in general.

1.2.9.1 Gene therapy as a cure for HIV-1

Methods to eradicate the viral reservoir include gene therapy (CRISPR/Cas9 mediated destruction of provirus; transplantation of altered autologous virus-resistant stem cells) (Dash et al., 2019; Xu et al., 2019), summarised in Table 1.2.

Table 1.2: HIV-1 cure strategies involving gene therapy

Strategy	**Target**	**Study design**	**Effect**	**References**
CCR5Δ32 allogenic haemopoietic stem-cell transplants	Replication and reservoir.	*In vivo*, human	Eradication of the viral reservoir and prevention of re-infection by CCR5-tropic HIV strains.	Gupta et al., 2020, Hütter et al., 2009
CRISPR *in situ* gene editing in combination with ART	Replication and reservoir.	*In vivo*, human	Prevention of viral spread and excision of provirus.	Dash et al., 2019
CRISPR *ex vivo* edited stem cell transplants	Replication and reservoir.	*Ex vivo* / *in vivo*, human	Reduction of the frequency of HIV-1 susceptible CD4 T cells.	Xu et al., 2019

Functional cure strategies aim for complete immune control or long-term inhibition of the viral life cycle instead of removing all proviruses from the body. It is known that the human immune system can effectively control an HIV-1 infection under certain conditions in the absence of ART, evident in a small number of

people living with HIV. These patients are termed controllers (<5000 HIV-RNA copies/mL), elite controllers or long term non-progressors (<50 HIV-RNA copies/mL, the threshold of many assays) (Morou et al., 2019). Even though different host and viral factors have been identified to have beneficial effects on containing the infection, no universal combination of factors is known to mediate long term HIV-1 control (Pernas et al., 2017). Extensive research is done to investigate the role of innate and adaptive immunity during viral control. While the detailed mechanisms of immune control stay unclear, it seems that the presence of broad-neutralising antibodies is not crucial as they are absent in most elite controllers (Baker et al., 2009).

1.2.9.2 Targeting PRRs to cure HIV-1

The so-called *shock and kill* attempt aims for the reactivation of the entire viral reservoir, inducing the death of infected cells while preventing viral spread to uninfected cells (reviewed in Kim et al., 2018 and Xu et al., 2017). Over the past years, innate immune receptors were included more frequently in studies for an HIV-1 cure. Activation of innate immunity has bee explored to boost reactivation of latent virus or to facilitate detection and subsequent cellular immune responses. Studies targeting the HIV-1 reservoir using PRR agonists are listed in Table 1.3 and will be further discussed in the following paragraphs.

Table 1.3: HIV-1 cure strategies involving innate immune sensor agonists.

Compound	Target	Study design	Effect	References
Pam3CSK4	TLR1/2	*In vitro*	NF-κB activation, TNFα secretion and viral reactivation.	Novis et al., 2013
Pam2CSK4 and GS-9620	TLR2 and TLR7	*Ex vivo*	NF-κB activation, TNFα secretion	Macedo et al., 2018

			and viral reactivation.	
GS-9620 and/or GS986	TLR7	*Ex vivo*, human and *in vitro* non-human primates	Induction of type-I IFNs and viral reactivation.	Tsai et al., 2017, Lim et al., 2018
MGN1703	TLR9	*In vivo*, human	Viral reactivation and enhancement of cellular immune responses.	Vibholm et al., 2017
Acitretin	RIG-I	*Ex vivo*	Reactivation of latent virus and induction of apoptosis in infected cells.	Li et al., 2016

The TLR7 agonist GS-9620 was used in PLWH on ART and induced type-I IFN dependent HIV reactivation (Tsai et al., 2017). Another study used two TLR7 agonists (GS-9620, GS986) and observed SIV reactivation and reduction of the reservoir size in macaques on ART (Lim et al., 2018). Combinational activation of TLR2 and TLR7 was found to induce viral reactivation and an antiviral state in CD4 T cells *ex vivo* (Macedo et al., 2018) and confirmed findings published by Novis et al., 2013, involving TLR1/2 activation and viral reactivation in CD4 T cells. TLR9 was targeted by agonist MGN1703 in a human study and showed latency-reversing action and enhanced innate immune responses (Vibholm et al., 2017).

The cytosolic innate immune sensor RIG-I was targeted with acitretin; an FDA approved retinoid used for the treatment of psoriasis. The study found that

latently infected cells were reactivated and preferentially underwent apoptosis *in vitro* (Li et al., 2016). A subsequent study evaluated the findings of Li et al. and was not able to replicate the results: Acitretin was found to have only modest effects on HIV-1 reactivation and did not mediate the targeted killing of infected cells (Garcia-Vidal et al., 2017).

1.3 Aims and Hypotheses:

RIG-I and MDA5 are important sensors for viral infections and possibly involved in the detection of HIV-1 infection. Apart from its role as an innate immune sensor, RIG-I can possibly modulate T cell differentiation and functions. There is a gap in literature on how the specific activation of RIG-I affects the biology of primary human CD4 T cells. This is also relevant in the context of HIV-1 infection, in which RIG-I is degraded by an unknown mechanism involving HIV-1 protease.

1.3.1 Hypotheses:

1. The activation of the RIG-I signalling pathway triggers an antiviral response in CD4 T cells and modulates biological processes within these cells.

2. HIV-1 protease directly degrades RIG-I independently of cellular factors.
3. The loss of RIG-I and MDA5 enhances latent and productive HIV-1 infection in primary CD4 T cells and Jurkat CD4 T cell line.

1.3.2 Aims:

1. To study the effects of RIG-I pathway activation on cellular processes and T cell effector functions in primary human CD4 T cells.

2. The identification of the molecular mechanism responsible for the degradation of RIG-I during HIV-1 *de novo* infection.

3. The generation of primary CD4 T cell and Jurkat RIG-I, MDA5 and MAVS knockout cell lines. To study these cell lines in productive and latent HIV-1 infection.

2. Materials and Methods

2.1 Materials

2.1.1 Chemicals

All chemicals were of analytical grade or higher and supplied by Sigma-Aldrich (St. Louis, MO, USA).

2.1.2 Oligonucleotides

Oligonucleotides used in this study were synthesised by IDT (Newark, NJ, USA) and Sigma-Aldrich and are outlined in Table 2.1. Unless otherwise stated, the oligonucleotides were desalt-purified and received dry. Oligos were reconstituted using nuclease-free water at 100 µM stock concentration.

Table 2.1: Oligonucleotides used for cloning and sequencing.

Name	Sequence 5'-3'	Description
RIG-2CARD-HINDIII	TAAGCAAAGCTTATGACCACCGAGCAGC	RIG-I 2CARD cloning, adds HindIII restriction site to PCR product.
RIG-2CARD_Rev1	TGCTTAGGATCCTTTTTTAAGATGATGTTCACATATAAGCAGTG	RIG-I 2CARD cloning, adds BamHI restriction site to PCR product.
pEF-BOS Seq fwd	ATGCGATGGAGTTTCCCCAC	Primer for pEF-BOS Sanger sequencing, forward
pEF-BOS Seq rev	TACTCTCAAGGGTCCCAGGT	Primer for pEF-BOS Sanger sequencing, reverse
pET28a+ Seq fwd	AGCTTCCTTTCGGGCTTTGT	Primer for pET28a+ Sanger sequencing, forward

Name	Sequence 5'-3'	Description
pET28a+ Seq rev	CCCTTATGCGACTCCTGCAT	Primer for pET28a+ Sanger sequencing, reverse

2.1.3 Plasmids

All plasmids cloned for use in this study are listed in Table 2.2. Correct products were confirmed using restriction digestion and Sanger sequencing. All plasmids obtained from other sources are listed in Table 2.3.

Table 2.2: Plasmids cloned for use in this study.

Name	Template		Description
	Name	Source	
pRP-puro-RIG284 / pRP-puro-RIG-I-2CARD	pRP-puro-FL-hnRNPM Flag	Steven Wolter	RIG-I 2CARD mammalian expression plasmid, first 284 N-terminal amino acids of RIG-I, untagged, lentiviral construct.
pEF-BOS HIV1 PR WT	pEF-BOS RIG-I WT	Prof. Veit Hornung	HIV-1 PR WT mammalian expression plasmid, C-terminal FLAG- and HIS-tag. Tags can be proteolytically processed by HIV-1 PR WT via the included factor-Xa site.
pEF-BOS HIV1 PR D25A	pEF-BOS RIG-I WT	Prof. Veit Hornung	HIV-1 PR D25A mammalian expression plasmid, C-terminal FLAG- and HIS-tag.
pEF-BOS HIV1 PR T26A	pEF-BOS RIG-I WT	Prof. Veit Hornung	HIV-1 PR T26A mammalian expression plasmid, C-terminal FLAG- and HIS-tag.

Name	Template		Description
	Name	Source	
pEF-BOS HIV1 PR D29N	pEF-BOS RIG-I WT	Prof. Veit Hornung	HIV-1 PR D29N mammalian expression plasmid, C-terminal FLAG- and HIS-tag.
ΔpET28a+ RIG-I WT	pET-28a+	Novagen	RIG-I WT bacterial expression plasmid, C-terminal HIS-tag.
ΔpET28a+ MDA5 WT	pET-28a+	Novagen	MDA5 WT bacterial expression plasmid, C-terminal HIS-tag.
ΔpET28a+ HIV PR WT	pET-28a+	Novagen	HIV-1 PR WT bacterial expression plasmid, C-terminal HIS-tag.
ΔpET28a+ HIV PR D25A	pET-28a+	Novagen	HIV-1 PR D25A bacterial expression plasmid, C-terminal HIS-tag.
ΔpET28a+ HIV PR T26A	pET-28a+	Novagen	HIV-1 PR T26A bacterial expression plasmid, C-terminal HIS-tag.
ΔpET28a+ HIV PR D29N	pET-28a+	Novagen	HIV-1 PR D29N bacterial expression plasmid, C-terminal HIS-tag.

Table 2.3: Plasmids used in this thesis and obtained from other sources.

Name	Owner/Source	Description	Reference
pEF-BOS RIG-I WT	Prof. Veit Hornung/Steven Wolter	Human RIG-I mammalian expression plasmid, C-terminal FLAG- and HIS-tag.	

Name	Owner/Source	Description	Reference
pEF-BOS-hsMDA5-3xFlag-His10	Dr. Thomas Zillinger	Human MDA5 mammalian expression plasmid, C-terminal FLAG- and HIS-tag.	
pNL-4.3	Dr. Jenny Anderson	X4-tropic HIV1 (Env-eGFP-IRES-nef)	Yamamoto et al., 2009
pNL-4.3(AD8)	Dr. Jenny Anderson	R5-tropic HIV1 (Env-eGFP-IRES-nef)	Yamamoto et al., 2009
pIFN-β-Gluc	Prof. Veit Hornung/Dr. Ann Kristin de Regt	Reporter plasmid. Gaussia luciferase expression under the control of the IFNβ promoter.	
pEF1-α-Fluc	Dr. Thomas Zillinger/Dr. Ann Kristin de Regt	Reporter plasmid. Firefly luciferase expression under the control of the EF1α promoter.	
pRSV-Rev	Didier Trono	3rd generation lentiviral packaging plasmid. Contains Rev.	Dull et al., 1998
pMD2.G	Didier Trono	VSV-G envelope expressing plasmid.	
pMDLg/pRRE	Didier Trono	3rd generation lentiviral packaging plasmid. Contains Gag and Pol.	Dull et al., 1998

2.1.4 Antibodies

All antibodies used in this study for immunoblotting and flow cytometry were supplied by BD (Franklin Lakes, NJ, USA), Cell Signaling Technologies (Danvers, MA, USA) or GeneTex (Irvine, CA, USA) and are listed in
Table 2.4.

Table 2.4: Antibodies used in this thesis.

Antibody	Supplier	Clone	Fluorophore	Dilution
CCR5	BD	2D7/CCR5	PE	-
CXCR4	BD	12G5	APC	-
CD4	BD	RPA-T4	FITC	-
RIG-I	Cell Signaling	D14G6	-	1:2,000
MDA5	Cell Signaling	D74E4	-	1:2,000
MAVS	Cell Signaling	-	-	1:2,000
IRF3	Cell Signaling	D6I4C	-	1:2,000
Anti-rabbit IgG, HRP-linked	Cell Signaling	-	-	1:2,000
beta Actin	GeneTex	-	-	1:10,000

2.2 Methods

2.2.1 General methods

2.2.1.1 Nucleic Acid Quantification

DNA and RNA were quantified using NanoDrop™ 2000 Spectrophotometer (Thermo Fisher Scientific, Waltham, MA USA) at wavelengths of 260/280 nm. Appropriate buffers were used to calibrate the instrument.

2.2.1.2 Cloning

PCR Amplification. Genes or gene fragments were amplified using 0.5 U of Phusion™ High-Fidelity DNA Polymerase and 0.2 mM final concentration (f.c.) dNTPs (both NEB, Ipswich, MA USA) in combination with forward and reverse primers at 0.4 µM f.c.. Phusion Buffer HF (5x) was used at 1x f.c. and volumes were adjusted to 25 µL with PCR-grade water. PCR cycling conditions as recommended by the manufacturer: Initial denaturation at 98 °C for 30 seconds, 30 cycles of 98 °C for 10 seconds, 45-72 °C for 30 seconds and 72 °C for 30 seconds per kilobase (kb) of template, and a final extension step at 72 °C for 5 minutes.

Restriction Digest. Restriction mixes included 20 Units (U) of each restriction enzyme (NEB), the appropriate buffer at 1x concentration and 1-3 µg of DNA. Reactions were incubated for 15-60 minutes at 37 °C or as indicated by the manufacturer.

Gel Electrophoresis and Purification. PCR reactions and restriction digests were mixed with DNA loading dye (NEB), loaded onto a 0.7-1.5 % agarose gel containing GelRed™ (Biotium, Fermont, CA USA) and resolved at 80-120 Volt (V) for 30-45 minutes. 1 kb Plus DNA Ladder (Thermo Fisher Scientific) was run on the same gel as size reference. Correctly sized bands were excised from the gel and purified using the NucleoSpin Gel and PCR Clean-up Kit (Macherey-Nagel, Dueren, Germany) following the manufacturers instructions.

Ligation. DNA insert ligation into vector DNA was done with 5U T4 DNA Ligase (Thermo Fisher Scientific). Up to 150 ng total DNA was ligated per reaction in a total volume of 20 µL of T4 DNA Ligase Buffer (1x f.c.). Molar ratios were varied between 1:3 to 1:5 (backbone to insert ratio) and the reactions were incubated at room temperature (RT) for 1 hour (sticky ends) or at 8 °C over night (blunt-end).

Transformation. Ligated products were transferred to tubes containing 25-50 µL chemically competent *Escherichia coli (E. coli)* DH5α or Stbl3 (both Thermo Fisher Scientific) and incubated on ice for 10-30 minutes. A heat shock was performed in a heat block at 42 °C for 45-60 seconds and tubes were returned to ice for 1-2 minutes. 500 µL of super optimal broth with catabolite repression (SOC) media was added to the tubes and bacteria were incubated at 37 °C and 180 rpm for 45 minutes. Bacteria were pelleted at 3,000 relative centrifugal force (rcf), 400 µL supernatant (SN) were discarded and cells were resuspended in the residual media. 5-50 µL cell suspension was plated on agar plates supplemented with Ampicillin (100 µg/mL) or Kanamycin (30 µg/mL) depending on the antibiotic resistance gene of the vector. Plates were incubated at 37 °C overnight or at RT over the weekend.

2.2.1.3 Plasmid preparation and confirmation of vectors

Bacterial clones were scratched from selective agar plates and used to inoculate 3 mL selective Luria-Bertani broth (LB) media (Media Preparation Unit, Department of Microbiology and Immunology, University of Melbourne Australia). Tubes were incubated for 6-9 hours at 37 °C and 180 rpm. Mini-preparation of plasmid DNA was performed with 2 mL of the bacterial culture using the NucleoSpin Plasmid Easypure Kit (Macherey-Nagel). For Midi-preparation of plasmid DNA 100 mL of selective LB media was inoculated with 1 mL of the 3 mL culture and grown over night at 37 °C. Column-based NucleoBond Xtra Midi Kit (Macherey-Nagel) was used, following the manufacturer's instructions.

Plasmids from Mini- and Midi-preparations were screened for correct plasmid assembly by restriction digestion and Sanger sequencing.

2.2.1.4 SDS-PAGE and western blot

Sample preparation. Cells were washed off the tissue culture plastic with phosphate buffered saline (PBS) (adherent cells) or harvested by centrifugation (suspension cells). Cells were resuspended in ice-cold radioimmunoprecipitation assay (RIPA) buffer (Scientifix, Clayton, Australia) complemented with protease inhibitor cocktail (cOmplete^{TM}, Mini, EDTA-free Protease Inhibitor Cocktail, Roche, Basel, Switzerland) at 2x concentration and incubated on ice for 30 minutes to complete cell lysis. The lysate was cleared by centrifugation at 12,000 rcf for 10 minutes in a chilled centrifuge and transferred to a new tube. The protein concentration was quantified using the Pierce BCA Protein Assay Kit (Thermo Fisher Scientific) following the manufacturers instructions.

SDS-PAGE. Sodium dodecyl sulphate (SDS)-polyacrylamide gel electrophoresis (PAGE) gels were prepared using the Bio-Rad (Hercules, CA, USA) gel casting system. The separation gel was prepared with 8-16 % Acrylamide (40 % Acrylamide/bis-Acrylamide solution 29:1, Bio-Rad), 0.375 M Tris-HCl pH 8.8, 0.1 % (w/v) SDS, 0.25 % (w/v) APS, 0.1 % TEMED in deionised water. The stacking gel was prepared with 4-10 % Acrylamide, 0.125 M Tris-HCl pH 6.8, 0.1 % (w/v) SDS, 0.25 % (w/v) APS, 0.1 % TEMED in deionised water. Equal amounts of protein (5-80 µg per sample) were prepared with SBL loading dye (4x: 250 mM Tris-HCl pH 6.8, 8 % SDS, 40 % Glycerol, 20 % 2-Mercaptoethanol, 0.04 % Bromophenol blue in deionised water) and incubated at 95 °C for five minutes to denature proteins. Samples were cooled on ice for 2 minutes and loaded along with the Precision Plus Protein Dual Colour standard (Bio-Rad) onto the cast SDS gel. The gels were run at constant 80 V for 20 minutes followed by constant 120-140 V for 45-60 minutes with SDS-PAGE running buffer (10x: 250 mM Tris-HCl, 1.92 M glycine, 1 % SDS in deionised water).

Transfer of proteins and western blot. Proteins were transferred from the SDS gel to a 0.45 µm nitrocellulose membrane (Bio-Rad). SDS gel, membrane and sponges were equilibrated for 2 minutes in transfer buffer (25 mM Tris-HCl, 0.192 M glycine, 20 % Methanol). The transfer buffer was pre-cooled and was

kept cool during the transfer with ice packs. The standard setting for the protein transfer was a constant 400 mA for 45 minutes. The membrane was washed with deionised water, stained with Ponceau S solution (Edwards Group, Narellan, Australia) for 2 minutes and washed for 2 minutes in deionised water to control the even transfer of proteins. Membranes were blocked using 5 % BSA in PBST (0.1 % Tween-20 in PBS) for 30 minutes at RT, followed by one five-minute wash with PBST. The primary antibodies were diluted 1:2,000 (rabbit-RIG-I, rabbit-MDA5, rabbit-MAVS, rabbit-TBK1, rabbit-IRF3) or 1:10,000 (beta Actin) in 5 % BSA in PBST and incubated together with the membrane for 1 hour at RT or over night at 4 °C. The membrane was washed three times for five minutes in PBST. The secondary antibody (anti-rabbit-HRP) was diluted 1:10,000 in 5 % BSA in PBST and incubated together with the membrane for 1 hour at RT. The membrane was washed three times for three minutes with PBST, incubated with 1 mL of the SuperSignal™ West Pico Chemiluminescence substrate (Thermo Fisher Scientific) for two minutes and imaged using the ChemiDoc Imaging System (BioRad). Stripping buffer (0.25 M glycine, 1 % w/v SDS, pH 2.0) was used to remove primary and secondary antibodies to allow the re-use of the membrane and the detection of more than one protein within one sample. Membranes were blocked again with BSA and the protocol described above was repeated.

2.2.1.5 Cell Culture

Adherent cell lines and maintenance. HEK293T (ATCC, Manassas, VA USA), HEK-Blue™ IFN-a/b (InvivoGen, San Diego, CA USA), Flp-In™ 293 T-REx RM (based on Flp-In™ 293 T-Rex - Thermo Fisher Scientific, genetically modified by Dr. Ann Kristin de Regt to achieve a double knockout of RIG-I and MDA5), and TZM-bl cells (NIH AIDS Reagent Program, Division of AIDS, NIAID, Dr. John C. Kappes, Xiaoyun Wu) were maintained in Dulbelco's Modified Eagle's medium (DMEM) (Media Preparation Unit), supplemented with GlutaMax™ (1x f.c.) and 10 % (v/v) foetal bovine serum (FBS) (both Thermo Fisher Scientific) and cultured at 37 °C in 5 % (v/v) CO_2.

Suspension cell lines and maintenance. Jurkat cells (ATCC) were maintained in Roswell Park Memorial Institute (RPMI) 1640 medium (Media Preparation Unit), supplemented with GlutaMax™ (1x f.c.) and 10 % (v/v) FBS (both Thermo Fisher Scientific) and cultured at 37 °C in 5 % (v/v) CO_2.

Primary CD4 T cells. Cells were maintained in RPMI 1640 medium (Thermo Fisher Scientific) supplemented with 5 % (v/v) of human AB serum (Sigma Aldrich) and 100 U/mL recombinant hIL-2 (Miltenyi Biotech, Bergisch-Gladbach, Germany) if not stated otherwise. Cells were incubated with Dynabeads Human T-Activator CD3/CD28 (Thermo Fisher Scientific) to induce activation and proliferation. 1E5 cells were plated together with 0.5E5 CD3/CD28 beads per 96-round-bottom well in 200 µL media. Cells were cultured at 37 °C in 5 % (v/v) CO_2. After three days, beads were removed and cells were seeded at a concentration of 1E6 cells/mL into 12- or 6-well plates or T25 or T75 tissue culture flasks. After 7-10 days, CD3/CD28 beads (0.1-0.5 beads/cell) were added to the culture vessel if prolonged activation and expansion was desired.

2.2.1.6 PBMC isolation and enrichment of CD14 and CD4 T cells

Peripheral blood mononuclear cells (PBMCs) were isolated from buffy coats. The blood was mixed with an equal volume of NaCl (0.9 %) or PBS and layered over 15 mL Ficoll-Paque (Cytiva, NSW, Australia) in a 50 mL tube. Gradient was established by centrifugation at 800 rcf for 20 minutes (acceleration 1, break 1). The intermediate layer containing the PBMCs was transferred to a new 50 mL tube. Cells were washed twice with 40 mL natrium chloride (NaCl) (0.9 %) or PBS and centrifuged at 200 rcf for 15 minutes to reduce the amount of platelets within the cell fraction. Erythrocytes were removed by incubation with 5 mL red blood cell lysis buffer (155 mM ammonium chloride, 10 mM potassium bicarbonate, 0.1 mM EDTA) and cells were washed with 45 mL NaCl (0.9 %) or PBS and centrifuged at 200 rcf for 15 minutes.

CD14 positive cells were positively selected using CD14 MicroBeads (human) and LS columns (both Miltenyi Biotec) according to the manufacturer’s

instructions. CD4 T cells were enriched from PBMCs using the CD4 T cell isolation kit and LS columns (both Miltenyi Biotec) following the manufacturer's instructions. If both cell types were prepared from one sample, first, CD14 cells were positively enriched and second, the leftover cells were used for negative selection of CD4 T cells.

2.2.1.7 DNA and RNA Transfection

HEK293T and FLP-IN™ 293 T-REX RM cell transfection. Cells were transfected with nucleic acids using Lipofectamine 2000 reagent (Thermo Fisher Scientific) following the manufacturer's protocol if not otherwise stated. In brief, cells were seeded 6-20 hours prior transfection to be 80-90 % confluent by the time of transfection. Nucleic acids were complexed with Lipofectamine 2000 in Opti-MEM™ Reduced Serum Medium (Thermo Fisher Scientific) free of Penicillin/Streptomycin and FBS with a ratio of 1 to 3-4 (Nucleic acids [µg] to Lipofectamine 2000 [µL]).

CD4 T cell and PBMC transfection. Cells were transfected with synthetic RNA using MACSfectin (Miltenyi Biotec), HiPerFect (Qiagen, Hilden, Germany), Lipofectamine LTX (Thermo Fisher Scientific), Lipofectamine 2000 (Thermo Fisher Scientific) or ScreenFectA (ScreenFect, Eggenstein-Leopoldshafen, Germany) following the manufacturer's protocol.

2.2.1.8 Flow Cytometry

Cells were washed and resuspended in FACS buffer (2 mM EDTA and 1 % BSA (v/v) in PBS). Live/Dead™ Fixable Near-IR Dead Cell Stain Kit (Thermo Fisher Scientific) was used to label apoptotic and dead cells if required. The dye was diluted 1:800 in FACS buffer and 100 µL staining solution were used per 1E6 cells. After 15 minutes of incubation cells were washed twice in FACS buffer and proceeded to extracellular antibody staining. Extracellular antibodies were diluted in FACS buffer and added to cells, followed by an incubation period on ice for 45 minutes. Unbound antibodies were removed with three washes with FACS buffer. Cells were fixed using 4 % PFA solution for 20 minutes and resuspended in 100-

200 µL FACS buffer. Samples were used immediately or stored up to 24 hours before acquisition.

Sample data was acquired using the Fortessa™ flow cytometer (BD) and analysed using the FACSDiva software (BD).

2.2.1.9 Statistical Analysis

Calculations of means and standard deviations (SD) were done in Microsoft Excel or Graphpad Prism. Statistical tests were done in Graphpad Prism and are specified in the figure legend.

2.2.2 Methods Chapter 3 – Aim 1

2.2.2.1 Sendai Virus infection of CD4 T cells and PBMCs

Different batches of Sendai virus (SeV) strain Cantell (Charles River Laboratories, Wilmington, MA, USA) were titrated and standardised to elicit a type-I IFN response of approximately 1000 U/mL in 4E5 CD4 T cells after 16 hours (typically 100-200 HAU/mL SeV). Insoluble components were removed from the allantoic fluid containing the virus by centrifugation at 200 rcf for two minutes and transferring the clear supernatant to a fresh microtube. Undiluted virus stock solutions were stored at -20 °C for short-term and at -80 °C for long-term storage.

CD4 T cells and PBMCs were infected with varying doses of SeV as indicated in corresponding figure legends. Cells were cultivated as previously described. The SeV stock solution was diluted prior to use in complete media (typically 1:10-1:100) and added to cells for 16 hours or as indicated. Media was not replaced during the incubation period.

2.2.2.2 Exosome stimulation of CD4 T cells

Exosomes were obtained from AG Coch (Dr. Juliane Daßler-Plenker and Bastian Putschli, The University Hospital Bonn, Germany) and were generated in primary human melanoma cells (D05mel) that were left untreated (unloaded exosomes)

or transfected with in vitro transcript 4 (IVT4) (IVT4-loaded exosomes). Exosomes were validated by Dr. Daßler-Plenker (unpublished data): While there is no experimental evidence that IVT4 is being loaded into exosomes, indirect proof exists. It was shown that the type-I IFN response to IVT4-loaded exosomes is 3pRNA- and RIG-I-dependent: RNA isolated from IVT4-loaded exosomes induced type-I IFN in RIG-I expressing recipient cells, but not after the removal of 3p with alkaline phosphatase. In addition, IVT4-loaded exosomes or RNA isolated from them failed to induce a type-I IFN response in RIG-I knockout cell lines. The potency of IVT4-loaded exosomes to induce a type-I IFN response in recipient cells was independent of RIG-I signalling in exosome producing cells: IVT4-loaded exosomes that derived from RIG-I wildtype or RIG-I knockout cells showed similar capacity of type-I IFN induction in recipient cells.

Primary CD4 T cells were seeded in 96-well plates (4E5 cells per well) and treated with 0, 2 or 10 µg exosome preparations for 18 hours at 37 °C and 5 % CO_2. Type-I IFN levels in cell-free supernatants were measured using the HEK-blue™ IFN-α/β reporter assay.

2.2.2.3 Electroporation of CD4 T cells

Nucleic acids or CRISPR/Cas9 complexes were delivered to Jurkat cell line or primary CD4 T cells using the Neon® Transfection System in combination with the 10 µL Neon® tips (Thermo Fisher Scientific). 5E5 cells were prepared per reaction in Buffer T as instructed by the manufacturer. The machine was set up to run with an optimised protocol (3 pulses of 10 ms width at 1600 V).

2.2.2.4 miRNA stimulation of CD4 T cells

RNA oligos 3p-antisense (5´-pppGACGCUGACCCUGAAGUUCAUCUU-3´) and GFP-Chol (CUGCGACUGGGACUUCAAGUAGAA-C6-Cholesterol) were ordered from IDT. The oligos were used at equimolar concentrations (120 µM) and denatured at 75 °C for 5 minutes and annealed by gradual reduction of the temperature (1 °C/min) to 18 °C. 4E5 CD4 T cells were plated per 96-well and treated with 10, 20 or 30 µM f.c. of the annealed oligo for 16 hours. Type-I IFN

levels in the supernatant were measured using a cell-based IFN reporter assay (2.2.2.5).

2.2.2.5 Type-I IFN Reporter Assay

HEK-blue™ IFN-α/β cells were used to measure type-I IFN levels in tissue culture supernatants according to the manufacturer's instructions. 5E4 cell were seeded in a 96-well culture plate in 180 µL medium. 20 µL cell free supernatant (sample) was added along to an IFNα standard dilution (15-2000 U IFN/mL) in duplicate or triplicate. Cells were incubated for 20-24 hours and the cell free supernatant was transferred to a clear 96-well plate. 40 µL para-Nitrophenylphosphate (pNPP) solution (1 mg/mL pNPP in 100 mM TRIS-HCl, 100 mM NaCl, 5 mM $MgCl_2$, pH 9.5) was added per well and plates were incubated for 15-60 mins at RT. The absorbance was measured at a wavelength of 405 nm using the FLUOstar® Omega microplate reader (BMG Labtech, Ortenberg, Germany).

2.2.2.6 IP-10 ELISA

Cells were stimulated for 16 hours and IP-10 levels in the cell-free supernatant were determined using the human IP-10 ELISA Kit (BD). Only minor changes were made to the manufacturer's protocol: final volumes and amounts of antibodies were halved. In brief, plate coating was performed over night at 4 °C using Coating Buffer (100 mM sodium bicarbonate, 33.6 mM sodium carbonate in PBS, pH 9.5). Blocking of the plate and sample dilution was carried out in Assay Buffer (10 % (v/v) FBS in PBS). Samples were added to the coated plate along with an IP-10 protein standard and incubated for 2 hours at RT to allow binding. Plates were washed five times with Wash Buffer (Tween-20 0.05 % (v/v) in PBS) and the detection antibody and horseradish peroxidase (HRP)-conjugate were added simultaneously for 1 hour at RT with light shaking in the dark. Plates were washed seven times with Wash Buffer. Substrate solution A and B were added to the plate and the reaction was stopped with sulfuric acid once the standard samples reached their final optical density (OD).

2.2.2.7 Real-Time Cell Metabolic Analysis

CD4 T cell metabolism was monitored during CD3/CD28 activation using a Seahorse XFe96 Analyser (Agilent, CA, USA). Primary CD4 T cells were prepared as described previously and treated with SeV or left untreated for 2 to 24 hours before activation. Cells were washed once with PBS and immobilised with Corning® Cell-Tak Cell Tissue Adhesive (Sigma-Aldrich) in a Seahorse 96-well plate (Agilent) following the manufacturer's instructions. The T cell activation assay was done following the manufacturer's protocol (Real-time Detection of T Cell Activation Using an Agilent Seahorse XFp Analyser). Briefly summarised as follows: Adhered cells in assay media (Seahorse RPMI 1640 medium without bicarbonate or phenol red (Agilent), 2 mM L-Glutamine (Corning, NY, USA), 1 mM Sodium Pyruvate (Corning), 10 mM Glucose (Corning), pH 7.4) were incubated at 37 °C / 5 % CO_2 for one hour. CD3/CD28 Dynabeads^{TM} were loaded into Port A of a hydrated XFp catridge (4 beads per CD4 T cell) just prior to the start of XFP calibration. The instruments protocol was set up as follows: Calibration, equilibration, basal measurement cycles (3 cycles, mix: 3 minutes, wait: 0 minutes, measure: 5 minutes), injection (Port A), measurement after injection (15 cycles, mix: 3 minutes, wait: 0 minutes, measure: 5 minutes). Cells derived from three different donors were used and each condition was monitored in triplicates.

2.2.2.8 Proliferation Assays

Metabolic Assay. 5E4 cells were seeded per 96-well in 100 µL media and incubated for 48 hours. Cell proliferation was monitored using CellTiter 96® AQ_{ueous} One Solution Cell Proliferation Assay (Promega, Madison, WI, USA) following the manufacturer's instructions.

Manual cell counting. CD4 T cells were activated with CD3/CD38 beads for 72 hours as described previously. The beads were removed prior to stimulation and 2E5 cells were seeded per 96-well in 100 µL media. Wells were topped up with 100 µL media containing IFNα2 (2000 U/mL, Miltenyi Biotec) or SeV (20, 100, 200 or 400 HAU/mL). Cells were incubated for 48 hours at 37 °C and 5 % CO_2.

Cell suspensions were diluted with 4 % Trypan blue solution (Sigma Aldrich) as required and counted using a Neubauer Chamber.

2.2.2.9 Next generation RNA Sequencing

RNA Extraction. Cells were harvested by centrifugation and homogenised using TRIzol™ Reagent (Thermo Fisher Scientific) following the manufacturer's protocol. The dried RNA pellet was resuspended in 10-15 µL nuclease-free water and stored at -80 °C. Purity and concentration of samples was estimated using Nanodrop 2000 Spectrophotometer as described previously.

Sample and library preparation. CD4 T cells were enriched as previously described and activated with CD3/CD28 beads or left untreated for 72 hours. Cells (>1E6 per sample) were infected with Sendai virus (100-200 Hemagglutination Units (HAU)) or left untreated for 7 hours. Total RNA was extracted using Trizol™ reagent as previously described. Library preparation and sequencing was done by the Next Generation Sequencing Facility (Life&Brain Center, University of Bonn, Germany). The library was prepared using the QuantSeq 3' mRNA-Seq Library prep Kit FWD for Illumina (Lexogen, Vienna, Austria) and the sequencing data was acquired using the HiSeq 2500 V4 platform (Illumina, San Diego, CA, USA).

Bioinformatic analysis. RNA sequencing data was analysed using the Partek® Flow software package (Partek, St. Louis, MO, USA). The analysis pipeline included filtering for contaminants (Bowtie 2 v2.2.5), adapter trimming, base trimming, sequence alignment (STAR aligner v2.6.1d, hg38), quantification and annotation (Partek E/M model, hg38, RefSeq Transcripts 93 – 2020-02-03), normalisation (TMM), differential gene expression analysis (ANOVA) and filtering of low expressed genes. Pre- and post-alignment QA/QC, PCA plots and hierarchical clustering were used to monitor data quality.

2.2.2.10 IFNγ enrichment and release assay

Fast DCs and CMV pp65 peptide loading. CD14 and CD4 positive cells were prepared from CMV positive blood donors as previously described. 2E6 CD14 positive cells were plated per 12-well in 2 mL of fast DC media A (RPMI-1640 (Gibco), 5 % human AB serum (Sigma Aldrich), Penicillin/Streptomycin (100 U/mL, Life Technologies), GM-CSF (1000 U/mL, Miltenyi Biotec), IL-4 (500 U/mL, Miltenyi Biotec)). PepTivator® CMV pp65 (15 pmol/well, Miltenyi Biotec) was added to 50 % of the wells. Cells were incubated at 37 °C and 5 % CO_2 for 24 hours. 1 mL of supernatant was aspirated, discarded and replaced with fast DC media B (RPMI-1640, 5 % human AB serum, Penicillin/Streptomycin (100 U/mL), GM-CSF (1000 U/mL), IL-4 (500 U/mL), IL-6 (2000 U/mL, Miltenyi Biotec), TNFα (20 ng/mL, Miltenyi Biotec), PGE-2 (2 µg/mL, Miltenyi Biotec), IL-1β (20 ng/mL, Miltenyi Biotec)). Cells were incubated for another 24-48 hours. The supernatant was removed and cells were washed off the tissue culture plastic. One half of the cells was stored at -80 °C in cryomedia (RPMI-1640, 10 % human AB serum, 10 % DMSO). The other half of the cells was plated in 500 µL of co-culture media (RPMI-1640, Penicillin/Streptomycin (100 U/mL), 10 % human AB serum) in a 12-well plastic plate.

Activation, enrichment and expansion of CMV pp65-specific CD4 T cells. To activate CMV pp65-specific CD4 T cells, the appropriate amount (T cell to DC ratio 5:1) of CD4 T cells was resuspended in 500 µL of co-culture media (see above) and added to the CMV pp65-loaded fast DCs in 12-well plates. Cells were incubated for 1 hour, mixed by cautious pipetting and incubated for another 3-4 hours at 37 °C and 5 % CO_2. Activated CD4 T cells were positively selected using the IFNγ Secretion Assay - Cell Enrichment and Detection Kit (Miltenyi Biotec) following the manufacturer's instructions. Enriched cells were expanded in T cell media (RPMI-1640, 5 % human AB serum, Penicillin/streptomycin (100 U/mL), IL-2 (100 U/mL)) for six to seven days without further activation. Media was replaced when required.

Treatment and re-activation of CMV pp65-specific CD4 T cells. CMV pp65-specific CD4 T cells were treated with SeV, type-I IFN (1000 U/mL, Miltenyi Biotec) or left untreated for 16 hours before re-activation. CMV pp65-loaded or unloaded DCs were thawed on the day of T cell re-activation, plated in 12-well plates and allowed to adhere. CD4 T cells were washed in media to remove virus or type-I IFN and added to the DCs (T cell to DC ratio 5:1) for 4-6 hours. The IFNγ Secretion Assay - Cell Enrichment and Detection Kit (Miltenyi Biotec) was used to label IFNγ-secreting cells and the read-out was done using flow cytometry.

2.2.3 Methods Chapter 4- Aim 2

2.2.3.1 Co-expression of RLRs and HIV-1 PRs

HEK293T cells were seeded in 12-well plates and transfected at 80-90 % confluency with expression plasmids for RIG-I or MDA5 (pEF-BOS RIG-I WT, pEF-BOS-hsMDA5-3xFlag-His10) and HIV-1 PR (ΔpET28a+ HIV PR WT / D25A / T26A or D29N) as described previously. Darunavir (NIH AIDS Reagent Program) was added prior to transfection and was maintained at 5 µM (f.c.) as indicated in the corresponding figure legend. Cells were incubated for at least 20 hours at 37 °C / 5 % CO_2 before harvest. RIG-I and MDA5 protein levels were evaluated via western blot as described previously (40 µg total protein was loaded per lane).

2.2.3.2 Recombinant protein expression in bacteria

E.coli BL21 were transformed with plasmids coding for RIG-I, MDA5, or different HIV-1 PRs (ΔpET28a+ RIG-I WT / MDA5 WT / HIV1 PR WT or HIV1 PR D25A) as described before. Cells were grown in Luria-Bertani broth (LB) medium supplemented with kanamycin (f.c. 30 ng/mL) and D-Glucose (f.c. 0.5 % w/v). Expression of recombinant proteins was induced with isopropyl β-d-1-thiogalactopyranoside (IPTG, f.c. 0.1 mM) once the cell suspensions reached 0.4-0.6 OD_{600}. Cells were harvested after 3 hours by centrifugation and were stored at -20 °C or used immediately.

Protein purification from inclusion bodies. Cell pellets were resuspended in 10 mL ice-cold Buffer A (50 mM TrisHCl, pH 8.0, 50 mM NaCl, 0.1 mM EDTA, NP-40 0.2 % (v/v), cOmplete^{TM} Protease Inhibitor (Roche)). Cell lysis was induced by freeze/thaw cycles on dry ice or at RT and completed by sonication on ice. Lysates were centrifuged and the pellets were washed twice with 7 mL ice-cold Buffer A + TritonX-100 (1% (v/v)). Residual inclusion bodies were resuspended in Buffer B (50 mM Tis-HCl, pH 8.0, 50 mM NaCl, 10 mM 2-Mercaptoethanol, 8 M Urea, 10 mM imidazole) at RT and gentle shaking. Resuspended recombinant proteins were passed through 0.45 µm pore-size filters, added to nickel charged affinity resin (Ni-NTA Agarose, Qiagen) and incubated with gentle shacking at 4 °C for one hour. Recombinant proteins were washed and re-folded on the column by gradual reduction of urea (Buffer B with 8 M to 0 M urea). His-tagged proteins were eluted with 3 mL of Buffer C (50 mM Tis-HCl, pH 7.7, 50 mM NaCl, 0.1 mM EDTA, 0.5 M imidazole). Amicon® Pro filters (Merck Millipore, Darmstadt, Germany) with cut-offs of 3 or 50 kDa were used to exchange Buffer C to Buffer D (50 mM Tris-HCl, pH 7.0, 50 mM NaCl, 1 mM 2-Mercaptoethanol, 10 % (v/v) glycerol). Protein expression and purification was followed by SDS-PAGE and Coomassie staining or western blot. Aliquots of recombinant HIV-1 PR were stored at -20 °C for short-term storage or at -80 °C for long-term storage.

2.2.3.3 Small scale recombinant protein expression in mammalian cells

HEK293 T cells were transfected with expression plasmids for RIG-I or MDA5 (pEF-BOS RIG-I WT, pEF-BOS-hsMDA5-3xFlag-His10) as described previously. Cells were harvested two days after transfection (six 12-wells per protein of interest). The cell pellet was washed with PBS and resuspended in ice-cold Lysis Buffer (20 mM TRIS-HCl (pH 7.2), 150 mM NaCl, 0.5 % NP40, 1 mM Dithiothreitol (DTT), cOmpleteTM Protease Inhibitor (Roche)). Recombinant proteins were enriched with anti-Flag M2 affinity gel (Sigma Aldrich) following the manufacturer's instructions. Recombinant proteins were eluted from the M2 affinity gel with 100 µL Elution Buffer (20 mM Tris-HCl (pH 7.2, 4 °C), 150 mM NaCl, 1 mM DTT, cOmplete Protease Inhibitor (Roche), 0.15 mg/mL Flag-Peptide

(Sigma-Aldrich)). Recombinant proteins were stored at 4 °C for up to 3 days or used immediately.

2.2.3.4 HIV-1 Protease Activity Assay

The activity of recombinant HIV-1 protease was validated using the HIV-1 Protease Activity Assay Kit Fluorometric (abcam, Cambridge, MA, USA) following the manufacturer's instructions. The assay is based on a synthetic peptide, which acts as a substrate for HIV-1 PR. Cleavage of the substrate releases a fluorophore which can be quantified using a fluorescence reader.

The HIV-1 PR activity was calculated as:

$$HIV\text{-}1\ PR\ Activity\ (nmol/min\ /mg) = \left(\frac{B}{\Delta T * M}\right)$$

Where B is the amount of product (nmol), ΔT is the reaction time T2-T1 (min) in the linear phase of the reaction, M is the amount of HIV-1 protease per well (mg).

2.2.3.5 HIV-1 Protease degradation Assays

Whole-cell-based assay. RIG-I or MDA5 were co-expressed with HIV-PR in HEK293T cells for 20 hours. Cells were harvested, lysed and samples analysed by western blot as described previously.

Whole-cell lysate-based assay. RIG-I or MDA5 were expressed in HEK293T cells as described previously. Cells were harvested by centrifugation and washed twice with PBS. Cells were lysed in ice-cold Lysis Buffer (50 mM MES (2-(N-morpholino)ethanesulfonic acid), 300 mM NaCl, 50 mM NaH2PO4, 1 mM DTT, protease inhibitor cocktail (2x f.c., Roche) in deionised water, pH adjusted to 6.85 with NaOH) on ice for 20 minutes. Samples were frozen and thawed once to complete cell lysis when necessary. Lysates were cleared by centrifugation at 12,000 rcf for 10 minutes in a chilled centrifuge and transferred to a new tube. 10 µL RIG-I- or MDA5-containing whole-cell lysate (60-70 µg of total protein) and 1 µL of recombinant HIV-1 PR were used per reaction. Optional: 1 µL IVT4 (generously provided by Dr. Thomas Zillinger) or polyinosinic polycytidylic acid

(poly(I:C), Sigma Aldrich) at 1 µg/µL or 1 µL Darunavir (5 µM f.c.) were added to samples and adjusted to a final volume of 12 µL with Lysis Buffer. Samples were incubated at 37 °C for 30-90 minutes. Degradation was monitored using western blot analysis (5 µL 4xSBL was added per reaction, heated to 95 °C for 3 minutes, chilled on ice and loaded onto an SDS-PAGE as described previously).

Purified protein-based *in vitro* assay. Recombinant RIG-I or MDA5 proteins (FLAG-tag purified) were used in combination with recombinant HIV-1 PR (HIS-tag purified). Reaction mixes included 3-4 µL recombinant RIG-I or MDA5, 0.5 µL recombinant HIV-1 PR and optional 1 µL IVT4 or poly(I:C) at 1 µg/µL or 1 µL Darunavir (DV, 5 µM f.c.) and were adjusted to a final volume of 12 µL with Reaction Buffer (20 mM TRIS-HCl, 150 mM NaCl, 1 mM DTT, pH 7.2, 4 °C). Samples were incubated at 37 °C for two hours using Eppendorf's flexlid Mastercycler nexus (Eppendorf, Hamburg, Germany). Of note, when heated to 37 °C the Reaction Buffer exceeds its buffer capacity and the pH value shifts to a slightly acidic pH of 6.72, which promotes the activity of HIV-1 PR (optimal pH range 4-6 (Ido et al., 1991)). Degradation was monitored using western blot analysis (5 µL 4xSBL was added per reaction, heated to 95 °C for 3 minutes, chilled on ice and loaded onto an SDS-PAGE as described previously).

2.2.3.6 Dual Luciferase Reporter Assay

Flp-In™ 293 T-REx RM cells were seeded in 96-well plates (3E4 cells/well in 100 µL media) on the day prior to transfection. Cells were co-transfected as described previously with pEF1-α-Fluc (5 ng), pIFN-β-Gluc (10 ng), pEF-BOS HIV1 PR (20 ng) and pEF-BOS RIG-I WT or pEF-BOS-hsMDA5-3xFlag-His10 (20 ng) and treated with Darunavir (5 µM f.c.) where indicated. After 8-10 hours, stimulatory RNAs IVT4 (100 ng) or poly(I:C) (100 ng) were delivered via a second transfection. Cells were incubated for 20 hours at 37 °C and 5 % CO_2. Supernatants were transferred to a white 96-well plate (Corning). An equal volume of coelenterazine solution (Cayman Chemical, Ann Arbor, MI, USA, 1 µg/mL in deionised water) was added to samples and *Gaussia* luciferase (GLuc) activity was measured immediately using Fluostar® Omega (BMG Labtech)

reader. Intracellular firefly luciferase (FLuc) expression was measured using the Britelite™ plus reporter gene assay system (PerkinElmer, Llantrisant, UK) following the manufacturer's instructions. GLuc is a surrogate for IFNβ promoter activation while FLuc is constitutively expressed and serves as a transfection control. Relative light units (RLUs) measured for GLuc were normalised to the corresponding RLUs measured for FLuc.

2.2.3 Methods chapter 5 – Aim 3

2.2.3.1 Generation of knock out cell lines

The CRISPR/Cas9 gene editing system

We chose a system that utilises recombinant CRISPR/Cas9 and synthetic tracrRNA and crRNAs over a plasmid-based system. Complexation of recombinant CRISPR/Cas9 with synthetic RNAs allows the quick adaptation of the system to new gene targets by exchanging the crRNA. In comparison to a plasmid-based system no free nucleic acids are introduced into the target cells, potentially reducing immunogenicity. This system has the advantage that a fully functional CRISPR/Cas9 complex is delivered to target cells, making plasmid-delivery to the nucleus und subsequent gene expression and CRISPR/Cas9 complex assembly in target cells unnecessary.

All reagents were obtained from IDT and sequences of the crRNAs are shown in Table 2.5. crRNA sequences were selected to target early exons within each target gene to increase the probability of a loss of function event. TracrRNA (f.c. 200 µM), crRNAs (f.c. 200 µM) and transfection enhancer (f.c. 100 µM) were resuspended in IDTE buffer and stored at -20 °C. The transfection enhancer was further diluted in IDTE buffer (f.c. 10.8 µM) on the day of use.

TracrRNA and crRNA were hybridised by heating equal amounts (1.1 µL each) in 2.8 µL IDTE buffer to 95 °C for 5 mins, followed by a 20 mins incubation period at RT. Reactions were stored at -20 °C or used immediately.

The ribonucleoprotein (RNP) complex was prepared fresh or on the day preceding the experiment in Buffer T from the Neon® Transfection Kit following the manufacturer's instructions.

Table 2.5: CRISPR/Cas9 gene targets and crRNA sequences.

Gene target	Sequence
DDX58 (RIG-I)	GGATTATATCCGGAAGACCC
IFIH1 (MDA5)	TTGGACTCGGGAATTCGTGG
MAVS	GTCCTGCTCCTGATGCCCGC or GTAGATACAACTGACCCTGT

Genetic manipulation of primary CD4 T cells and Jurkat cell lines

The RNP complex was delivered to primary CD4 T cells (activated for 72 h, beads removed) and Jurkat cell lines as described previously (2.2.2.3 Electroporation of CD4 T cells).

Generation of single cell or polyclonal cell lines

Cells manipulated in the previous step were manually counted and seeded into 384 well plates at densities of 1 or 5 cells per well. After 3 days, cells were monitored on a daily basis for 4-6 weeks and stimulated with Dynabeads Human T-Activator CD3/CD28 (Thermo Fisher Scientific). The amount of beads was adjusted to each individual well depending on the number of cells. Re-activation was repeated every 7 days until cells reached 50-80 % confluency. The media was replaced 1-2 times per week. Cells were transferred to plates with increasing well sizes (96-, 48-, 12-, 6-well plates). Once the 6-well format was reached one 6-well was used for western blot analysis and one 6-well was stored in liquid nitrogen (LN) per cell line. Cell lines that were identified as knockouts were thawed, expanded and stored in LN.

2.2.3.3 Preparation of HIV-1 stocks

HEK293T cells were transfected with X4- or R5-tropic HIV-1 coding plasmids that were complexed with FuGene® HD Transfection Reagent (Promega) according

to the manufacturer's instructions. The media was replaced on the day following the transfection. Supernatants were harvested two days after the transfection. Cell debris was removed by centrifugation and passing through 0.45 µm pore-size filters. Virus stocks were concentrated using the Lenti-X™ Concentrator (Takara Bio, Mountain View, CA, USA) following the manufacturer's instructions and stored in 30 µL aliquots at -80 °C. The median tissue culture infectious dose (TCID50) was estimated for each batch of virus using the TZM-bl reporter cell line.

2.2.3.4 TZM-bl Assay – TCID50s of HIV-1 stocks

2E4 TZM-bl cells were seeded in 100 µL per 96 flat-bottom well. Cells were incubated over night at 37 °C and 5 % CO_2. A 1:10 serial dilution of the viral stock (1:10-1:100,000,000) was performed in 96-wells (15 µL virus stock added to 135 µL DMEM) in triplicates. The media was removed from the TZB-bl cells (70 % confluent) and 100 µL of the diluted viral stocks were added per well. 100 µL DMEM was added to negative control wells. Cells were incubated at 37 °C and 5 % CO_2. One day after infection, virus containing supernatants were replaced with 100 µL fresh DMEM. Cells were incubated for another day before reading the assay.

The media was removed and replaced with 50 µL 1x Cell Culture Lysis Reagent (Promega) per well. The plates were incubated at RT for 10 minutes to complete cell lysis. Cell lysates were resuspended and 10 µL per sample were transferred per well of a white 96-well plate. 25 µL Luciferase Assay Buffer (Promega, E1501) were added per well using the auto-injector function of the FLUOstar® Omega microplate reader and read immediately. The TCID50 was done following the protocol published by Reed and Muench, 1938.

3. Aim 1: Activation of the RIG-I signalling pathway modulates CD4 T cell biology

3.1 Introduction

CD4 T cells are an essential part of the adaptive immune response against infections and are also involved in autoimmune dysregulation (reviewed by Raphael et al., 2020). Different viruses, including HIV-1, specifically target CD4 T cells (Agosto et al., 2018; Rahimi et al., 2014). The understanding of the effects of innate immune pathway activation in CD4 T cells and the effects on effector functions is currently incomplete. CD4 T cells express several innate immune receptors, but it is less clear if associated pathways are functional and how their activation affects CD4 T cell biology. Given that the activation of endosomal toll-like receptors (TLRs) can promote or diminish CD4 T cell differentiation and effector functions (Dominguez-Villar et al., 2015; Liu et al., 2017; Meås et al., 2020), it is feasible that these pathways are indeed active. In addition, RIG-I activation has been linked to reduced proliferation in the Jurkat cell line, and RIG-I knockout mice show an imbalance of CD4 T cell subtypes (Yang et al., 2017; L. Zhang et al., 2019). This chapter aims to understand the effects of RIG-I activation on the biology of primary human CD4 T cells.

We aimed to deliver stimulatory RNAs to the cytoplasm of CD4 T cells, a prerequisite to study the effect of RIG-I signalling pathway stimulation. Using cationic lipid-mediated transfection of CD4 T cells, we were unable to stimulate RIG-I, consistent with prior reports demonstrating that CD4 T cells were widely refractory towards transfection with Lipofectamine 2000 (Zhao et al., 2006). We therefore first investigated different methods to induce RIG-I signalling in CD4 T cells, which include exosome-mediated transport, live virus (Sendai virus (SeV)), electroporation and chemically engineered RNA, Figure 3.1.

Next, we assessed the gene transcript levels of known members of the RIG-I signalling pathway in resting and CD3/CD28 activated CD4 T cells and whether RIG-I activation affects the transcriptome of resting CD4 T cells. We found that important pathways involved in CD4 T cell activation were differentially expressed following RIG-I activation. We validated these findings using metabolic, proliferation and IFNγ-release assays.

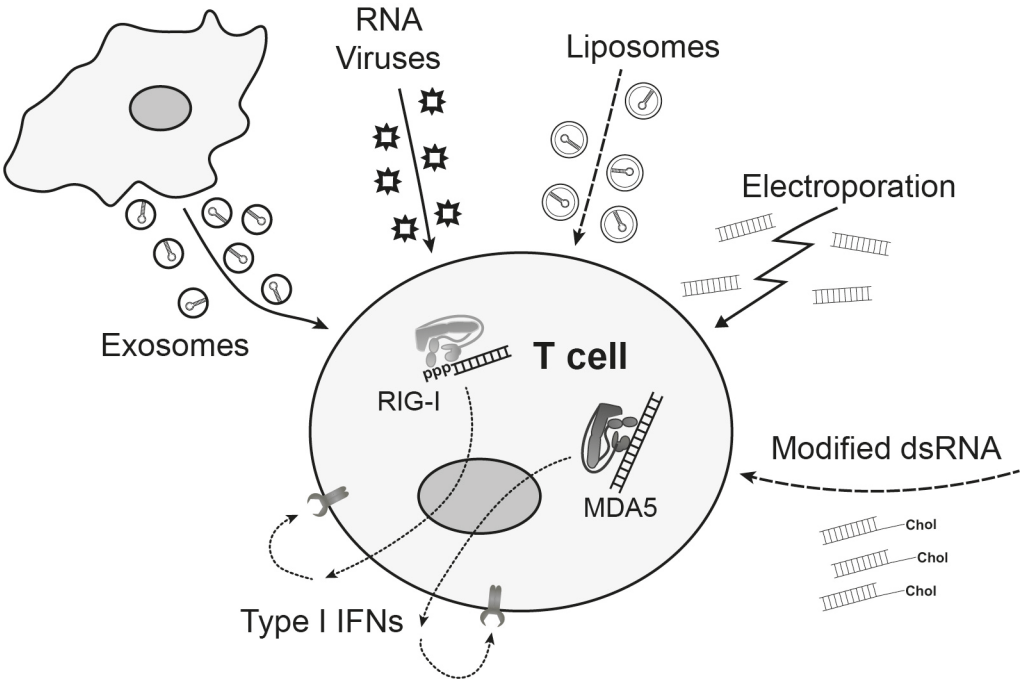

Figure 3.1: Techniques to activate cytosolic RNA sensing pathways in CD4 T cells. Exosomes can deliver stimulatory RNAs to CD4 T cells. RNA viruses like Sendai Virus (SeV) can activate cytosolic RNA signalling pathways. Lipofection and electroporation are widely used techniques to deliver nucleic acids to various cell types and were assessed in this thesis. Chemically modified RNAs are used for gene silencing in CD4 T cells and were studied for their capability to stimulate RIG-I. Dashed arrows indicate techniques that were not efficient in stimulating a type-I IFN response in CD4 T cells.

3.2 Results

3.2.1 Stimulating the RIG-I signalling pathway in CD4 T cells

3.2.1.1 CD4 T cells are widely refractory to cationic lipid transfection

Cationic lipid transfection is a well-studied method to deliver nucleic acids to cells. CD4 T cells have been described as difficult to transfect and we assessed different commercially available formulations to deliver RNA analogues to CD4 T cells. We utilized a FITC-labelled RNA analogue and measured cell association using flow cytometry Figure 3.2A, or an unlabelled RNA analogue and measured IP10 induction using ELISA, Figure 3.2B.

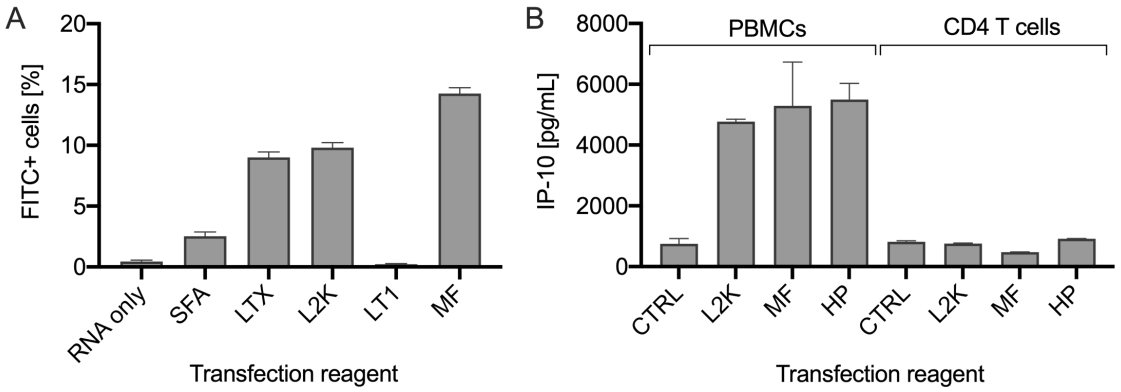

Figure 3.2: Efficacy of cationic lipid transfection of CD4 T cells. A) CD3/CD28 activated CD4 T cells were transfected with synthetic RNA analogue FITC-poly(I:C) using different cationic lipid formulations. Four hours after transfection, frequencies of FITC positive cells were estimated using flow cytometry. B) PBMCs and CD3/CD28 activated CD4 T cells were transfected with unlabelled RNA analogue poly(I:C) using different cationic lipid formulations. IP-10 levels were measured in the supernatant using an ELISA assay sixteen hours after transfection. Uncomplexed FITC-poly(I:C) (RNA only), untreated control (CTRL), Lipofectamine LTX (LTX), Lipofectamine 2000 (L2K), ScreenFectA (SFA), TransIT-LT1 (LT1), MACSfectin (MF), HiPerFect (HP). N = 2, mean + SD.

We observed different frequencies of cell-associated FITC-labelled RNA depending on the cationic lipid formulation that was used. MACSfectin (MF), Lipofectamine LTX and 2000 (LTX and L2K, respectively) showed the highest transfection efficiencies of the tested formulations with 10-15 % FITC positive cells. We compared L2K, MF and HiPerFect (HP) reagents towards their ability to deliver RNA analogue poly(I:C) to the cytoplasm of CD4 T cells. Even though we found cell-associated FITC-labelled RNA, we could not detect an increase of IP-10 in the supernatant of transfected CD4 T cells. In contrast, transfection of PBMCs with poly(I:C) induced high levels of IP-10.

3.2.1.2 Sendai virus induces a type-I IFN response in primary human CD4 T cells

SeV is a well-described stimulator of the RIG-I signalling pathway (Strähle et al., 2007). It is a negative ssRNA virus with a dsRNA intermediate within the viral replication cycle. SeV copy-back defective interfering dsRNAs have been reported to potently stimulate the RIG-I signalling pathway (Baum et al., 2010;

Sánchez-Aparicio et al., 2017). We assessed the immuno-stimulatory capacity of the SeV strain Cantell in CD4 T cells derived from three healthy donors.

In brief, CD4 T cells were enriched from PBMCs and infected with SeV. Type-I IFN levels in the supernatants were measured using a cell-based reporter assay (2.2.2.5) 16 hours post-infection. Type-I IFNs were detected in activated but not in resting CD4 T cells following stimulation with SeV, and the magnitude of the type-I IFN response differed widely between the three donors, Figure 3.3.

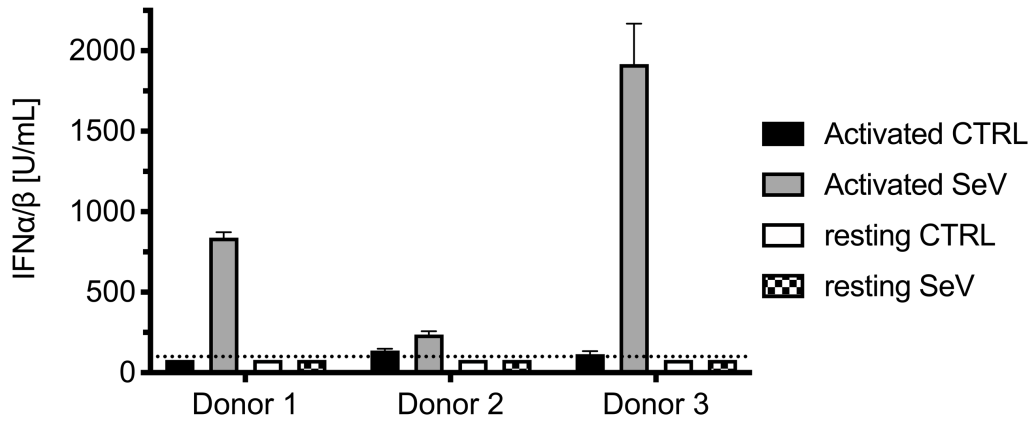

Figure 3.3: Type-I IFN release by CD4 T cells after Sendai virus infection. CD4 T cells were infected with Sendai Virus (200 HAU/mL). After 16 hours, type-I IFN levels were measured using a HEK.blue cell-based reporter assay. Activated = CD4 T cells activated by CD3/CD28, resting = unstimulated CD4 T cells, SeV = Sendai virus, CTRL = uninfected control. Type-I IFN detection limit (dotted line) as estimated by using a recombinant IFNα2 standard. N = 3, one experiment, columns and error bars represent the mean + SD.

3.2.1.3 Exosomes induce a type-I IFN response in primary human CD4 T cells

Exosomes are extracellular vesicles that can carry different cargo, including nucleic acids, proteins, and lipids present within the secretory cell (Sork et al., 2018). Given that exosomes can be engineered to deliver micro RNAs (miRNAs) to cancer cells (Naseri et al., 2018), we evaluated the capability of exosomes to deliver the RIG-I agonist *in vitro* transcript 4 (IVT4) to CD4 T cells.

Activated CD4 T cells were incubated with exosomes derived from untreated or IVT4-treated D05mel cells. Exosomes from untreated cells did not induce a type-I IFN response (Figure 3.4). IVT4-loaded exosomes induced a dose-dependent type-I IFN response. The highest exosome dose tested (10 µg / 4E5 cells) induced type-I IFN levels as high as 75 % of the amount of type-I IFN released upon Sendai virus infection, Figure 3.4.

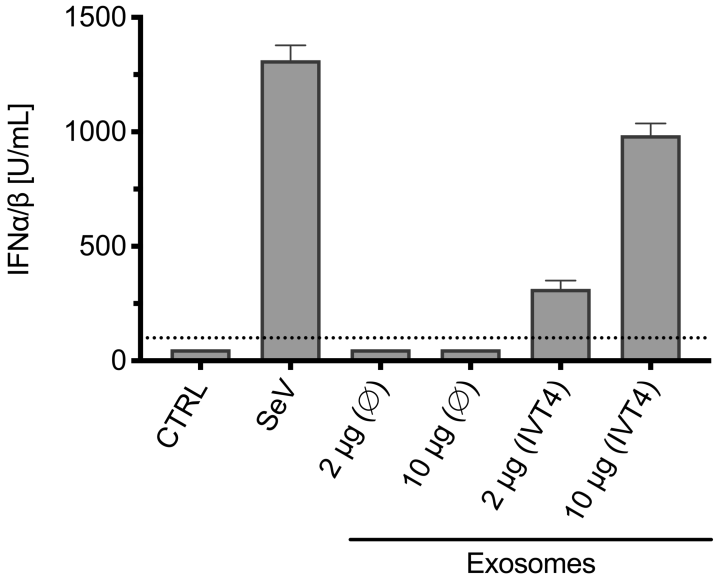

Figure 3.4: IVT4-loaded exosomes induce type-I IFNs in CD4 T cells. CD3/CD28 activated CD4 T cells were treated with 2 µg or 10 µg exosomes. Exosomes were derived from untreated D05mel cells (ø) or IVT4-treated D05mel cells (IVT4). Type-I IFN detection limit (dotted line) as estimated by using a recombinant IFNα2 standard. N = 2, one experiment, columns and error bars represent mean + SD.

IVT4-loaded exosomes induced a dose-dependent type-I IFN response in activated CD4 T cells. Unloaded exosomes did not stimulate the release of type-I IFNs. Relatively high amounts of exosomes (10 µg) were necessary to elicit a type-I IFN response similar to the response induced by SeV.

3.2.1.4 Electroporation delivers RIG-I agonists to CD4 T cells

Electroporation of chemically modified in-house RIG-I agonists (triphosphorylated, synthetic RNA) induced a type-I IFN response in activated CD4 T cells, and no type-I IFN was detected in resting CD4 T cells, Figure 3.5.

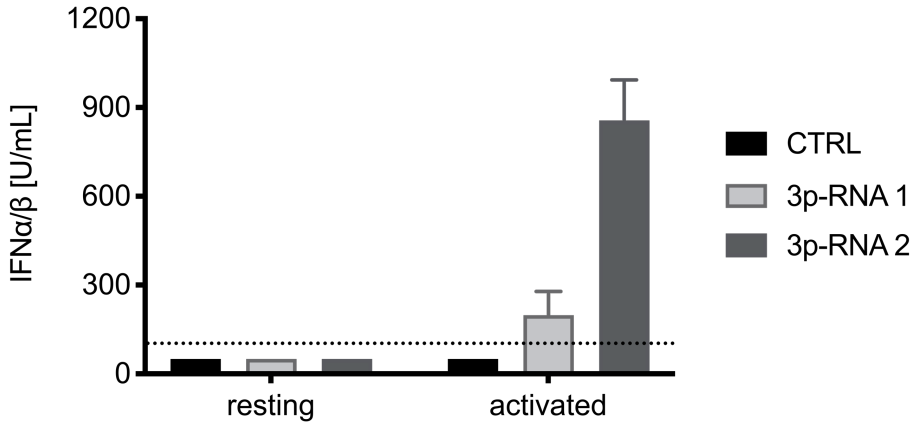

Figure 3.5: Type-I IFN response to RIG-I ligands delivered to CD4 T cells by electroporation. Two chemically engineered RIG-I stimuli (3p-RNA 1 or 2) were electroporated into either resting or activated CD4 T cells. 200 ng of 3p-RNA 1 or 75 ng of 3p-RNA 2 were used. Type-I IFN detection limit (dotted line) as estimated by using a recombinant IFNα2 standard. N = 2 (resting) or 4 (activated), pooled data from two biological replicates, columns and error bars represent mean + SD.

The specificity of the chemically modified in-house RIG-I agonists to stimulate the RIG-I signalling pathway has been extensively studied by the Schlee laboratory (Dr. Ann Kristin de Regt, unpublished data). Small amounts of stimulatory molecules were necessary to induce a type-I IFN response in activated CD4 T cells, and no type-I IFN was detected in resting CD4 T cells. We observed high amounts of cell debris after electroporation, indicating a negative effect on cell viability.

3.2.1.5 A chemically engineered micro RNA is a weak inducer of type-I IFNs in CD4 T cells

Chemically engineered anti-miRNAs were previously shown to translocate from the supernatant into the cytoplasm of CD4 T cells and subsequently silencing gene expression (Haftmann et al., 2015). The authors used cholesterol-tagged, single-stranded miRNAs. We therefore investigated the ability of a similarly designed RNA to stimulate the RIG-I signalling pathway in CD4 T cells. Functional dsRNA (3p-ds-GFP-Chol) was formed by hybridising the triphosphate-bearing antisense strand (3p-antisense) and the GFP-Chol sense strand, Figure 3.6A. High doses (30 µM) 3p-ds-GFP-Chol induced low levels of type-I IFNs in activated CD4 T cells, Figure 3.6B.

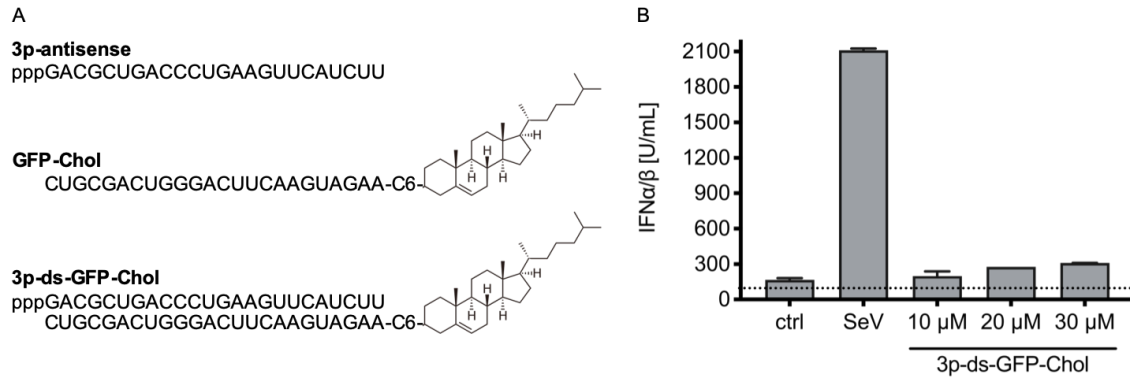

Figure 3.6: Type-I IFN response to a chemically modified dsRNA in CD4 T cells. A) Design of the 24 base pair long chemically modified dsRNA. The hybridisation of the triphosphorylated antisense RNA strand (3p-antisense) and cholesterol-tagged sense strand (GFP-Chol) led to the formation of the functional dsRNA (3p-ds-GFP-Chol). B) CD3/CD28 activated CD4 T cells were treated with 3p-ds-GFP-Chol or Sendai Virus (SeV). Type-I IFN levels were measured using a cell-based reporter assay. Type-I IFN detection limit (dotted line) as estimated by using a recombinant IFNα2 standard. N = 2, one experiment, columns and error bars represent mean + SD. Control (ctrl).

In summary, SeV induced repeatedly high levels of type-I IFNs (1000 IU/mL and above) in different donors. Exosomes were not found to induce higher levels of type-I IFN compared to SeV. Relatively large amounts of exosomes were necessary to induce a strong type-I IFN response. In addition, exosomes are of a less known composition than SeV particles and can deliver unwanted cargo to CD4 T cells. Electroporation was found to deliver stimulatory RNAs with medium to high efficiencies. The negative impact on cell viability nullified this method's advantage to deliver stimulatory RNAs independently of other factors. Others have reported high frequencies of dead cells in the context of electroporation of CD4 T cells as well (Aksoy et al., 2018; Zhao et al., 2006). Therefore, SeV infection was the method of choice for the induction of a type-I IFN response in primary, human CD4 T cells acknowledging that the response to SeV varied between donors.

We next aimed to determine if SeV induced a type-I IFN response exclusively via the RIG-I signalling pathway and not through other innate immune sensors expressed in CD4 T cells. Primary CD4 T cells were genetically modified to disrupt the DDX58 (RIG-I) gene using CRISPR/Cas9 and subsequently infected

with SeV. The type-I IFN response to SeV infection was measured using a cell-based reporter assay (2.2.2.5), Figure 3.7.

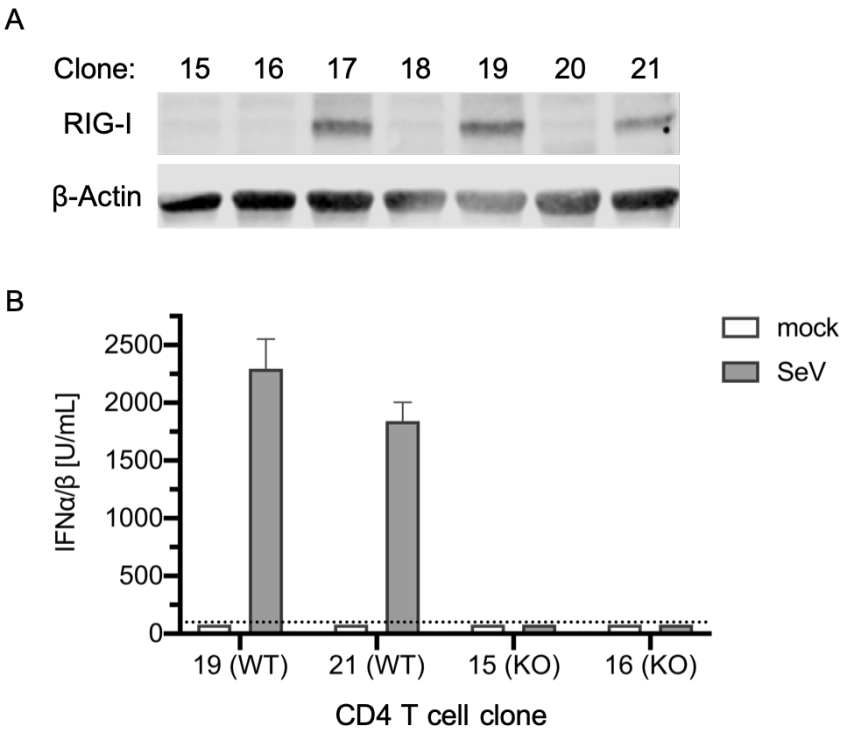

Figure 3.7: RIG-I senses Sendai virus in primary CD4 T cells. (A) The RIG-I coding region (DDX58) was targeted by CRISPR/Cas9 in primary CD4 T cells. Single-cell clones were expanded and stimulated with IFNα (1000 U/mL) to induce RIG-I expression. 30 µL whole cell lysate per sample was loaded onto an SDS PAGE and subjected to immunoblotting using anti-RIG-I and anti-β-actin antibodies. (B) Different wild-type (WT) and RIG-I knockout (KO) CD4 T cell clones were mock-infected (mock, open column) or SeV-infected (40 HAU/mL, SeV, grey column) for 16 hours. The release of type-I IFNs was detected using a cell-based reporter assay. Type-I IFN detection limit (dotted line) as estimated by using a recombinant IFNα2 standard. N = 4, one experiment, column and error bars represent mean + SD.

Wild-type CD4 T cell clones released high amounts of type-I IFNs upon SeV infection. In contrast, no type-I IFNs were detected in CD4 T cells deficient for *DDX58* (RIG-I) following SeV infection.

3.2.2 Modulation of the CD4 T cell transcriptome upon RIG-I activation

3.2.2.1 Expression levels of the RIG-I signalling pathway in CD4 T cells

Experiments performed in the previous sections found high type-I IFN levels in activated CD4 T cells following SeV infection and during electroporation, but not

in resting CD4 T cells. RIG-I mediated this as the production of type I IFN was eliminated in RIG-I knock out cells. Next-generation sequencing was next used to assess if CD4 T cell activation affected the expression level of members of the RIG-I signalling pathway. CD4 T cells were enriched from PBMCs from healthy donors by depletion of unwanted cell populations. CD4 T cells were enriched to purities of 94 % or higher. Transcripts of markers for B cells, NK cells, monocytes, macrophages and granulocytes were detected at low levels (Appendix, figure 8.1), confirming expected contaminating cell types within the samples.

The expression levels of the RIG-I and MDA5 signalling pathways in resting and activated CD4 T cells were analysed, Figure 3.8.

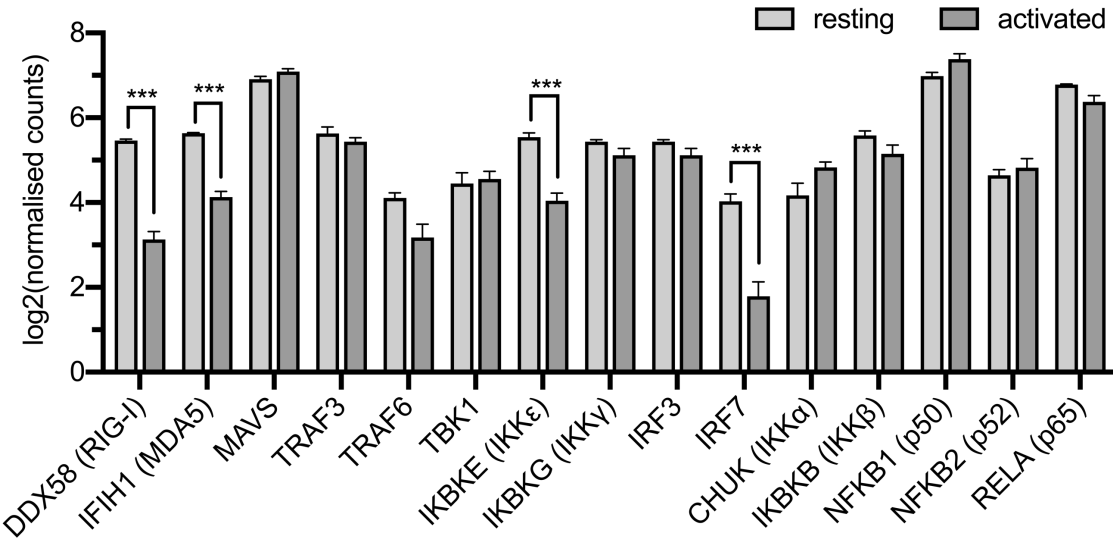

Figure 3.8: Expression levels of members of the RIG-I and MDA5 signalling pathways in CD4 T cells. Next-generation sequencing was used to assess mRNA expression of cytosolic RNA receptors RIG-I and MDA5 and their downstream signalling proteins in resting (light grey) or after 72 hours of stimulation with CD3/CD28 (activated, dark grey) of CD4 T cells. RIG-I (retinoic acid-inducible gene I), MDA5 (melanoma differentiation-associated protein 5), MAVS (mitochondrial antiviral-signalling protein), TRAF3/6 (tumour necrosis factor associated factor 3/6), TBK1 (TANK-binding kinase 1), IKKε/γ/α/β (inhibitor of nuclear factor kappa-B kinase subunit ε/γ/α/β), IRF3/7 (interferon regulatory factor 3/7), NFKB (nuclear factor kappa B subunit), RELA (RELA proto-oncogene). N = 3, mean + SD, three technical replicates from one of two biological replicates (representative data). The gene expression levels were compared between resting and activated CD4 T cells: no statistically significant differences were found if not otherwise indicated, two-tailed student's t-test, ***$p<0.001$.

We found transcripts coding for RIG-I and MDA5 and known members of their signalling pathways in resting and activated CD4 T cells. Some of the gene transcripts (DDX58, IFIH1, IKBKE, IRF7) were more abundant in resting compared to activated CD4 T cells. Based on these data we conclude that the changes in the transcriptome following T cell activation alone did not explain different responses to SeV in resting and activated CD4 T cells.

3.2.2.2 Transcriptomic changes during Sendai virus infection in resting CD4 T cells

Genes involved in the innate immune response against RNA viruses were found to be expressed in resting CD4 T cells, but type-I IFNs were not detected in the supernatant of those cells using a cell-based type-I IFN reporter assay (2.2.2.5). One potential explanation of these findings is that resting CD4 T cells show less translational activity than activated cells and that the transcriptome and proteome do not necessarily match in resting cells (Ricciardi et al., 2018). Therefore, we assessed the changes in gene expression in resting CD4 T cells following SeV infection, Figure 3.9.

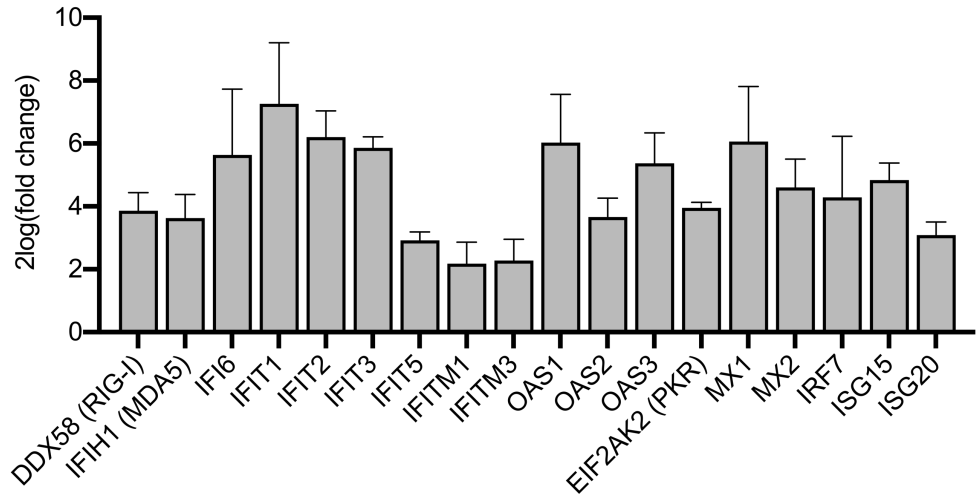

Figure 3.9: Type-I IFN-stimulated genes are upregulated in resting CD4 T cells upon Sendai virus infection. Resting CD4 T cells were inoculated with Sendai virus or left untreated for seven hours. Total RNA was extracted using TRIZol reagent. Next-generation sequencing of the polyA-RNA transcriptome was performed. The relative expression of interferon-stimulated genes (ISGs) in the Sendai virus treated cells to the untreated cells is shown. DDX58 (DExD/H-box helicase 58), IFIH1 (interferon induced with helicase C domain 1), IFI6 (interferon alpha inducible protein 6), IFIT (interferon-induced protein with

tetratricopeptide repeats), IFITM (interferon-induced transmembrane protein), OAS (2'-5'-oligoadenylate synthetase), EIF2AK2 (eukaryotic translation initiation factor 2 alpha kinase 2), MX (MX dynamin-like GTPase), IRF7 (interferon regulatory factor 7), ISG (interferon-stimulated gene). N = 3, mean + SD, three technical replicates from one of two biological replicates (representative data).

Resting CD4 T cells respond to SeV infection with the upregulation of multiple interferon-stimulated genes (ISGs), indicating a functional RIG-I signalling pathway. IFNα and IFNβ transcripts were detected in SeV treated CD4 T cells but not in the untreated control. Furthermore, the analysis of differentially expressed genes revealed an enrichment or reduction of different cellular pathways, Figure 3.10A and B.

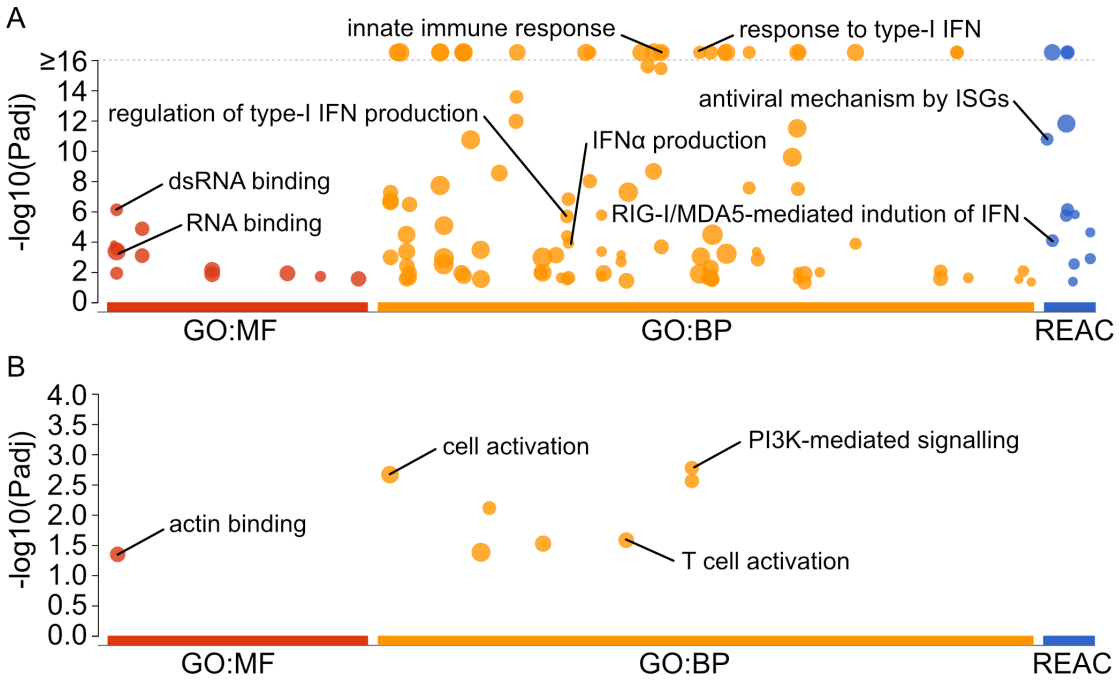

Figure 3.10: Differentially regulated pathways in resting CD4 T cells upon Sendai virus infection. Resting CD4 T cells were inoculated with SeV or left untreated for seven hours. Next-generation sequencing of the polyA-RNA transcriptome was performed. Functional gene set enrichment analysis (g:GOSt, version: e100_eg47_p14_7733820, organism: hsapiens, Raudvere et al., 2019) identified enriched (A) and downregulated (B) pathways in resting CD4 T cells seven hours after SeV inoculation. N = 6 (three technical replicates per donor, two donors in total, pooled data). Each dot represents one pathway. GO:MF (gene ontology term (GO) molecular function), GO:BP (GO biological process), REAC (reactome pathway database). The Y-axis shows the adjusted enrichment p-values in a negative decadic logarithm scale.

The sequencing data revealed a broad antiviral response in resting CD4 T cells upon SeV infection and stimulation of the RIG-I signalling pathway. Pathways

involved in RNA binding, type-I IFN production, innate immune responses and RIG-I and MDA5-mediated induction of type-I IFNs were found to be upregulated, among others. A few pathways were found to be downregulated; all of them connected to T cell activation. Therefore, we decided to investigate the effects of RIG-I activation on the different steps of CD4 T cell activation, including metabolic reprogramming, proliferation and release of effector cytokines.

3.2.3 Effects of RIG-I activation on CD4 T cell activation and proliferation

A hallmark of CD4 T cell activation is the upregulation and modulation of metabolic pathways, reviewed in Shyer et al., 2020. We therefore assessed the metabolic response of resting CD4 T cells to activation using CD3/CD28 beads. Cells were either left untreated or were infected with SeV before activation, Figure 3.11.

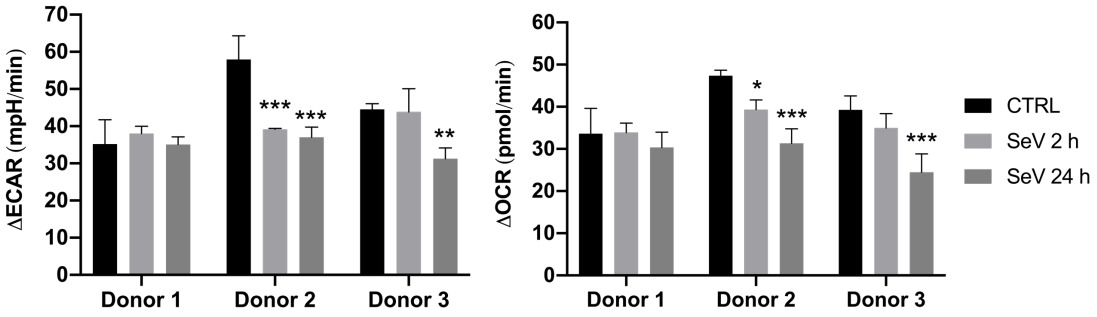

Figure 3.11: Metabolic activity of CD4 T cells after Sendai virus infection. The extracellular acidification rate (ECAR, left) and oxygen consumption rate (OCR, right) were measured to monitor oxidative phosphorylation and glycolysis. Resting CD4 T cells were mock-infected (CTRL), or Sendai virus (SeV) infected for 2 or 24 hours before activation with CD3/CD28 beads. ΔECAR and ΔOCR were calculated as the differences between the metabolic rates before and after activation. Two-way ANOVA, Tukey's test. *($p<0.05$), **($p<0.01$), ***($p<0.001$). N = 3, mean + SD, one experiment.

We used a Seahorse flux analyser to measure the oxygen consumption rate (OCR) and the extracellular acidification rate (ECAR). Both parameters serve as surrogate markers to monitor oxidative phosphorylation and glycolysis, respectively. One out of three donors (donor 1, Figure 3.11) was non-responsive to SeV infection. Two donors showed a decrease in their metabolic response upon activation 24 hours after SeV infection. This was true for both monitored markers OCR and ECAR. One donor showed a reduction of the metabolic

response (ECAR and OCR) upon activation as soon as two hours after SeV infection.

Clonal expansion is tightly connected to the metabolic activity of CD4 T cells and is a prerequisite for an effective T cell-mediated immune response, (reviewed in Dimeloe et al., 2017). Next, we studied if RIG-I activation during SeV infection affected the proliferative activity of CD4 T cells, Figure 3.12.

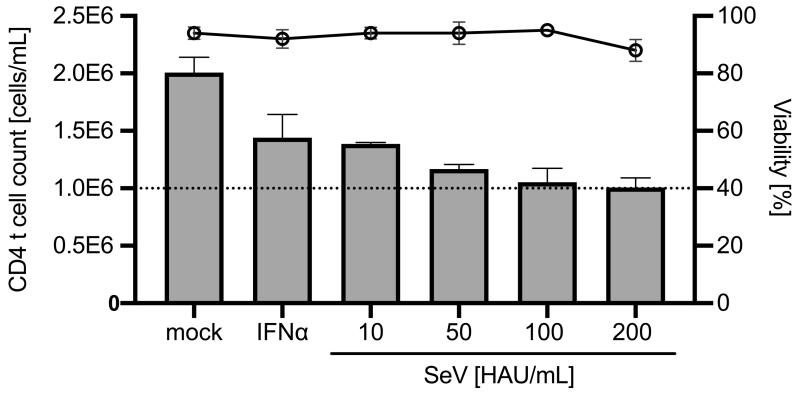

Figure 3.12: Effects of Sendai virus infection and RIG-I activation on proliferation and viability of CD4 T cells. CD4 T cells were activated with CD3/CD28 for 72 hours and then mock-infected (mock), treated with IFNα (1000 U/mL IFNα) or infected with different doses of Sendai virus (SeV). Cell count (columns) and viability (line) were determined 36 hours after infection. The starting cell density of 1E6 cells/mL is indicated as a dotted line. A significant decline ($p < 0.001$) in cell numbers was found for the groups treated with IFNα or SeV when compared to the mock-treated control. No statistically significant changes in cell viability were observed. One-way ANOVA, Dunnett's test. N = 3, mean + SD, one experiment.

SeV infected cells showed significantly lower total cell numbers compared to the mock-infected control. This effect was dose-dependent with increasing amounts of SeV, causing a decrease of total CD4 T cell numbers. At the same time, cell viability was not affected at low and medium doses of SeV. A slight drop of cell viability was observed in samples infected with a high dose of SeV (200 HAU/mL) but was not found to be statistically significant. Also, a significant reduction in total cell numbers was observed in the type-I IFN treated group.

3.2.4 Effects of RIG-I activation on CD4 T cell effector function

CD4 T cells interact with antigen-presenting cells (APCs) (Burgdorf et al., 2007). Upon the engagement with their specific antigen in combination with self molecules, T cells become activated and are primed to release effector cytokines (Zinkernagel and Doherty, 1974). It has been described in the literature that type-I IFNs can affect the biology of CD4 T cells, and we confirmed some of these effects in the context of RIG-I and SeV infection. We used a model of CD4 T cell activation that resembles processes of T cell activation *in vivo* to study the effect of RIG-I activation and SeV infection on CD4 T cell effector functions.

CD14 monocytic cells and CD4 T cells were enriched from peripheral blood mononuclear cells (PBMCs) from cytomegalovirus (CMV) infected individuals. The CD14 positive cell fraction was differentiated into antigen-presenting dendritic cells (DCs) by adding a cytokine cocktail, and these cells were loaded with an overlapping peptide pool to the CMV phosphoprotein 65 (pp65). Pp65 peptide-loaded DCs were co-cultured with CD4 T cells. T cells specific for pp65 became activated and were enriched using an IFNγ capture assay. Cells were clonally expanded and allowed to finish their activation cycle. Six to seven days after primary activation, pp65-specific CD4 T cells were infected with SeV, treated with type-I IFN or left untreated for 16 hours. After that, cells were co-cultivated with pp65-loaded or unloaded DCs, and the release of IFNγ was measured using an IFNγ capture assay, Figure 3.13.

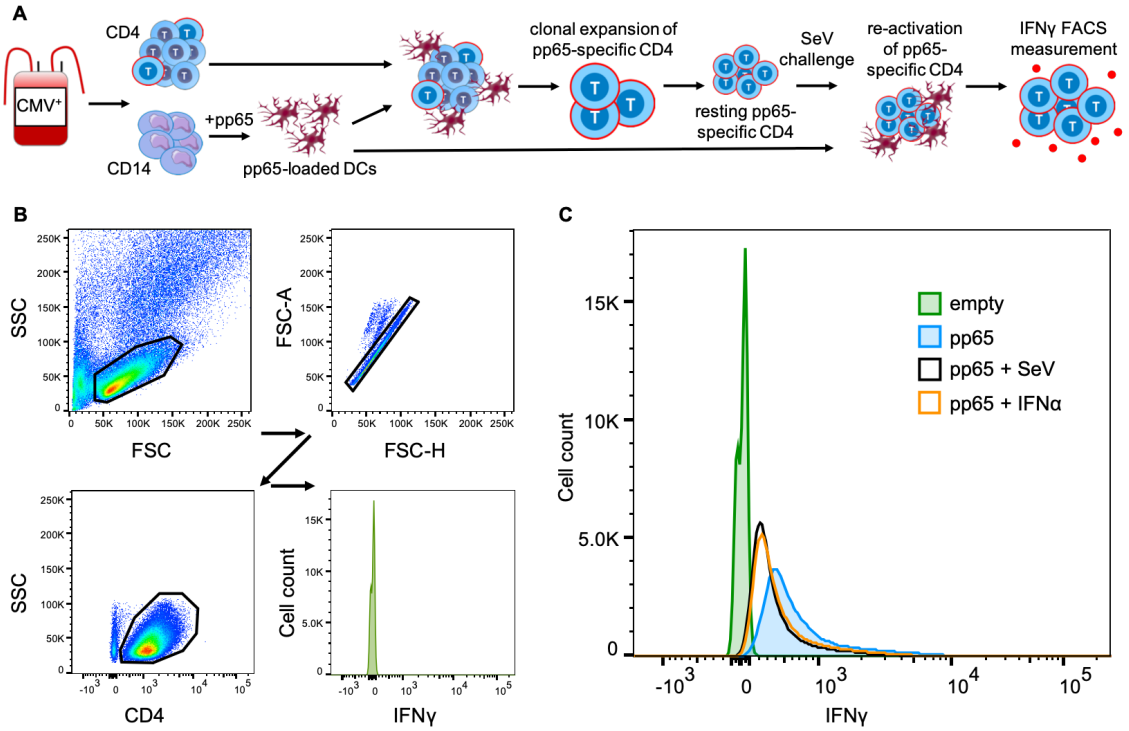

Figure 3.13: Effects of Sendai Virus infection and stimulation of RIG-I on CD4 T cell effector function. A) CD4 T cells and monocytes were derived from blood donors with IgG to Cytomegalovirus (CMV). Monocytes were differentiated into dendritic cells (DCs) and loaded with an overlapping peptide pool to the CMV pp65, a structural protein. Pp65-specific CD4 T cells became activated and clonally expanded during co-cultivation with pp65-loaded DCs. CD4 T cells were harvested and allowed to revert back into a resting state leading to an enriched population of CD4 T cells with known antigen-specificity. Cells were then challenged with SeV, incubated with IFNα (1000 U/mL) or left untreated for 16 hours. B) Cells were incubated with empty or pp65-loaded DCs, and the release of IFNγ was monitored using flow cytometry. Similar results were obtained in two independent experiments.

Co-cultivation of pp65-specific CD4 T cells with unloaded DCs did not induce the release of IFNγ. However, more than 95 % of CD4 T cells released IFNγ when co-cultured with pp65-loaded DCs. Cells infected with SeV showed a reduction of IFNγ released, and only 85 % of CD4 T cells were found positive for IFNγ. A similar decrease of IFNγ levels was detected when cells were pre-treated with type-I IFN.

Together these data demonstrate that SeV infection triggers a RIG-I dependent type-I IFN response in CD4 T cells. And that the activation of RIG-I negatively

affects the activation cascade in CD4 T cells, including metabolic rate, proliferation and the release of effector cytokine IFNγ.

3.3 Discussion

Innate immune sensor activation plays an important role during the priming of adaptive immune responses. The role of innate immune receptors in CD4 T cells has been addressed by others but is not fully understood to date. Here we studied the effect of RIG-I stimulation on the biology of CD4 T cells. Different methods to stimulate the RIG-I signalling pathway in CD4 T cells were assessed and RIG-I was strongly and reproducibly activated by infection with live virus (SeV). High amounts of type-I IFNs were present in the supernatant of activated CD4 T cells following SeV infection. In contrast, no type-I IFNs were found in the supernatant of resting CD4 T cells, but RNA deep sequencing data revealed that these cells initiate a broad antiviral response by altering their transcriptomic profile. Gene enrichment analysis uncovered the downregulation of cellular pathways connected to T cell activation. This finding was confirmed on the level of T cell activation (metabolic rate), proliferation and effector function.

Electroporation, exosomes and SeV infection mediated the stimulation of RIG-I in CD4 T cells while cationic lipid-mediated transfection and a chemically modified microRNA had no effect. We observed the association of a FITC-labelled RNA analogue with CD4 T cells shortly after cationic lipid transfection but did not detect the induction of IP-10. One explanation for this could be that the cationic lipid encapsulation of the labelled RNA analogue mediates cell association but not incorporation. Or the particles are internalised but do not enter a compartment where sensing is possible (cytoplasm or endosome).

Electroporation negatively impacted cell viability and was excluded from subsequent studies. We decided to use SeV for various reasons: The SeV Cantell strain is a well-described, specific activator of the RIG-I signalling pathway, commercially available and easy to grow in a laboratory environment. In comparison, relatively large amounts of exosomes were necessary to elicit a

type-I IFN response similar to SeV infection in CD4 T cells. Exosomes have a less known composition compared to a viral particle. They can incorporate a wide range of nucleic acids and proteins that may affect cellular processes apart from the RIG-I signalling pathway (Nolte-'t Hoen et al., 2009; Okoye et al., 2014). Therefore, exosomes were not found to be advantageous over SeV, which was subsequently used to stimulate the RIG-I signalling pathway in CD4 T cells.

Using RIG-I knockout cell lines, we confirmed that the type-I IFN response following SeV infection is dependent on RIG-I. We further characterised the effect of SeV on CD4 T cells and found that SeV caused a reduction of the proliferative activity, while the cell viability was unaffected. We observed a similar effect in CD4 T cells treated with type-I IFN alone, which is in line with what has been previously reported by others. It has been shown that type-I IFNs can have an antiproliferative effect on CD4 T cells *in vitro* (Dondi et al., 2004; Havenar-Daughton et al., 2006; Tanabe et al., 2005). We explain the reduced proliferation of SeV-infected CD4 T cells with the release of high levels of type-I IFNs upon infection.

SeV infection caused a reduced metabolic activity in resting CD4 T cells following activation with CD3/CD28 beads. This result supports observations made by others in which type-I IFNs induced a cell cycle arrest and inhibited proliferation of resting CD4 T cells (Dondi et al., 2003), as well as data obtained during RNA sequencing experiments shown in this thesis.

IFNγ is a signature cytokine for the Th1 CD4 T cell linage (Bradley et al., 1996). We did not control for other cytokines or markers that identify different T cell subsets. Therefore, we can not exclude that the inflammatory environment during SeV infection or type-I IFN treatment caused plasticity in the T cell responses due to the re-assignment of cells to different T cell subclasses. Even though a loss of Th1 T cell function is unlikely, according to previous publications, which include the following: Memory CD4 T cells were found to show certain plasticity upon reactivation depending on their microenvironment but maintained their initial

effector fate (Lee et al., 2009). Instead of acquiring an entirely different phenotype, they maintained the capability to express effector cytokines specific to their original linage and additionally released cytokines that were commonly found in other T cell subclasses (Krawczyk et al., 2007). Experiments shown in this thesis monitored early time points after reactivation of CD4 T cells. Hence, we can only determine the effect of RIG-I activation during SeV infection on the early stages of CD4 T cell activation. Cells may acquire full metabolic activity and effector functions at later time points after activation, but the initial response is diminished.

Similar effects on proliferative activity and IFNγ release were found when cells were treated with type-I IFNs or infected with SeV. This indicates that the stimulation of RIG-I and the subsequent release of type-I IFNs are involved in the modulation of CD4 T cell responses. We did not detect type-I IFNs in resting CD4 T cells using a cell-based reporter assay, with a detection limit of approximately 100 U/mL type-I IFN. Transcriptomic data confirmed the presence of type-I IFN mRNA upon SeV infection in resting CD4 T cells. A more sensitive assay, e.g. ELISA, could be used to assess the type-I IFN levels in SeV infected resting CD4 T cells. Antibodies blocking the interferon receptor (IFNAR) could also be used to further differentiate between the direct effect of RIG-I activation and the effect of the subsequent release of type-I IFNs on CD4 T cells.

Using a replication-competent virus in a living cell system can significantly modulate the biology of the host cell. The immunomodulatory effects of SeV have been extensively studied elsewhere. The multiple effects include the following. First, the C- and V-proteins of SeV have been described to inhibit type-I and type-II IFN induction and their signal transduction via MDA5, RIG-I, STAT1 and IFNAR2 (Andrejeva et al., 2004; Kitagawa et al., 2020; Oda et al., 2015; Sánchez-Aparicio et al., 2018). Accumulation of defective interfering RNAs allows the infected cell to overcome the immunosuppressive effects during SeV strain Cantell replication (Takeuchi et al., 2008). Transcriptomic changes during SeV infection have been studied in different cell types and were similar to antiviral

responses observed in the presence of type-I IFNs, even though some gene expression patterns were exclusively found during SeV infection (Mandhana and Horvath, 2018). No changes in the protein biosynthesis rate of cellular proteins were found during SeV infection (Takeuchi et al., 2008). Even though we can not exclude effects other than RIG-I activation during SeV infection, controls including RIG-I knockout cell lines and supplementation of media with type-I IFNs indicate that the activation of RIG-I and the subsequent type-I IFN response is at least partly involved in modulating CD4 T cell responses as studied in this thesis.

Our findings could have significant implications for HIV-1 cure strategies. Pharmacological activators of the RIG-I signalling pathway have been exploited in the context of other viral infections, including Ebola, Hepatitis B, Influenza A and Dengue virus, in order to prevent or clear the infection (Coch et al., 2017; Ho et al., 2019; Jasenosky et al., 2019; Korolowicz et al., 2016). Effects of RIG-I activation on HIV-1 latency reversal has been discussed controversially. Li et al., 2016, reported latency-reversal and the specific killing of HIV-1 infected cells by acitretin, an FDA-approved drug that activates RIG-I. A subsequent study could not reproduce the specific killing of HIV-1 infected cells and only found modest effects on latency reversal by acitretin (Garcia-Vidal et al., 2017).

RIG-I activation alone may not be sufficient to reverse latency or trigger the killing of latently infected cells, but the pathway could play an important role in multifactorial HIV-1 cure approaches. One cure strategy being tested includes activating latent HIV-1 to induce expression of viral proteins and virus-induced or immune-mediated clearance of the infected cell. HIV-1 relies on activated, metabolically active CD4 T cells for efficient replication and viral spread (Valle-Casuso et al., 2019). Active viral HIV-1 replication also has cytotoxic effects on uninfected bystander cells (Ahr et al., 2004; Maccarrone et al., 1998). If activation of latent virus activated RIG-I, as seen in productively HIV-1 infected CD4 T cells, this would reduce the metabolic activity of the cell and could also reduce the number of viral particles released by these cells, thereby decreasing cytotoxic effects in bystander cell populations.

An indication for the importance of the RIG-I signalling pathway is the fact that HIV-1 established a mechanism to evade RIG-I immune surveillance in infected cells (Solis et al., 2011). In the following chapters, we will focus on the mechanism that HIV-1 utilises to circumvent RIG-I sensing and what role RIG-I-like receptors play during productive HIV-1 infection.

4. Aim 2: HIV-1 protease cleaves RIG-I and MDA5 – a potential immune evasion mechanism for HIV-1

4.1 Introduction

Despite the advances of antiretroviral therapy (ART) in people living with HIV-1 leading to substantially reduced morbidity and mortality, treatment is needed life long and there is no cure (reviewed in Pitman et al., 2018). HIV-1 persists in PLWH on ART as long-lived and latently infected cells (Bui et al., 2017). We now know that in nearly all PWLH on ART, low levels of cell-associated HIV-1 RNA (Anderson et al., 2020; Lewin et al., 1999) and plasma HIV-1 RNA (Palmer et al., 2008) are always detected and in some individuals, constitutive expression of viral proteins also persists (T. Wang et al., 2015). Although RNA producing cells in both blood and tissue are less common in PLWH who have been on ART for prolonged compared to shorter periods of time (Banga et al., 2016), others have shown that detection of plasma HIV-1 RNA in plasma is associated with slower decay of the latent reservoir (Bachmann et al., 2019). What remains unclear is why or how virus-producing cells can persist on ART and whether HIV-1 employs an immune evasion mechanism to escape detection of infected cells by either the innate or adaptive immune system. These immune evasion pathways could also hamper efforts to eliminate HIV-1 infected cells through activation or reversal of latency (reviewed in Zerbato et al., 2019)

RNA and DNA viruses use various strategies to evade the host's innate immune defence (reviewed in Beachboard and Horner, 2016). An important pathway for early detection of viral nucleic acid are the cytosolic RNA sensors RIG-I and MDA5, which are targeted directly or indirectly by sequestration of downstream signalling adaptors or activating factors (Feng et al., 2014; Gack et al., 2009; Li et al., 2005; Papon et al., 2009). In fact, the RIG-I like receptors (RLR) RIG-I and MDA5 have been shown to recognise HIV-1 RNA species (Nasr et al., 2017; Ringeard et al., 2019; M. Q. Wang et al., 2015). Despite their high structural similarity and a shared downstream signalling pathway, their specificity towards RNAs during HIV-1 infection differs. It has been shown that MDA5 detects unmethylated, genomic HIV-1 RNA (Ringeard et al., 2019), while RIG-I is

activated by HIV-1 RNA as well as by endogenous RNA species that only occur during viral replication (Berg et al., 2012; Vabret et al., 2019).

A previous study demonstrated that RIG-I was degraded during HIV-1 infection through a mechanism involving HIV-1 protease (HIV-1 PR) (Solis et al., 2011). They claimed that during HIV-1 infection of THP-1 cells, RIG-I protein levels were decreased by a mechanism involving HIV-1 PR, but not via the catalytic activity of the enzyme. They used an HIV-1 PR deficient virus or the protease inhibitor saquinavir during overexpression of RIG-I and HIV-1 PR in HEK293 cells to demonstrate the effects of HIV-1 PR on RIG-I. When they co-expressed HIV-1 PR and MDA5 in HEK293 cells, they found that MDA5 protein levels were not affected by HIV-1 PR. These experiments first warrant independent confirmation as well as an exploration of the mechanism of how HIV-1 PR mediates degradation of RIG-I.

HIV-1 PR is essential for viral maturation and infectivity and has been identified as an antiviral drug target with multiple protease inhibitors licensed for the treatment of HIV-1 (reviewed in Lv et al., 2015). The catalytically active enzyme comprises two identical subunits with two aspartic acid residues at position 25, forming the catalytic centre (Maximova et al., 2019), Figure 4.1.

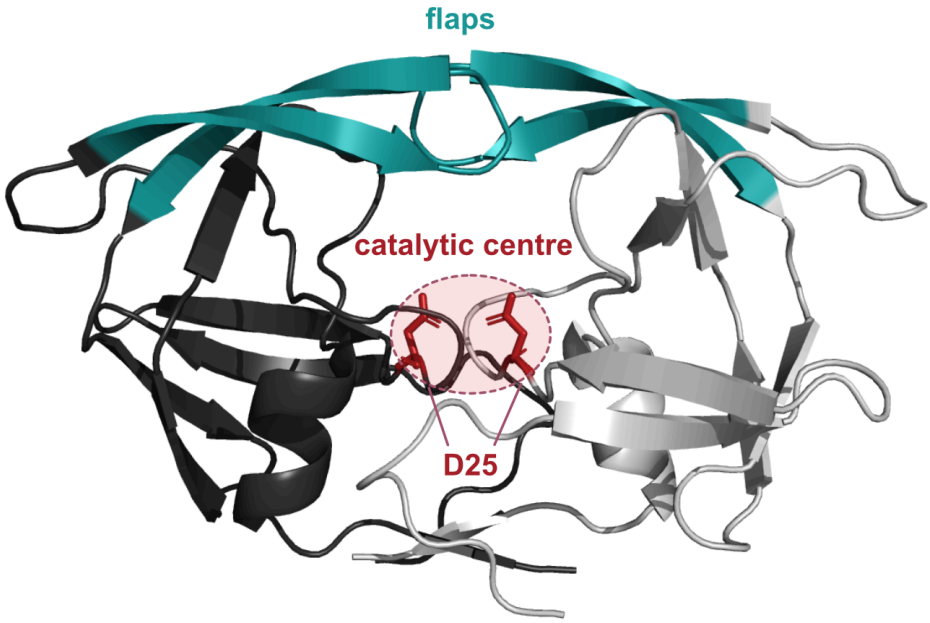

Figure 4.1: 3D structure of HIV-1 protease. Two identical subunits (dark and light grey) form a catalytically active dimer. Two aspartic acid residues (one from each monomer, in red) form the catalytic centre, which is covered by flexible flaps (teal). Each monomer is made up of 99 amino acids with a total molecular weight of 11 kDa and 22 kDa for the homodimer. (Image rendered with PyMOL 2.4.0, using PDB data file 1ODW.)

Introduction of mutation D25A renders the enzyme inactive (Pettit et al., 2003). Residues T26 and D29 have been identified to be essential for dimerization and the mutations T26A and D29N prevent the formation of homodimers and cause the loss of enzymatic activity, too (Louis et al., 2003).

We hypothesised that the enzymatic function of HIV-1 PR is required for RIG-I degradation and that the mechanism was independent of other cellular factors. To address this hypothesis, wild-type HIV-1 PR or different protease mutants were co-expressed with RIG-I and MDA5 in HEK293T cells in combination with the protease inhibitor darunavir. Furthermore, recombinant proteins expressed in *E. coli* or HEK293T cells were purified, and interactions between HIV-1 PRs and RIG-I or MDA5 were studied in the presence or absence of cellular factors. Finally, we investigated if the presence of stimulatory RNAs affected RIG-I and MDA5 protein levels in the presence of HIV-1 PR.

4.2 Results

4.2.1 Wild-type HIV-1 protease but not dead mutant D25A reduces protein levels of RIG-I and MDA5 during co-expression

To determine if the catalytic centre of HIV-1 PR was required for RIG-I degradation, we co-expressed wild type or a mutated version of HIV-1 protease with RIG-I and MDA5 in HEK 293T cells. DNA transfection was first optimised in HEK293T cells, Figure 4.2A. The expression constructs included a protease cleavage site, which separated the recombinant protein from the C-terminal His-tag and enabled HIV-1 PR to cleave off the tag. Therefore, HIV-1 PR expression levels were not monitored during co-expression experiments using a His-tag antibody, Figure 4.2B.

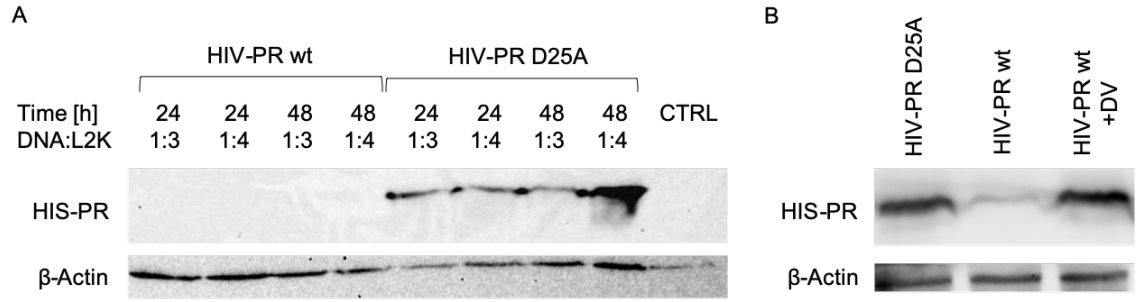

Figure 4.2: Transfection optimisation of recombinant HIV-1 proteases in HEK293T cells. A) Different ratios of DNA to Lipofectamine2000 (L2K) were tested, and protein expression was assessed after 24 to 48 hours using immuno-blot. The expression constructs included a protease cleavage site, which separated the recombinant protein from the His-tag and enabled wild-type HIV-1 PR to auto-process the tag. Recombinant proteases were detected using an anti-HIS antibody which therefore detected mutant but not wild type PR. B) Efficient expression of wild-type PR was confirmed in the presence of darunavir (DV), which inhibited cleavage of the HIS-tag and enabled detection via immuno-blot.

The wild-type or dead mutant D25A HIV-1 PR were co-expressed with RIG-I, in combination with the protease inhibitor darunavir in HEK293T cells, to assess whether the catalytic centre of HIV-1 PR was required for the degradation of RIG-I. Wild-type HIV-1 PR induced reduced levels of RIG-I in a concentration-dependent manner. There was no change in RIG-I levels in the presence of the dead mutant D25A. The addition of the protease inhibitor darunavir restored RIG-I levels during co-expression with the wild-type protease, Figure 4.3.

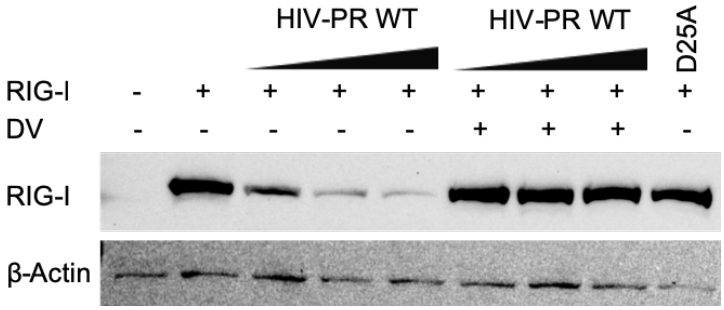

Figure 4.3: Effect of HIV-1 PR on RIG-I protein levels during co-expression. A constant amount of RIG-I expressing plasmid (1.5 µg/12-well) was used across all conditions. Increasing amounts of wild-type HIV-1 protease (HIV-1-PR WT; 0.5, 1.0 or 1.5 µg/12-well) were co-expressed with RIG-I in HEK293T cells for 20 hours. The dead mutant D25A HIV-1 PR (1.5 µg/12-well) and darunavir (5 µM) were used as controls. 40 µg whole cell lysate was loaded per lane, RIG-I was detected using an anti-RIG-I antibody and an anti-β-Actin antibody was used as a loading control. Similar results were obtained in three independent experiments.

RIG-I and MDA5 share similar domain structures and MDA5 was also investigated as a potential target for HIV-1 PR. Solis et al., 2011, observed that a GFP-tagged HIV-1 PR did not target MDA5. We suspected steric hindrance of HIV-1 PR by the GFP tag and used a tag-free HIV-1 PR to ask whether MDA5 was also degraded by the HIV-1 PR. MDA5 was co-expressed with increasing amounts of wild-type HIV-1 PR in HEK293T cells. Wild-type HIV-1 PR co-expression reduced MDA5 levels in a concentration-dependent manner, while high levels of MDA5 protein were maintained during co-expression with the HIV-1 PR mutant D25A, Figure 4.4.

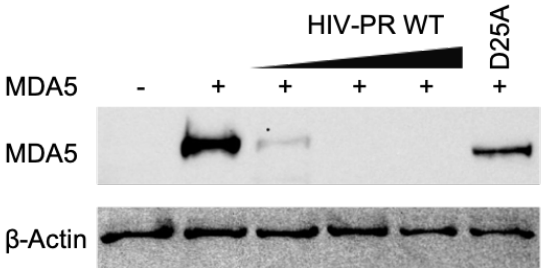

Figure 4.4: Effect of HIV-1 PR on MDA5 protein levels during co-expression. A constant amount of MDA5 expressing plasmid (1.5 µg/12-well) was used across all conditions. Increasing amounts of wild-type HIV-1 protease (HIV-1-PR WT; 0.5, 1.0 or 1.5 µg/12-well) were co-expressed with MDA5 in HEK293T cells for 20 hours. Protease dead mutant D25A (1.5 µg/12-well) was used as a control. 40 µg whole cell lysate per lane, MDA5 was detected using an anti-MDA5

antibody, an anti-β-Actin antibody was used as a loading control. Similar results were obtained in two independent experiments.

4.2.2 Wild-type HIV-1 protease induces cleavage of RIG-I and MDA5 in a cell-free assay

Even though no cytotoxic effects were observed during the previous co-expression experiments, off-target effects of an active protease could potentially occur in living cells. We therefore used a different experimental approach to provide evidence that the reduction in recombinant protein levels was due to degradation processes and not due to off-target effects of HIV-1 PR on cellular biosynthesis pathways. HIV-1 PR expression was optimised in the *E. coli* strain BL21. The bacterial expression constructs added a cleavage resistant six-HIS-tag to the recombinant proteases. Ni-NTA resins bind six tandem histidine residues with high affinity and selectivity and were used to purify the HIS-tagged recombinant proteins. Activity or loss of activity of recombinant proteases was analysed using an HIV-1 protease activity assay. The assay is based on the proteolytic cleavage of a commercially provided substrate and the release of a fluorescent product. The formation of the fluorescent product can be followed using a fluorometer and is directly proportional to the activity of the assayed HIV-1 PR, Figure 4.5.

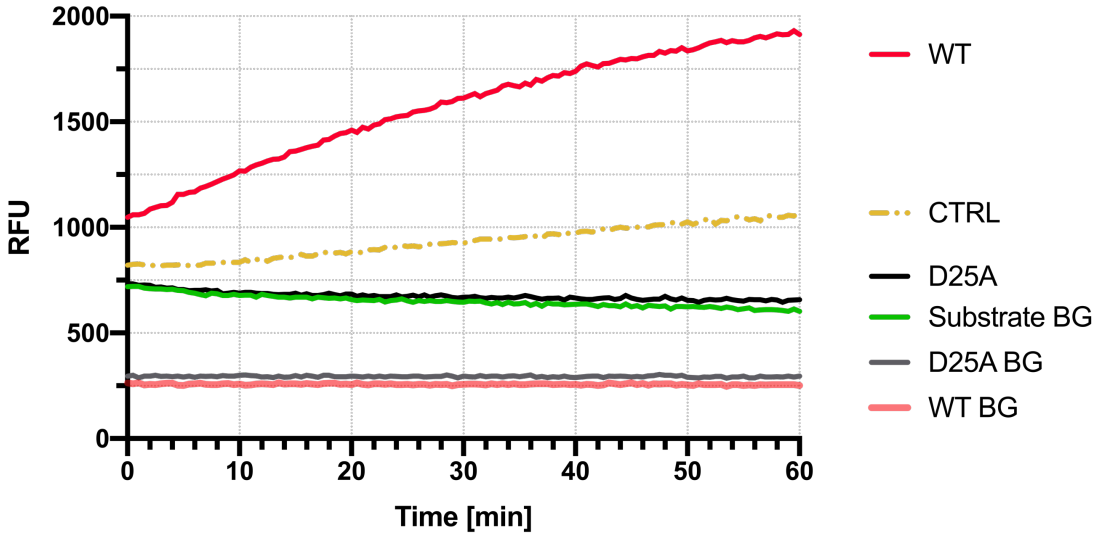

Figure 4.5: HIV-1 protease activity assay. Recombinant HIV-1 PRs were analysed for enzymatic activity. In this assay, enzymatic processing of a synthetic

substrate releases a fluorescent product upon cleavage, which is detected by a change in fluorescence. Wild-type or mutant HIV-1 PR or substrate alone was used to control for background fluorescence (salmon-coloured, grey and green, respectively). Wild-type HIV-1 PR (red) induced cleavage of the substrate and mutant protease D25A (black) was catalytically inactive as expected. Positive control (dashed yellow) included recombinant HIV-1 protease provided with the assay kit. 2 µL recombinant protein was used per reaction. Wild-type (WT), activity assay kit internal control (CTRL), Aspartic acid to alanine HIV-1 PR dead mutant (D25A), background control (BG).

The enzymatic activity of the recombinant wild-type HIV-1 PR was estimated to be 3.4 µmol/min/mg, which is within the same range as reported previously by Leuthardt and Roesel, 1993, who measured a specific activity of 4.4 µmol/min/mg for a recombinant HIV-1 PR.

RIG-I and MDA5 were expressed in HEK293T cells as described before. Cell lysates were prepared in the presence of protease inhibitors targeting endogenous proteases but not HIV-1 PR. Purified, recombinant HIV-1 PRs were added to the whole-cell lysates containing recombinant RIG-I or MDA5. Cleavage of RIG-I and MDA5 was observed in the presence of wild-type HIV-1 PR but not in samples incubated with dead mutant D25A. The protease inhibitor darunavir prevented degradation of RIG-I and MDA5 in samples containing wild-type HIV-1 PR, Figure 4.6.

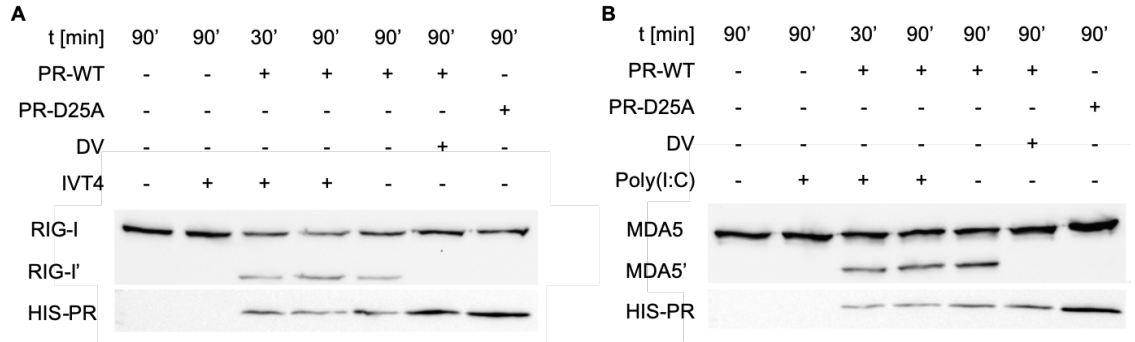

Figure 4.6: HIV-1 protease degrades RIG-I and MDA5 *in-vitro*. Whole-cell lysates of RIG-I or MDA5 expressing HEK293T cells were incubated with purified, recombinant wild-type or mutant HIV-1 PR for indicated times. Wildtype HIV-1 PR induced degradation of RIG-I and MDA5 and degradation was inhibited in the presence of 5 µM darunavir. Degradation products are indicated as RIG-I' and MDA5'. D25A did not cause degradation. RIG-I and MDA5 RNA ligands (*in-vitro* transcript 4 (IVT4) and poly(I:C)) were added to determine their effect on degradation kinetics. Recombinant RNA sensors were detected using specific antibodies against RIG-I or MDA5. Membranes were stripped, and HIV-1 PRs

were detected using an anti-HIS antibody. Similar results were obtained in two independent experiments.

The addition of MDA5 ligand poly(I:C) did not affect degradation kinetics of MDA5. In contrast, *in-vitro* transcript 4 (IVT4), a RIG-I ligand, accelerated the degradation of RIG-I. Reduced levels of full-length RIG-I and increased levels of degraded RIG-I (RIG-I') were found in the presence of IVT4, Figure 4.7.

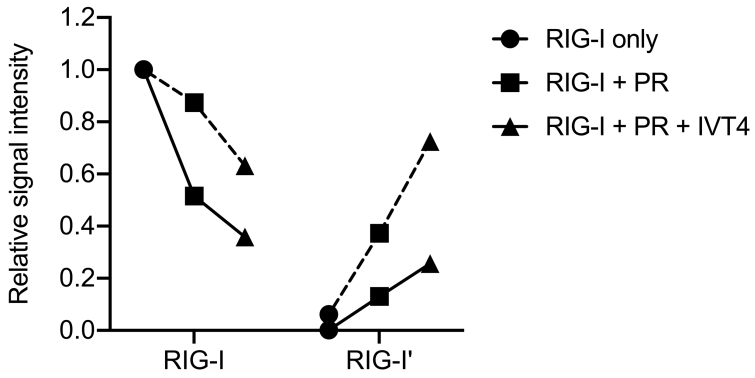

Figure 4.7: Effect of IVT4 on RIG-I degradation by HIV-1 PR. Whole-cell lysates of RIG-I expressing HEK293T cells were incubated with purified, recombinant wild-type HIV-1 PR in the presence or absence of *in-vitro* transcript 4 (IVT4), a RIG-I ligand. Detection of full-length RIG-I (RIG-I) and its degradation product (RIG-I') was determined using immunoblotting and quantified using ImageStudioLite software. Signal intensities were normalised to the control group (RIG-I only). RIG-I + PR (RIG-I incubated with HIV-1 PR), RIG-I + PR + IVT4 (RIG-I incubated with HIV-1 PR and 1 µg IVT4). Data are shown from two independent experiments (indicated by dashed and solid lines).

These experiments provide evidence that degradation of RIG-I in the presence of HIV-1 PR is dependent on the catalytic activity of the enzyme and that MDA5 is a novel target for HIV-1 PR.

We next screened for effects on endogenous downstream signalling adaptor mitochondrial antiviral signalling protein (MAVS), TANK binding kinase 1 (TBK1) and interferon regulatory factor 3 (IRF3) as possible targets for HIV-1 PR. We saw no degradation of these proteins following exposure to wild type or the D52A mutant HIV-1 PR in HEK293T cells, Figure 4.8.

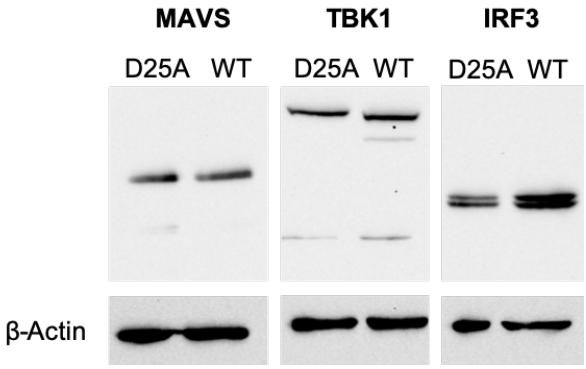

Figure 4.8: MAVS, TBK1 and IRF3 are not targeted by HIV-1 protease. Whole-cell lysates of IFNα stimulated HEK293T cells, transfected with plasmids coding for wild-type or D25A HIV-1 protease were analysed for endogenous protein levels of mitochondrial antiviral signalling protein (MAVS), TANK binding kinase 1 (TBK1) and interferon regulatory factor 3 (IRF3). 30 µg total protein per lane, anti-MAVS, anti-TBK1 or anti-IRF3 antibodies were used for detection. β-Actin was used as a loading control. Similar results were obtained in two independent experiments.

4.2.3 Wild-type HIV-1 protease degrades RIG-I and MDA5 independently of endogenous cellular factors

The previous experiments clearly show the necessity of an active catalytic centre of HIV-1 PR to mediate RIG-I and MDA5 degradation. The involvement of other cellular factors could not be excluded at this stage as experiments were carried out *in-vivo* or using whole cell lysates. To address this issue, we used *in-vitro* digestion of recombinant RIG-I and MDA5 by recombinant HIV-1 PRs. Expression of recombinant RIG-I and MDA5 in *E.coli* BL21 was attempted but was not successful after two rounds of optimisation, Figure 4.9.

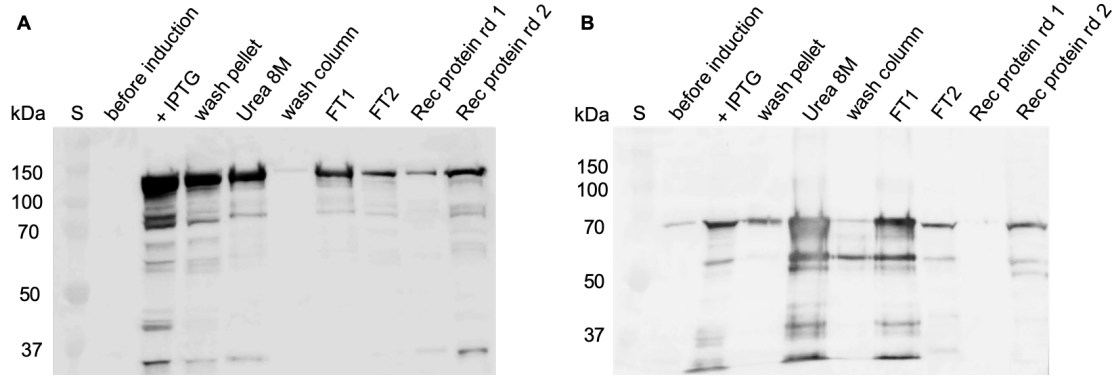

Figure 4.9: Recombinant expression of RIG-I and MDA5 in *E.coli* BL21. RIG-I and MDA5 were expressed analogous to HIV-1 PRs as described before. Two rounds of optimisation did not result in sufficient amounts or purity of recombinant proteins. The two rounds of optimisation are shown as the second round (rd 2) or

the first round (rd 1). Considerable amounts of RIG-I were recovered in round two but were contaminated with a degraded protein. Full-length MDA5 was not recovered at all. Anti-RIG-I and anti-MDA5 antibodies were used for detection. Flow-through (FT), protein standard (S).

We next attempted to express recombinant proteins using a mammalian expression system. RIG-I and MDA5 were successfully expressed in HEK293T cells and purified via FLAG affinity gel. RIG-I and MDA5 were incubated with purified, recombinant wild-type HIV-1 PR in the presence or absence of their ligands IVT4 or poly(I:C) for indicated times to assess if ligand-binding impacts degradation in a cell-free system. HIV-1 PR successfully degraded both proteins, with levels of the full-length proteins decreasing over time while degradation products accumulated, Figure 4.10, (quantification: Appendix Figure 8.2).

In the presence of IVT4, there was an accelerated degradation of RIG-I and accumulation of the degradation product RIG-I', as previously shown in a cell-based assay (Figure 4.6 and Figure 4.7). RIG-I' was further degraded to RIG-I'' in the absence of IVT4 as seen in immuno-blots using anti-HIS antibodies. In contrast, full-length MDA5 levels decreased over time, and the kinetic and products were not altered in the presence of poly(I:C). Band patterns that were observed during MDA5 degradation differed depending on the antibody used for detection (anti-MDA5 or anti-HIS), consistent with a degradation site between both antibody detection sites. This was not the case for the degradation of RIG-I by HIV-1 PR as the main degradation product RIG-I' was detected with anti-RIG-I and anti-HIS antibodies, indicating that the degradation site was likely nearer to the N-terminal from the recognition site of the RIG-I antibody. The significance of this observation will be further addressed in section 4.2.4.1.

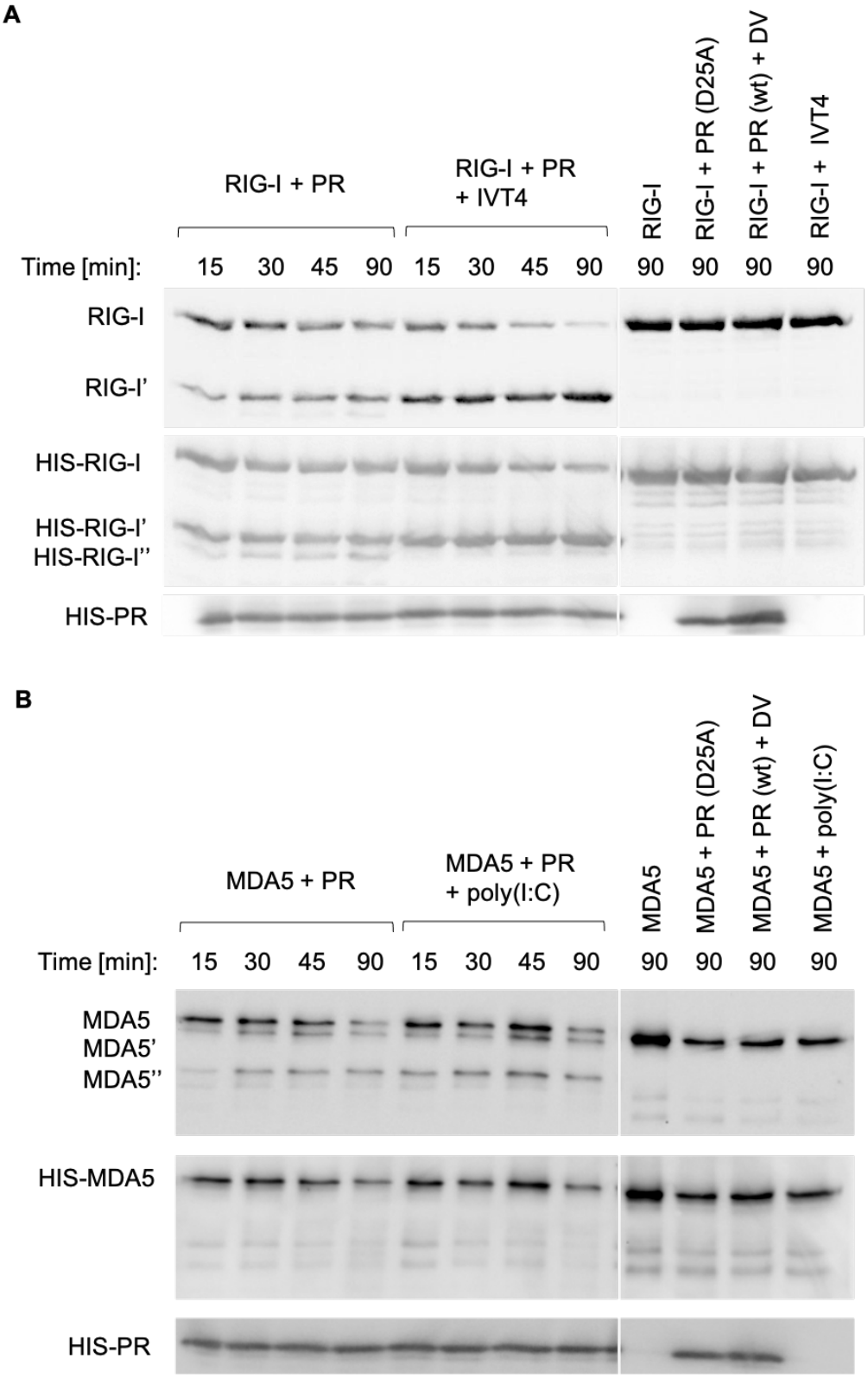

Figure 4.10: *In-vitro* digestion of RIG-I and MDA5 by HIV-1 PR. Recombinant RIG-I (A) and MDA5 (B) were incubated for indicated times with recombinant wild-type HIV-1 PR and degradation was quantified over time by immuno-blotting. The effect of stimulatory RNAs IVT4 (in-vitro transcript 4) or poly(I:C)

(poly(inosine:cytidine) on degradation kinetics was compared to the protease only control. Controls included recombinant protein only, incubation with HIV-1 PR dead mutant D25A, wild-type HIV-1 protease (PR) in combination with the protease inhibitor darunavir (DV), and stimulating RNA. Controls are shown in the right panel of each blot. Membranes were incubated with antibodies against RIG-I and MDA5 and stripped after imaging. HIS-tagged proteins RIG-I, MDA5 and HIV-1 PR were detected using an anti-HIS antibody. Similar results were obtained in two independent experiments.

4.2.4 Degradation of RIG-I and MDA5 by HIV-1 protease disrupts innate immune recognition of stimulatory RNA species

RIG-I and MDA5 induce downstream signalling upon binding of specific ligands, which induce conformational changes and the release of the CARD signalling domains. A dual-luciferase reporter assay was used to determine the impact of HIV-1 PR on innate immune signalling through RIG-I and MDA5 pathways.

Flp-In™ 293 T-REx RM cells, deficient for endogenous RIG-I and MDA5 (RM), were transfected with RIG-I or MDA5 in combination with wild-type or proteolytically inactive HIV-1 PR mutant (T26A or D25A) expressing plasmids. Stimulatory RNAs (IVT4, poly(I:C)) were transfected at a later timepoint and expression of the Gaussia luciferase (IFNβ-GLuc) reporter gene was measured in the supernatant 20 hours after stimulation through detection of luciferase. Signals were normalised to expression levels of Firefly luciferase (CMV-FLuc) in whole-cell lysates to adjust for different transfection efficiencies between replicates.

Co-expression of wild-type HIV-1 PR abrogated RIG-I and MDA5 signalling, which was restored in the presence of the protease inhibitor darunavir. By contrast, co-expression of mutant HIV-1 PRs T26A and D25A did not affect signal induction by stimulatory RNAs, Figure 4.11.

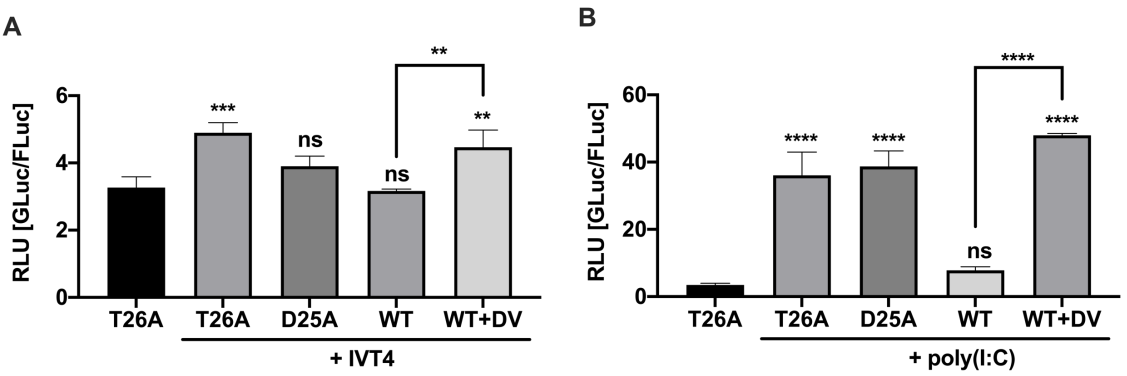

Figure 4.11: RIG-I and MDA5 signaling is abolished in the presence of wild-type HIV-1 PR. FLP-IN™ 293 T-REX RM cells expressing RIG-I (A) or MDA5 (B) were stimulated with IVT4 or poly(I:C) (p(I:C)), respectively, (100 ng/96-well). The IFNβ response was determined 20 hours after RNA transfection using a dual-luciferase reporter assay. RNA stimulated samples were compared to the unstimulated control T26A. Additional comparisons were made by a horizontal line as indicated. N = 3, mean + SD, one-way ANOVA, Dunnett's test. ***(p<0.001), ****(p<0.0001). Similar results were obtained in two independent experiments.

4.2.4.1 RIG-I 2CARD signalling domain is targeted by HIV-1 protease

As mentioned before (4.2.3, Figure 4.10), similar degradation patterns of RIG-I (but not MDA5) were observed regardless of the antibodies (anti-RIG-I or anti-HIS) that were used. Considering the band sizes observed in immuno-blot experiments, we predicted a cleavage site located within the N-terminal linker region or the C-terminal region of the 2nd CARD, Figure 4.12A. This was of interest as free RIG-I CARD can induce type-I IFN signalling on its own (Yoneyama et al., 2004). Therefore the degradation of RIG-I could either abrogate or induce RIG-I signalling.

A series of experiments were conducted to investigate if degradation of RIG-I releases the signalling domain (2CARD) and induces an IFNβ response or if the signalling domain is itself a target for degradation by the HIV-1 PR, Figure 4.12C-E.

We co-expressed HIV-1 PR and RIG-I and did not observe an induction of type-I IFN signalling following RIG-I degradation by HIV-1 PR, Figure 4.12C.

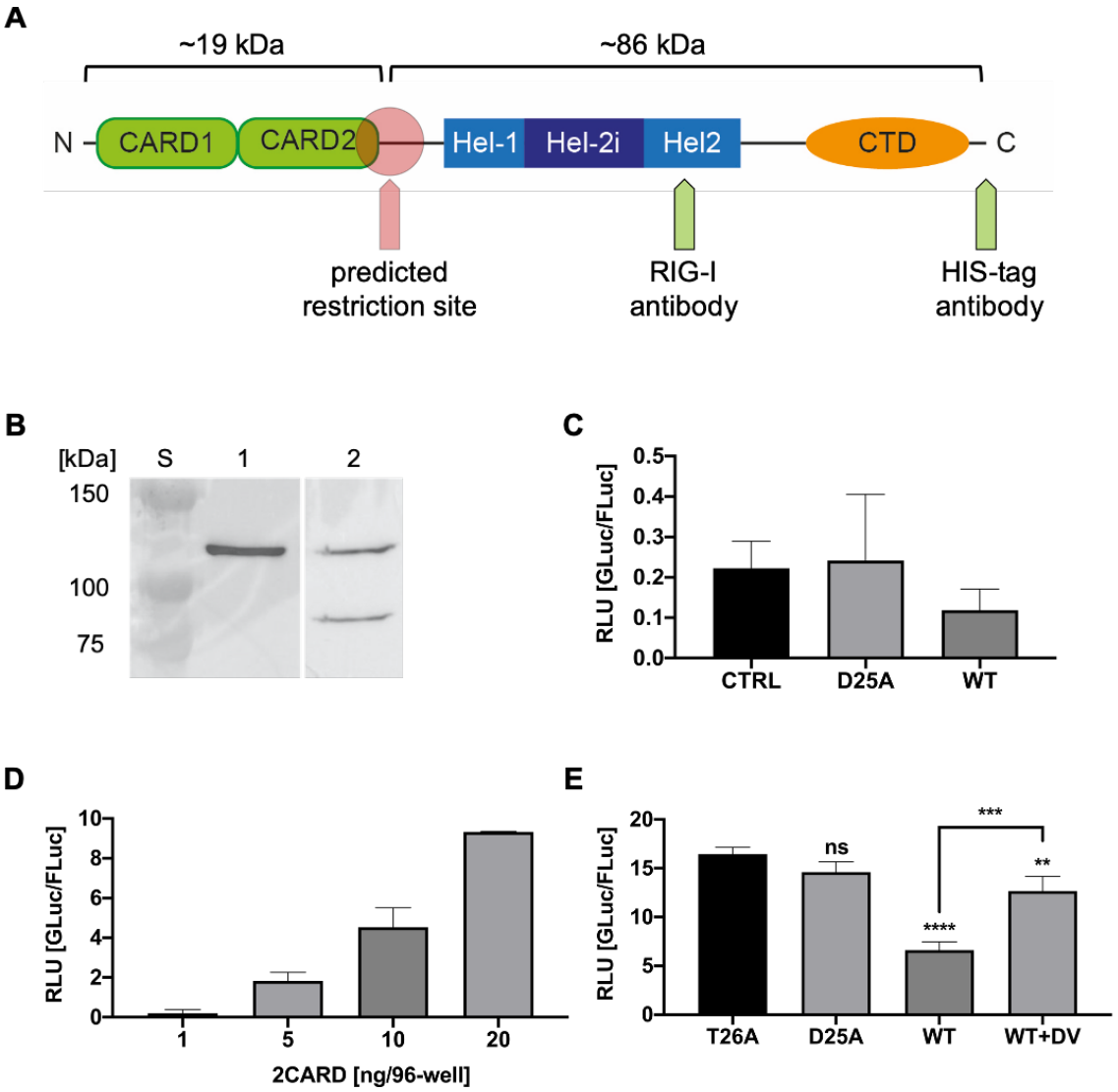

Figure 4.12: HIV-1 protease abrogates signal induction by RIG-I 2CARD. (A) RIG-I domain structure: RIG-I consists of two N-terminal signalling domains (CARD1/2), a helicase domain (Hel-1/2i/2) and a C-terminal domain (CTD). Green arrows indicate binding sites of antibodies used in this study (anti-RIG-I, anti-HIS). The red arrow and circle indicate the predicted area where restrictions by HIV-1 PR occurs. The molecular weight of indicated fragments was calculated based on the gene size using DNA to protein converter on molbiol.ru/eng/scripts. (B) Immuno-blot of RIG-I expressing HEK293T cells, RIG-I only (1) or in combination with wild-type HIV-1 PR (2). Bands detected with anti-RIG-I (B) and anti-HIS (not shown) antibodies show the same fragment sizes. (C) FLP-IN™ 293 T-REX RM cells expressing RIG-I were transfected with HIV-1 PRs, and the IFNβ response was determined 20 hours after transfection using a dual-luciferase reporter assay. Degradation of RIG-I did not induce 2CARD signalling as no IFNβ response was detected in the presence of wild-type HIV-1 PR. RIG-I only (CTRL). N = 3, mean + SD, one-way ANOVA, Dunnett's test. (D) FLP-IN™ 293 T-REX RM cells were transfected with a 2CARD expression plasmid, and a dose-

dependent IFNβ response was detected in a dual-luciferase reporter assay 20 hours after transfection. N = 2, mean + SD. (E) Wild-type and mutant HIV-1 PRs were co-expressed with the 2CARD construct. Protease inhibitor darunavir (DV) was used to control the catalytic activity of the wild-type HIV-1 PR. All samples were compared to control T26A. Additional comparisons as indicated. N = 3, mean + SD, one-way ANOVA, Dunnett's test. **($p<0.01$), ***($p<0.001$), ****($p<0.0001$). Similar results were obtained in two independent experiments.

We confirmed the finding of Yoneyama et al., 2004, that the expression of free RIG-I CARD is sufficient to elicit an IFNβ response, Figure 4.12D. Therefore, to counteract RIG-I signalling, the CARDs have to be destroyed.

RIG-I expressing HEK T-REx RM cells were transfected with a wild-type HIV-1 PR expression plasmid and the IFNβ response was measured using a dual-luciferase reporter assay. No induction of the IFNβ promoter was observed, Figure 4.12C. An expression plasmid containing the same 2CARD expression sequence as published by Yoneyama et al., 2004, was used in a dual-luciferase reporter assay. Dose-dependent induction of the IFNβ promoter was observed, Figure 4.12D. When co-expressed with wild-type HIV-1 PR, the induction of the IFNβ promoter decreased and was restored in the presence of darunavir. Mutant HIV-1 PRs T26A and D25A did not affect the induction of the IFNβ promoter.

4.3 Discussion

HIV-1 PR plays an essential role in the viral life-cycle. It is necessary for the proteolytic processing of the Gag and Gag-Pol polyproteins and the formation of infective particles. Here we show that HIV-1 PR is also capable of mediating the degradation of RIG-I and MDA5, two important innate immune receptors in the context of viral infections. We provide experimental evidence that catalytically active HIV-1 PR directly targets both receptors and that the interaction occurs independently of other cellular factors. The degradation of RIG-I and MDA5 abrogated the detection of stimulatory RNAs and the subsequent induction of type-I IFNs, indicating its potential role as an innate immune evasion mechanism of HIV-1.

We assessed the involvement of the catalytic activity of HIV-1 PR in the degradation of RIG-I using the HIV-1 PR dead mutant D25A, which failed to induce degradation of RIG-I. Further, we showed that wild-type HIV-1 PR induced reduced levels of RIG-I in a concentration-dependent manner and that the protease inhibitor darunavir reversed this effect. These results are contrary to the findings obtained by Solis et al. with the protease inhibitor saquinavir. Different IC50 values have been published for saquinavir in the literature, ranging from 2 nM in C8166 cells to 26 nM in MT4 cells (Dierynck et al., 2007; Roberts et al., 1990). Although the final concentration of saquinavir (5 µM) used by Solis et al. exceeded these concentrations, it needs to be considered that the antiviral activity of saquinavir was determined in cell models or primary cells using live virus with MOIs as low as 0.01 (Dierynck et al., 2007). Higher concentrations may be needed during plasmid expression of HIV-1 PR in mammalian cells. Solis et al. did not control the effectiveness of saquinavir in their experimental setting. In contrast, we used the protease inhibitor darunavir, which has a higher binding affinity to the catalytic centre of HIV-1 PR, of about 100 fold compared to saquinavir (Dierynck et al., 2007). This may explain the different results in overcoming the effect of wild type PR using an HIV-1 protease inhibitor.

An *in-vitro* degradation assay was used to exclude the involvement of cellular factors in the degradation of RIG-I and MDA5. Thereby, MDA5 was identified as a novel, direct target for HIV-1 PR. This finding is contrary to previously published data by Solis et al., who did not observe any effect of HIV-1 PR on MDA5. The different experimental design can explain the outcome of the experiments presented in this thesis. First, Solis et al. used an HIV-1 PR that was tagged with GFP. In contrast, we used an HIV-1 PR that was untagged or incorporated a short signal sequence (HIS-tag). The proteolytic activity of HIV-1 PR is tightly controlled by a mechanism involving structural changes of the protein. Flexible flap regions restrict or allow access to the catalytic centre (Figure 4.1), and different conformational stages have been described for HIV-1 PR (Tóth and Borics, 2006; Yu et al., 2017). The wide-open confirmation is assumed to be necessary for binding of the substrate and is energetically less favoured in comparison to the

closed conformation (Gardner and Abrams, 2019). Maximova et al., 2019, published data providing experimental evidence for the reduced enzymatic activity of HIV-1 PR in crowded solutions. The authors explain their observations with the dynamics of the HIV-1 PR flaps and a slower substrate-enzyme association. We speculate that the GFP-tag used by Solis et al. inhibited the open confirmation of HIV-1 PR and therefore, the interaction of MDA5 and HIV-1 PR was sterically hindered in the presence of the GFP-tag.

It is known that RIG-I and MDA5 undergo conformational changes upon binding of stimulatory RNAs (Zheng et al., 2015). We showed that degradation of MDA5 was not affected by stimulatory RNA analogue poly(I:C). In contrast, degradation of RIG-I was accelerated in the presence of stimulating ligand IVT4. In addition, the degradation pattern of RIG-I changed in the presence of IVT4 and the large degradation product RIG-I' accumulated. The nature of RIG-I and MDA5 could explain the different effects of IVT4 and poly(I:C). First, free MDA5 has a dynamic structure with flexible CARDs (Berke and Modis, 2012), which may expose restriction sites for HIV-1 PR independently of ligand binding. In contrast, free RIG-I was found to have a closed, auto-repressed conformation (Kowalinski et al., 2011). Second, binding of IVT4 may induce conformational changes that expose vulnerable structures and make them more accessible for HIV-1 PR. Finally, IVT4 may mask a restriction site within the helicase domain of RIG-I.

In-vitro degradation experiments revealed a distinct degradation pattern for RIG-I independently of the antibodies (anti-RIG-I or anti-HIS) that were used for detection. We predicted a restriction site within the 2nd CARD or N-terminal linker region based on the fragment sizes observed in immuno-blot experiments. Even though others made attempts to identify and predict HIV-1 PR cleavage sites, no ubiquitous applicable sequences were identified (Impens et al., 2012; Rögnvaldsson et al., 2015). The localisation of the restriction site was of particular interest as free RIG-I CARDs are sufficient to induce an IFNβ response. We questioned if RIG-I degradation by HIV-1 PR could cause an IFNβ response by freeing the CARDs or if a cleavage within the 2nd CARD sequestered RIG-I

signalling: The latter is true. Co-expression of RIG-I and HIV-1 PR did not induce an IFNβ response and signalling induced by a RIG-I 2CARD construct was abrogated by HIV-1 PR. This was shown using a dual-luciferase reporter assay.

We showed that RIG-I and MDA5 are directly targeted by HIV-1 PR and that degradation of both receptors is sufficient to disrupt sensing of stimulatory RNA species. HIV-1 can escape innate immune recognition by MDA5 through other pathways, including the recruitment of cellular factors TAR RNA-binding protein (TRBP) and 2´-O-methyltransferase FTSJ3, which methylates the viral genomic RNA and thereby renders it non-stimulatory for MDA5 (Ringeard et al., 2019). The fact that HIV-1 PR degrades MDA5 hints at the role of MDA5 in affecting or sensing virus production. Others have shown that the overexpression of MDA5 increased viral replication as measured by p24 expression in HIV-1 infected HeLa-CD4 cells (Cocude et al., 2003).

In other work, translocation of MDA5 to the nuclear fraction in HIV-1-infected but not in mock-infected cells was impaired. The effect occurred during late (after 24 h) but not during early (4-8 h) infection. MDA5 has also been identified as a target for caspase-3 and caspase-8 during apoptosis, freeing the helicase domain from the CARDs, allowing for translocation to the nucleus and the modulation of the chromatin structure (Kovacsovics et al., 2002). The lack of follow-up studies limits the understanding of the biological function of these effects and if viral replication is positively or negatively affected by the degradation of MDA5. On the one hand, the complete degradation of MDA5 may prevent excessive production of viral proteins, thereby limiting cytotoxic effects and inhibiting apoptosis. On the other hand, cleavage of MDA5 may mimic the processing by caspases eight and three, thereby boosting viral replication.

For RIG-I, the triphosphatase DUSP11 is downregulated by the viral protein vpr during HIV-1 infection. This leads to the accumulation of endogenous triphosphate Y-RNAs, which can stimulate RIG-I (Vabret et al., 2019). Degradation of RIG-I by HIV-1 PR may counteract this mechanism.

In future work, it would be of interest to determine how the use of small molecule protease inhibitors affects the innate immune response during untreated HIV-1 infection or on viral protein expression in CD4+ T-cells from PLWH on ART. It is known that type-I IFN in the blood of HIV-1 infected individuals decreases to base levels after antiretroviral therapy (ART) is started (Hardy et al., 2013). Plasmacytoid dendritic cells (pDCS) were identified as the main producers of type-I IFN during primary HIV-1 infection, which sense the virus mainly through TLR7 (Beignon et al., 2005; Lepelley et al., 2011; Li et al., 2014). The substantial contribution of pDCs to type-I IFN levels may mask other effects at the level of infected CD4 T cells. Even though the overall type-I IFN response is reduced during ART, treatment regimens, including HIV-1 PR inhibitors, may demonstrate different outcomes compared to regimens, including other classes of antiretrovirals. One relevant example is the demonstration of ongoing expression of ISGs during *de novo* HIV-1 infection of monocyte-derived macrophages in the presence of protease inhibitor ritonavir, but not during treatment with other antiretrovirals (reverse transcriptase inhibitor zidovudine; integrase inhibitor raltegravir) (Nasr et al., 2017). The same study found that the expression of ISGs was dependent on MAVS, the signalling adaptor for RIG-I and MDA5. One potential explanation for this is that in the setting of a protease inhibitor, detection of cellular viral RNA can occur by activation of RIG-I or MDA5. In the absence of a protease inhibitor, this pathway is inactive due to the degradation of RIG-I or MDA5.

The impact of protease inhibitors on RIG-I and MDA5 may also be relevant in the context of shock and kill strategies. These aim to increase the expression of RNA from the latent virus with the aim of stimulating virus-induced or immune-mediated cytolysis. Restoring innate immune sensing during viral reactivation could promote more robust cellular defence mechanisms and probably the clearance of productively infected cells. HIV-1-PR inhibitors could play an essential role in the redesign of shock and kill strategies.

5. Aim 3: Generation of RIG-I-, MDA5- and MAVS-deficient cell lines and the effect on HIV-1 infection

5.1 Introduction

We showed that HIV-1 protease targets innate immune sensors RIG-I and MDA5 and that sensing of foreign RNA species is abrogated following their degradation. This is of importance as others have reported that RIG-I and MDA5 can directly or indirectly sense HIV-1 replication in infected cells (Nasr et al., 2017; Ringeard et al., 2019; M. Q. Wang et al., 2015). Activation of these sensors can induce an antiviral type-I IFN response in infected and uninfected cells, as outlined in previous sections, and the ability of the virus to eliminate sensors of the innate immune system could be beneficial for its replication and spread. Each HIV-1 particle contains an estimated 93-316 copies of protease (depending on the size of the particle, 60-100 nm), which are released into the cytoplasm following infection (Carlson et al., 2008). It was shown that the protease content of HIV-1 particles was sufficient to reduce RIG-I protein levels during early time points of *de novo* HIV-1 infection of THP-1 cells (Solis et al., 2011). The release of type-I IFNs by pDCs was shown to prevent the establishment of latent HIV-1 infection (van der Sluis et al., 2020). The same study has found that *in vitro* or *ex vivo* IFNα treatment-induced latency reversal in a model of latency or in cells derived from PLWH, respectively. It remains unclear if the remaining RIG-I and MDA5 protein levels in *de novo* or productively HIV-1 infected CD4 T cells affect latency formation, replication and spread of the virus. Assuming that residual RIG-I and MDA5 protein levels would allow viral sensing to a certain degree, we hypothesised that the establishment of latency and viral replication would be more efficient in RIG-I- and MDA5-deficient cells when compared to wildtype cells.

To address our hypothesis, we aimed to generate Jurkat and primary CD4 T cell lines that were deficient for RIG-I, MDA5 and their signalling adaptor MAVS. We identified and characterised several cell lines that were deficient for one of the targeted proteins and studied HIV-1 replication in some of these cell lines.

5.2 Results

5.2.1 Generation of RIG-I, MDA5 and MAVS deficient cell lines

We generated RIG-I-, MDA5- and MAVS-deficient cell lines by using the CRISPR/Cas9 gene-editing system (Jinek et al., 2012). Recombinant endonuclease (Cas9) was complexed with a guide RNA targeting *DDX58* (RIG-I), *IFIH1* (MDA5) or *MAVS*. The complexes were delivered to cells by electroporation. Manipulated cells were expanded from single cells or small cell populations (≤ 5 cells) to generate monoclonal or polyclonal cell lines. Cell lines deficient for RIG-I, MDA5 and MAVS, were identified using western blot analysis. Representative results for the analysed Jurkat cell lines are shown in Figure 5.1.

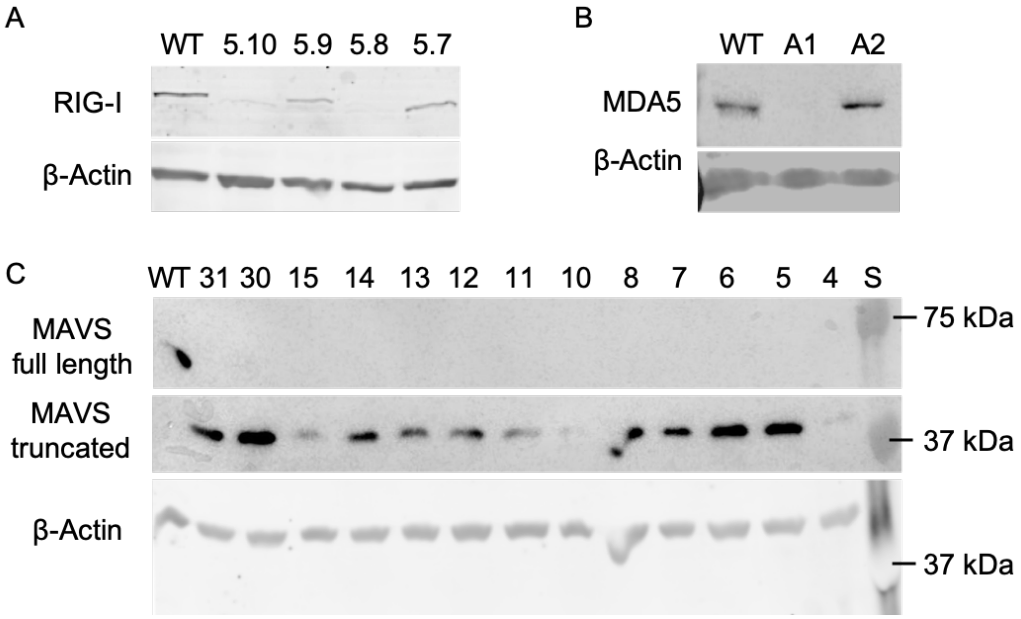

Figure 5.1: Verification of RIG-I-, MDA5- and MAVS-deficient Jurkat cell lines. Jurkat cells were treated with the CRISPR/Cas9 system that targeted either *DDX58* (RIG-I), *IFIH1* (MDA5) or *MAVS*. Cell lines were grown from single cells or polyclonal cell populations (≤5 cells). RIG-I and MDA5 deficient cell lines were incubated with type-I IFN (1000 U IFN/mL) overnight to upregulate RIG-I and MDA5 expression and to allow detection via immuno-blotting. Representative western blots of RIG-I (A), MDA5 (B) and MAVS (C) are shown. Each column represents a different clone which was labelled with either a number or letter. Proteins were detected with antibodies against RIG-I, MDA5, MAVS and β-Actin was used as a loading control. Wildtype (WT), protein standard ladder (S).

The guide RNAs efficiently targeted *DDX58*, *IFIH1* and *MAVS* and we identified Jurkat cell lines deficient for RIG-I, MDA5 and MAVS (see Figure 5.1). The guide RNA targeting *MAVS* did not cause the loss of MAVS in all clones but led to the

formation of a truncated protein with a molecular weight of approximately 37 kDa in some of the clones. Only one *IFIH1* (MDA5) KO cell line was recovered.

We next used the same approach to generate RIG-I-deficient primary CD4 T cell lines. Due to expected donor variation, we generated these cell lines using CD4 T cells derived from four different blood donors. A representative western blot to confirm RIG-I-deficiency is shown in Figure 5.2.

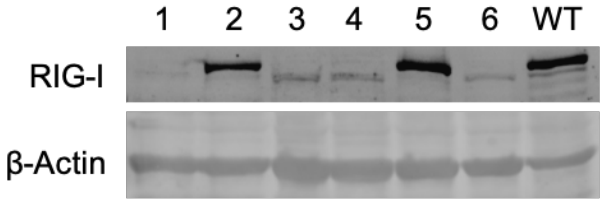

Figure 5.2: Verification of RIG-I-deficient primary CD4 T cells. CRISPR/Cas9 treated primary CD4 T cells were clonally expanded and incubated with type-I IFN to induce RIG-I expression. Whole-cell lysates were analysed for RIG-I using immunoblotting. β-Actin was used as a loading control. Each column represents a different clone. The immunoblot shows samples derived from donor 4 and is representative of a total of four donors

An overview of the generated Jurkat and primary CD4 T cell lines is shown in Table 5.1.

Table 5.1: RIG-I-, MDA5- and MAVS-deficient cell lines generated in this thesis. Jurkat and primary CD4 T cells were treated with the CRISPR/Cas9 system targeting either *DDX58* (RIG-I), *IFIH1* (MDA5) or *MAVS*. The table summarises all knockout cell lines (KO) that were confirmed via western blot.

Target	#KO cell lines – Jurkat	#KO cell lines – primary CD4 T cells
DDX58 (RIG-I)	8	47 (four different blood donors)
IFIH1 (MDA5)	1	-
MAVS	15 (truncated or KO)	-

5.2.2 Maintenance and characterisation of RIG-I deficient primary CD4 T cell lines

The generation of primary KO CD4 T cell lines took between six to ten weeks, a reasonable long propagation time for primary cells. In comparison to Jurkat cell lines, which proliferate without external stimulation, CD4 T cells had to be repeatedly activated with CD3/CD28 beads to maintain their proliferative state.

Some of these clones became unresponsive towards further CD3/CD28 activation and cell lines with this feature were discontinued and excluded from other experiments.

Given that the activation status of CD4 T cells affects their susceptibility towards HIV-1 infection and viral replication (Stevenson et al., 1990), we characterised the expression of early and late activation markers CD25 and HLA-DR, respectively, in selected cell clones, Figure 5.3.

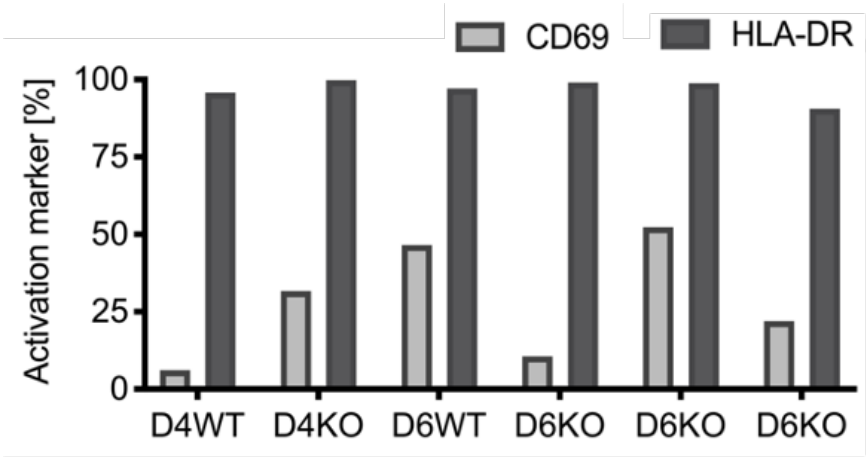

Figure 5.3: Activation status of RIG-I-deficient primary CD4 T cells. RIG-I KO clones from two donors were analysed for early and late activation markers CD69 and HLA-DR. D4 (Donor 4), D6 (Donor 6), WT (wildtype control), KO (knockout (*DDX58*/RIG-I)).

Each of the CD4 T cell lines showed a high expression of late activation marker HLA-DR. Expression of the early activation marker CD25 differed widely between cell lines (5-50 % of cells were positive for CD25). Once the activation with CD3/CD28 beads was ceased, cell numbers significantly decreased (near complete loss of cells).

As mentioned before, susceptibility to HIV-1 infection and the progression to a productive or latent infection is dependent on multiple factors, including the activation status of the infected cell. To study the effect of RIG-I on HIV-1 infection, it was essential to reduce other factors that affect HIV-1 infection and replication. We therefore next aimed to synchronise CD4 T cell activation to generate cell lines with a similar activation status. One way to achieve this was

to induce activated CD4 T cell lines to revert to a memory or resting state and simultaneously re-activate them at the start of an experiment. Therefore, we tried an experimental condition that was previously described in literature to promote memory formation in activated CD4 T cells by reduced levels of IL-2 (Firpo et al., 1994; Kaartinen et al., 2017). At first, we removed the CD3/CD28 beads from the cells to prevent further rounds of activation. Cells were then cultivated with gradually reduced levels of IL-2. The reduction of IL-2 after the removal of the CD3/CD28 beads did not improve cell survival. Removal of the CD3/CD28 beads while maintaining high levels of IL-2 (100 U/mL) also induced the near complete loss of cells.

The heterogeneity of the primary CD4 T cell lines in regards to their activation status was a major obstacle to study HIV-1 infection and latency formation in these cells. We were expecting difficulties in comparing and interpreting experimental outcomes of HIV-1 infection experiments. Since it appeared not possible to achieve synchronisation of T cells within the time frame of this doctoral thesis, this project was not pursued.

5.2.2 Effect of RIG-I on productive infection of Jurkat cell line

To determine the effects of RIG-I on productive HIV-1 infection, RIG-I deficient and wildtype Jurkat cells were infected with an X4-tropic HIV-1 GFP reporter virus. Productively infected cells become GFP positive and can be detected with a flow cytometer, Figure 5.4.

HIV-1 productively infected wildtype Jurkat cells with a frequency of 2.5-3.0 %. RIG-I deficiency was not found to affect the susceptibility of Jurkat cell lines to productive HIV-1 infection. The frequency of productively infected cells varied from 2.0 to 7.0 % in RIG-I-deficient cell lines. We further characterised these cells and measured the expression of co-entry receptor CXCR4, which is differentially expressed in dependence of the T cell activation status (Bermejo et al., 1998), Figure 5.5A.

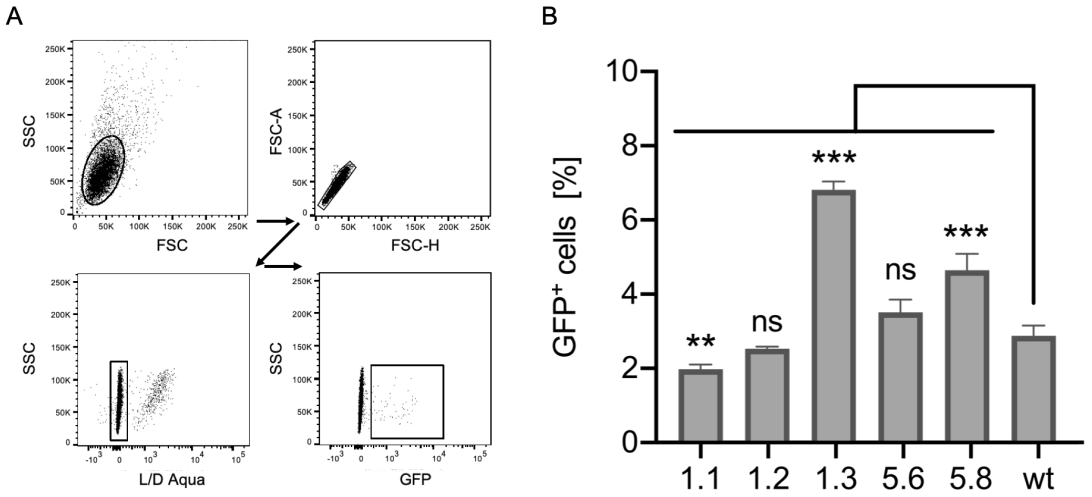

Figure 5.4: Productive HIV-1 infection in RIG-I deficient Jurkat cell clones. RIG-I deficient Jurkat cell clones were infected with an X4-tropic HIV-1 GFP reporter virus (MOI of 0.5). Forty-eight hours after infection, the frequency of GFP positive (productively infected) cells was estimated using flow cytometry. A) Gating strategy of the flow experiment, gate hierarchy as indicated by arrows. Gates were set on the target cell population, followed by the selection of single cells and live cells. GFP positive cells were selected from the live cell population. B) Frequency of GFP positive cells in wildtype (wt) or RIG-I deficient cell clones. Each Jurkat knock out clone is indicated by a different number. N = 3, mean + SD. One-way ANOVA, Dunnett's test. **($p<0.01$), ***($p<0.001$), ns (not significant).

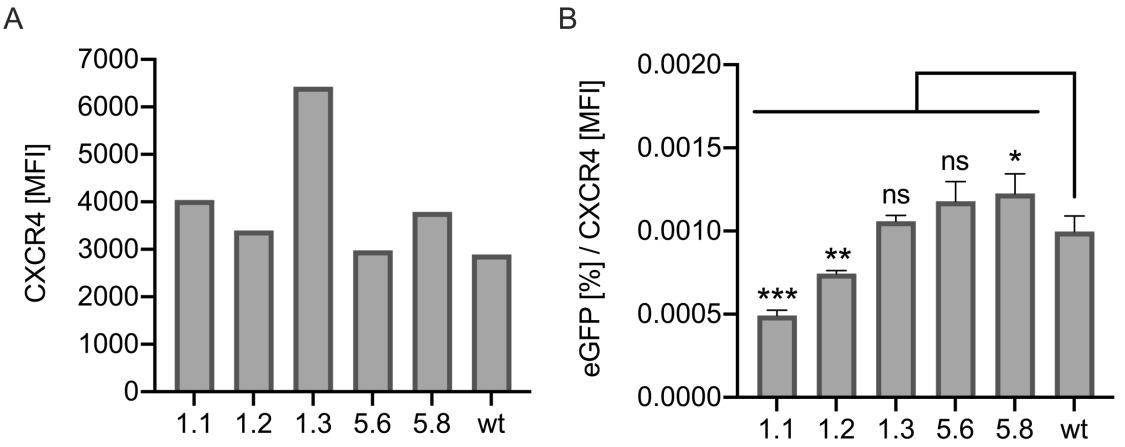

Figure 5.5: CXCR4 expression levels in Jurkat cell clones and the effect on productive HIV-1 infection. A) RIG-I deficient of wildtype (wt) Jurkat cell clones were stained with an anti-CXCR4 antibody, measured using flow cytometry, and the mean fluorescence intensity (MFI) was estimated using FACSDiva software. B) The frequency of HIV-1 productively infected (GFP positive) cells (as shown in Figure 5.B) was divided by the MFI of the CXCR4 receptor (as shown in this figure, part A). RIG-I deficient cell lines were compared to the wildtype. One experiment with n = 3, mean + SD. One-way ANOVA, Dunnett's test. *($p<0.05$), ***($p<0.001$), ns (not significant).

We found that the expression levels of co-entry receptor CXCR4 varied between different Jurkat cell clones. Susceptibility towards productive HIV-1 infection correlated with the expression levels of CXCR4. The frequency of productively HIV-1 infected cells were normalised to the expression levels of CXCR4, Figure 5.5B. One cell line (1.1) showed a significant reduction of productive HIV-1 infection, while clones 1.3 and 5.8 showed an increase in infection.

We next hypothesised that the RIG-I knock out effected proliferative activity and this could alter HIV-1 infection. Proliferative activity was measured with CellTiter96® and only one out of five analysed RIG-I-deficient cell lines (1.1) showed a significantly reduced proliferative activity compared to the wildtype control, Figure 5.6.

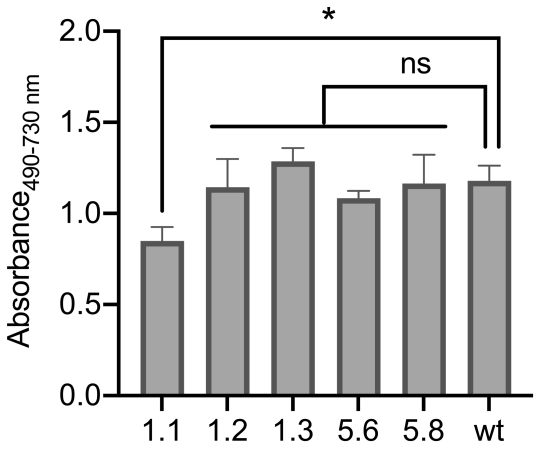

Figure 5.6: Proliferative activity of selected RIG-I-deficient Jurkat cell lines. A reporter assay (CellTiter 96®) was used to determine the proliferative activity of RIG-I-deficient Jurkat cell lines. Wildtype (wt). N = 3, mean + SD. One-way ANOVA, Dunnett's test. *($p<0.05$), ns (not significant).

In summary, Jurkat cell lines deficient for RIG-I, MDA5 and MAVS and primary cell lines deficient for RIG-I were generated in this thesis. Clonal effects in Jurkat and primary cell lines, which can possibly affect HIV-1 infection, became evident. In one pilot experiment, levels of productive HIV-1 infection in Jurkat cells varied between clones and could not be explained with the presence or absence of RIG-I. Time constraints put a stop to this part of the project. Cell lines generated in this thesis will be further characterised (e.g. the expression of exhaustion markers PD-1 and LAG-3 (Niu et al., 2019)) for their use in future projects.

5.3 Discussion

We generated RIG-I-, MDA5- and MAVS-deficient Jurkat and RIG-I-deficient primary CD4 T cell lines using the CRISPR/Cas9 gene-editing system. We observed effects of the clonal selection of cell lines on the HIV-1 entry receptor CXCR4 expression and this level of expression correlated with the susceptibility of these cells for productive HIV-1 infection. Primary CD4 T cell lines with a RIG-I knock out were successfully generated and maintained but showed signs of activation with high levels of expression of HLA-DR. The RIG-I deficient Jurkat cell lines were permissive to HIV-1 infection, but meaningful comparisons to wild type cell lines will require further experiments.

5.3.1 Generation of knockout cell lines

Guide RNAs targeting *DDX58* and *IFIH1* were successful in generating RIG-I- and MDA5-deficient Jurkat cell lines. The *MAVS*-targeting guide RNA did not induce the loss of MAVS in all clones but led to the formation of a truncated protein with a molecular weight of approximately 37 kDa in some cell lines. In comparison, full-length MAVS has a predicted molecular weight of approximately 75 kDa (we repeatedly detected wildtype MAVS at ~70 kDa in CD4 T cell lysates). Several polycistronic *MAVS* splice variants that give rise to at least nine MAVS isoforms have been identified so far (Brubaker et al., 2014; Lad et al., 2008; Ota et al., 2004; Qi et al., 2017; Seth et al., 2005), Figure 5.7.

The Crispr/Cas9 guide RNA used in this thesis targets a sequence that is located within exon five of *MAVS*, Figure 5.7. Interruption of this exon may not be sufficient to eliminate all existing MAVS isoforms. We speculate that the expression of a truncated MAVS isoform is sufficient to disrupt the signalling of RLRs.

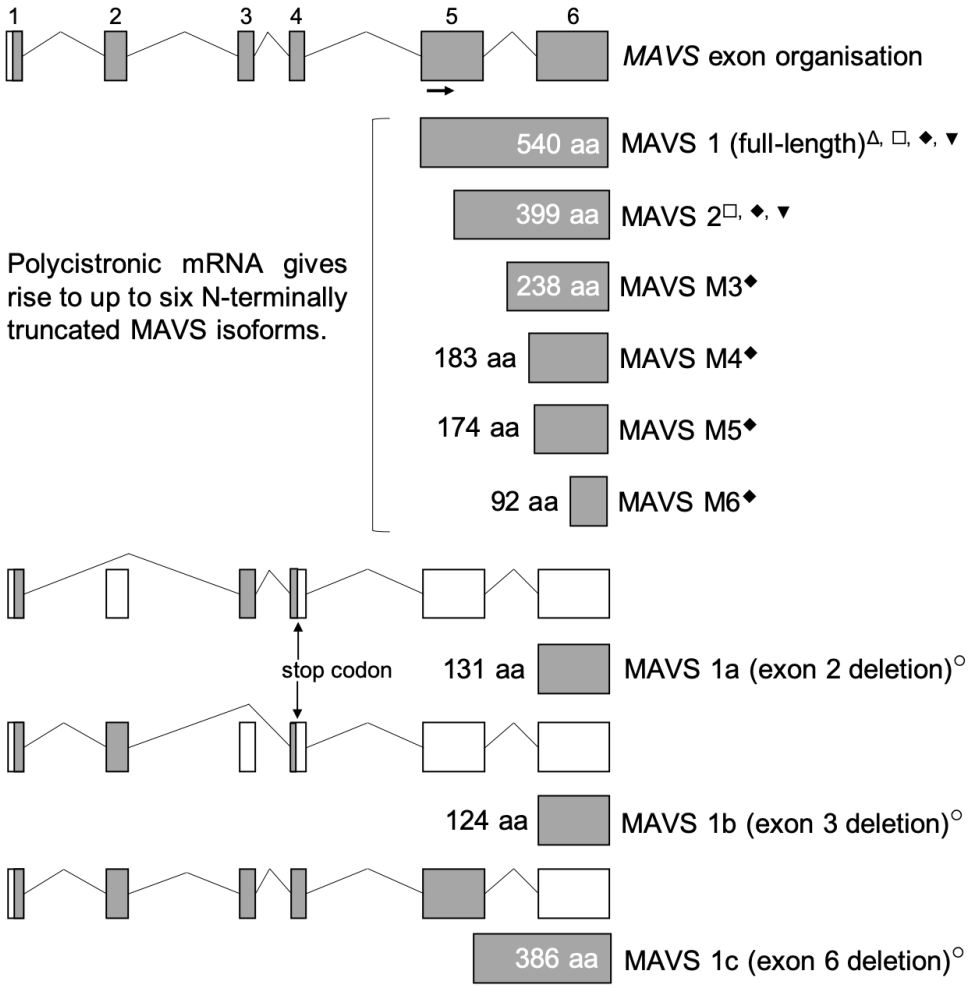

Figure 5.7: MAVS isoforms. Several isoforms of the mitochondrial antiviral-signalling protein (MAVS) were observed in many reports. Up to six isoforms are translated from a single full-length *MAVS* transcript and an additional three isoforms were described to result from alternative splicing. The CRISPR/Cas9 system used in this thesis was targeted against a gene region within exon 5 of *MAVS* (indicated with →). References: Seth et al., 2005 (Δ), Brubaker et al., 2014(□), Qi et al., 2017(◆), Ota et al., 2004(▼), Lad et al., 2008(○).

Full-length MAVS has an N-terminal CARD and a C-terminal transmembrane domain and both domains are essential for signal transduction and localisation within the mitochondrial membrane, respectively (Hou et al., 2011; Seth et al., 2005). All previously described MAVS isoforms other than full-length MAVS are either N-terminally truncated and are missing the CARD domain, or are splice variants with reading-frame shifts or are missing the C-terminal transmembrane domain (Lad et al., 2008; Qi et al., 2017).

Further characterisation of the cell lines generated in this thesis will be necessary to prove that the knockouts are functional. This could be done using specific ligands for RIG-I and MDA5 and by measuring the type-I IFN response in wildtype and knockout cell lines following stimulation. Additionally, the CRISPR/Cas9-targeted gene regions could be sequenced to confirm the genetic manipulation and to specify the introduced mutations.

The process of generating RIG-I-deficient primary CD4 T cells was successful. We observed unresponsiveness towards CD3/CD28 activation in several clones during the expansion phase following the CRISPR/Cas9 manipulation. This indicates a state of CD4 T cell exhaustion which can occur following prolonged T cell activation (Balkhi et al., 2018). Together, these observations show that the time-consuming process of generating knockout cell lines from small CD4 T cell populations can induce T cell exhaustion and cellular senescence. This is of importance in the context of HIV-1 infection as exhausted CD4 T cells show epigenetic, transcriptional, metabolic and functional abnormalities which can potentially affect their susceptibility to HIV-1 infection (Balkhi et al., 2018; Crawford et al., 2014; Patsoukis et al., 2015; Rezaei, 2018).

The characterisation of some of the generated primary cell lines showed apparent differences in their activation status, which prevented their direct use in HIV-1 infectivity assays. The removal of activating beads resulted in the loss of cells, which reflects the process of effector cell contraction after pathogen clearance observed *in vivo* (De Boer et al., 2003; Román et al., 2002).

Despite the availability of different latently HIV-1 infected cell lines, it is crucial to study host-virus interactions in primary cells. Others have shown that latently infected cell lines differ from each other and primary cells derived from PLWH (Telwatte et al., 2019). The authors identified differences in HIV-1 integration sites, HIV-1 transcription profiles and expression levels of antiviral defence pathways. Therefore, further optimisation is needed to generate primary CD4 T cell lines that can be used to study HIV-1 infection. These cells will require

monitoring for different immune checkpoint markers to ensure low and similar levels of exhaustion to minimise secondary effects on HIV-1 replication.

5.3.2 The effect of RIG-I on HIV-1 infection in Jurkat cells

We performed HIV-1 infection experiments in RIG-I-deficient Jurkat cell lines and a significantly lower productive HIV-1 infection was observed in one clone (1.1). One explanation could be the reduced proliferative activity of this clone, which was reduced considerably in comparison to wildtype cells. Based on these data, the role of RIG-I during productive HIV-1 infection in Jurkat cells stays inconclusive. We only studied a small proportion of the generated RIG-I-deficient cell lines in comparison to one wildtype control so far. More knockout and wildtype cell lines need to be included in further studies to conclude the effect of RIG-I on productive HIV-1 infection. Furthermore, the degradation of RIG-I by HIV-1 PR, as shown in Aim 2 of this thesis, could diminish the effects of the complete loss of RIG-I during productive HIV-1 infection. The generated cell lines could be used as controls in experiments involving HIV-PR inhibitors to restore innate immune sensing and to differentiate between effects mediated by RIG-I and protease inhibitors.

Furthermore, the characterisation of the studied cell lines was limited to their proliferative activity and CXCR4 co-receptor expression. Additional data with more cell lines are needed. Utilising MDA5- and MAVS-deficient cell lines will add more knowledge on the role of the RIG-I and MDA5 signalling pathways during HIV-1 infection. Studies, including the MDA5- and MAVS-deficient cell lines, exceeded the scope of this thesis. Still, the generation of these cell lines provides the foundation for future investigations addressing the role of these proteins and their underlying pathways in HIV-1 infection.

Clonal effects could be circumvented in future studies by using bulk cell populations. We observed satisfactory knockout efficiencies above 50 % in Jurkat and primary CD4 T cells. Knockout efficiencies could be further increased by a second round of CRISPR/Cas9 editing. The bulk approach could significantly

reduce the handling time of the cells and probably positively affect cell viability and signs of T cell exhaustion in primary cells.

6. General Discussion

Our overall goal was to determine the role of the innate RNA sensor RIG-I in viral infection of CD4 T cells. Several studies have reported transcriptomic data for resting and activated CD4 T cells in different settings (Helgeland et al., 2020; Sousa et al., 2019). To our knowledge, we were the first to study changes of the transcriptome in resting human CD4 T cells following the specific stimulation of the innate immune sensor RIG-I. We detected the induction of ISGs, indicative of the effective priming of these cells for a broad, cell-autonomous antiviral response. Furthermore, we demonstrated the downregulation of pathways that are connected to T cell activation. We validated our findings *in vitro* and found decreased metabolic and proliferative activities in CD4 T cells following RIG-I activation. By utilising an antigen-specific, co-culture model for CD4 T cell activation, we could show that the effector function (measured by IFNγ release) of CD4 T cells were also decreased following RIG-I activation.

We discovered that HIV-1-PR directly degrades RIG-I and MDA5. The sensing of RIG-I and MDA5 agonists was abrogated in the presence of HIV-1-PR, hinting to a possible immune evasion mechanism for HIV-1.

During the course of this project, Jurkat and primary CD4 T cell lines were generated, which will allow future *in vitro* studies of the role of RIG-I, MDA5 and their downstream adaptor MAVS during HIV-1 infection.

6.1 Harnessing the RIG-I-mediated T cell priming for novel HIV-1 therapies

It remains unclear if the *in vitro* effects on CD4 T cells (reduced proliferation, metabolic activity and effector function) following RIG-I activation occur *in vivo*. While many preclinical and clinical studies report benefits of RIG-I activation as part of novel cancer therapies or as an adjuvant in immunisation regimens against viral infections (reviewed in Iurescia et al., 2020 and Yong and Luo, 2018), RIG-I activation in CD4 T-cells has not been studied *in vivo* to date. The main limitation in undertaking these studies is the lack of a CD4 T cell-specific delivery system for RIG-I ligands *in vivo*. The development of such a system is one area of

research undertaken by members of our group, where we are generating nanoparticles that can be loaded with RIG-I agonists (and other drugs) to target surface receptors on CD4 T cells to enhance cell-type-specific uptake.

An orally administered RIG-I agonist (inarigivir soproxil) was recently investigated as a treatment for chronic hepatitis B virus (HBV) in a clinical trial but caused severe liver injury in some virally-suppressed chronic HBV patients (NCT04059198). In a previous study with healthy subjects, no severe adverse effects became evident, but more than 40 % of the participants reported non-severe adverse effects (NCT034936). The study outcomes were not published in full to date, and it stays unclear if the liver toxicity was primarily caused by inarigivir soproxil (e.g. toxic metabolites) or RIG-I activation and its effects on chronic HBV patients. Immunologic responses following RIG-I activation might cause adverse effects in infected tissues and might limit its use in the clearance of persistent, viral infections.

In contrast to this clinical trial in chronic HBV, RIG-I agonists have been effectively used in cancer cure strategies. RIG-I activation can mediate NK and CD8 T cell-dependent killing of tumour cells *in vitro* (Daßler-Plenker et al., 2019; Duewell et al., 2014) and intratumorally delivered compounds were found to be safe in animal and human studies (reviewed in Iurescia et al., 2020). The systemic administration of a RIG-I agonist enhanced survival and led to long-term remission in mice with acute myeloid leukemia (Ruzicka et al., 2020). These studies highlight that therapeutic RIG-I activation can be safe in certain settings. The potential to harness this pathway for viral infections like HIV-1 will depend on the generation of drugs and drug-delivery methods that have a tolerable side-effect profile (e.g. targeted delivery of RIG-I agonists with nanoparticles, as mentioned above).

6.2 Protecting cellular RNA sensing pathways to sensitise cells for HIV-1 and therapeutic RLR activation

RIG-I and MDA5 are known sensors for HIV-1 infection, as discussed previously (chapter 1). We identified active HIV-1 PR was responsible for the specific degradation of RIG-I. We also demonstrated that HIV-1 PR targets and can degrade MDA5. HIV-1 protease inhibitors are widely used for the treatment of HIV-1 infection (Phanuphak and Gulick, 2020) and could potentially be used to specifically prevent the degradation of RIG-I and MDA5 *in vivo* as a novel strategy to enhance innate immune activation and potentially cell death following latency reversal. In HIV-1 latency, there is limited expression of HIV-1 RNA or HIV-1 protein from the integrated pro-virus. Following latency reversal, the production of viral RNA and protein and endogenous Y-RNAs should theoretically be detected by innate factors such as RIG-I and MDA5 (Ringeard et al., 2019; Vabret et al., 2019). Our work is consistent with a hypothesis that these pathways are potentially disabled by HIV-1 protease. We therefore provide a rationale for investigating the effects of latency reversal in the presence and absence of protease inhibitors.

Precursor HIV-1 protease is translated as part of the Gag-pol polyprotein and has limited activity and possibly a different specificity than mature HIV-1 protease (Huang et al., 2019, 2011). The processing of Gag and Gag-pol by HIV-1 protease mainly occurs during particle assembly or shortly after and small amounts of mature HIV-1 protease do not interfere with this process (Könnyű et al., 2013). In contrast: the overexpression of the Gag-pol polyprotein enhanced the proteolytic processing of Gag and Gag-pol and abrogated virion production (Park and Morrow, 1991). Some non-nucleotide reverse transcriptase inhibitors (NNRTIs) accelerated Gag-pol processing by promoting the formation of Gag-pol homodimers (Figueiredo et al., 2006). NNRTI-accelerated Gag-pol maturation induced CARD8-dependend pyroptosis in productively HIV-1 infected cell lines and *ex vivo* samples, which was dependent on HIV-1 protease activity (Wang et al., 2021). The existence of processed Gag and Gag-pol polyproteins in productively infected cells indicated the presence of active HIV-1 protease in

absence of NNRTIs (Figueiredo et al., 2006; Park and Morrow, 1991; Wang et al., 2021). Basal levels of mature HIV-1 protease might be sufficient to silence RIG-I- and MDA5-mediated immune sensing. Wang et al, 2021, showed that CARD8 cleavage occurred in the absence of NNRTIs and was significantly accelerated once NNRTIs were added to the cells, but only the latter induced cell death. It stays unclear if CARD8 activation plays a role during *de novo* HIV-1 infection, as incoming viral particles release mature viral protease into the cytoplasm (degradation of RIG-I occurred during *de novo* infection and was mediated by HIV-1 protease (Solis et al., 2011)). The effects of latency reversal on RIG-I and MDA5 protein levels require evaluation in future studies.

There are limited data available on the effects of HIV-1 treatment regimens with or without protease inhibitors on the innate immune response and the HIV-1 reservoir size. The protease inhibitor ritonavir, but not other antivirals, mediated the ongoing expression of ISGs following HIV-1 infection of monocyte-derived macrophages *in vitro* (Nasr et al., 2017). In another study, there was no difference in the size of the reservoir in PLWH on ART who were receiving a protease inhibitors (lopinavir/ritonavir) containing regimen compared to those who were not (Pasquereau et al., 2018). The specific role of protease inhibitors in restoring innate immune sensing during *in vivo* reactivation of latent virus and their potential to increase cellular sensitivity to therapeutic RLR activation (as discussed above) has not been addressed yet.

It would be of interest to validate the results obtained by Nasr et al., 2017, in T cell lines and primary CD4 T cells. If protease inhibitors mediated ongoing ISG expression in these cells, the experimental layout could be extended to study immune activation in different settings, including activated T cells (productive HIV-1 infection) or resting T cells (latent HIV-1 infection) and the impact of different CD4 T cell subsets. We would expect sustained type-I IFN expression during productive infection in activated CD4 T cells in the presence of protease inhibitors. The effects of protease inhibitors on immune activation in resting CD4 T cells during latent infection would be expected to be less significant, assuming

there is low or incomplete HIV-1 transcription in a non-activated cell (Yukl et al., 2018).

The effect of protease inhibitors on immune activation during HIV-1 infection is of particular interest in HIV-1 cure strategies. If innate immunity could be restored by protease inhibitors during latency reversal, the clearance of the viral reservoir could be more efficient. Clearance of infected cells involves innate and adaptive immune responses, which can only be studied *in vivo* due to their full complexity. Well established humanised mouse models are available to study HIV-1 infection and the interactions with the human immune system *in vivo* (reviewed in Marsden and Zack, 2017). These models are based on immunodeficient mice that support engraftment with transplanted human cells to partly or near-completely re-constitute the human immune system. Restoring innate immune sensors with protease inhibitor treatment could be investigated in combination with latency-reversing agents, RIG-I agonists (immune activation) or immune checkpoint blockades (cell death) in mouse models for HIV-1 infection. It is noteworthy that these animal models are limited by their relatively short timeframe of infection, possible adverse effects of immune transplants (GvHD) and ongoing immune cell activation despite ART (reviewed in Marsden, 2020). The latter might be an obstacle in evaluating chronic immune activation in HIV-infected mice on ART, in the presence or absence of protease inhibitors.

Antiretroviral treatment regimens with or without protease inhibitors are well established and human *ex vivo* studies could be easily undertaken to investigate the impact of protease inhibitors on the immune system and ongoing inflammation. It would be of interest to monitor immune activation markers (e.g. type-I IFNs, ISGs) in human blood samples from PLWH and if these markers differ depending on the treatment type (incl./excl. protease inhibitors). This is of importance as type-I IFN responses help to control early viral infection but could have detrimental long-term effects (chronic immune activation), as discussed in the next section. If protease inhibitors enhance the expression of ISGs *in vivo* (indicative for ongoing innate immune activation) as seen in HIV-1 infection of

monocyte-derived macrophages *in vitro* (Nasr et al., 2017) and do not help to reduce the reservoir size in humans (Pasquereau et al., 2018), they should be avoided in long-term ART to prevent ongoing immune activation.

6.3 RIG-I activation – more effective than type-I IFN monotherapies?

Type-I IFNs are widely used as therapeutics for different indications: recombinant IFNα2 is used to treat cancer and chronic viral infections (HBV, HCV) and recombinant IFNβ is in use to treat multiple sclerosis (reviewed in Lazear et al., 2019). RIG-I mediates type-I IFN responses and is under investigation as a therapeutic target with similar applications to type-I IFNs, e.g. for cancer and viral infections.

The effect of type-I IFNs on HIV-1 infection has been broadly studied. Our group has recently shown that IFNα can induce T cell activation and reverse HIV-1 latency using an in vitro model of HIV-1 latency and also CD4 T-cells from people with HIV-1 (van der Sluis et al., 2020). IFNα alone has been extensively studied in HIV-1 infection of humans and humanised mice and following SIV infection of macaques, including the following. In humanised mice, IFNα reduced the replication of HIV-1 once acute infection was established (Lavender et al., 2016). In PLWH on ART, IFNα monotherapy reduced HIV-1 replication and cell-associated HIV-1 DNA (Azzoni et al., 2013). A follow-up study by the same group reported IFNα-mediated changes of the cell-surface glycome in CD8 T cells. The authors hypothesised that this could potentially explain reduced HIV-gag-specific CD8 T cell responses, and therefore an adverse effect of IFNα treatment (Giron et al., 2020). Long-term recombinant IFNα treatment-induced IFNα antibodies or autoantibodies, which caused the unresponsiveness to IFNα treatment and the onset of auto-immune diseases (Aruna and Li, 2018; Mandac et al., 2006; Scagnolari et al., 2012). It is unclear if RIG-I agonists would have similar adverse effects to exogenous type-I interferons. Prolonged endogenous type-I IFN signalling has been associated with autoimmune diseases like systemic lupus erythematosus and rheumatoid arthritis (Castañeda-Delgado et al., 2017; Shao et al., 2016).

The wide-ranging effects of IFNα have also been studied following SIV infection. In SIV infected macaques on ART, IFNα had no effect on the viral reservoir (Palesch et al., 2018). When IFNα was administered prior to SIV infection, there was reduced acquisition of SIV infection and also reduced numbers of founder viruses if infection occurred (Sandler et al., 2014).

Although we didn't directly examine this in our work, it would be of interest to determine the impact of CD4 T cell-specific delivery of RIG-I ligands on the latent HIV-1 reservoir. Linehan et al., 2017, reported broad immunologic effects of systemic RIG-I activation in mice. They found a strong upregulation of type-I IFNs and ISGs, but also of chemokine receptors (*CCR5, CCR7*), chemokines (*CCL2, CCL3, CCL4*), cellular remodelling factors (*VAV3, SATB2*) and other known immune factors (*TNFSF4* (OX40L), *VDR*), among others. Given the broad effects of RIG-I activation on the immune system, its activation might be superior to type-I IFN treatment and could be targeted as a novel component in future HIV-1 cure strategies and treatment regimen.

We would expect varying outcomes of RIG-I activation relative to different stages of HIV-1 infection: 1) Before infection, 2) during the acute phase of infection, 3) during viral suppression on ART.

1) Even though RIG-I activation could possibly reduce the risk of acquiring HIV-1 similar to IFNα, it should not be considered as a preventive treatment for the following reasons. RIG-I agonists are strong immunomodulators, which can induce an immunologic response with possible short- and long-term adverse effects in otherwise healthy individuals. Also, very efficient and well-tolerated FDA-approved drugs that block different steps in the early viral lifecycle are available to prevent the acquisition of HIV-1 infection (reviewed in Riddell et al., 2018).

2) Once HIV-1 infection is established, blood viremia levels rise during the acute phase of infection, which is accompanied by immune activation and antiviral responses, which are not sufficient to clear the infection (reviewed in chapter 1). Long-term recombinant IFNα monotherapy delayed and reduced the progression to AIDS, maintained CD4 T cell counts and prolonged survival in asymptomatic, treatment naïve PLWH prior to the availability of antivirals as treatments for HIV-1 (Rivero et al., 1997, 1994). We would expect that RIG-I agonists have similar or extended effects during the acute phase of HIV-1 infection. RIG-I activation induces the expression of type-I IFNs (IFNα and IFNβ) (reviewed in Schlee and Hartmann, 2016). IFNβ has a higher binding affinity to the IFNAR1 receptor than IFNα and induces a different transcriptional program (reviewed in Lazear et al., 2019). The resulting broader immune response might be more efficient in controlling viral replication than IFNα treatment alone.

The early onset of ART was positively correlated with a smaller reservoir size (Ho et al., 2019; Kuhn et al., 2018). We would expect a beneficial effect of short-term RIG-I activation accompanying ART during the acute phase of infection due to the additional induction of type-I IFNs and their effects on viral replication and spread. Transmitted HIV-1 strains were identified as more type-I IFN resistant and associated with higher numbers of cell-free virus *ex vivo* when compared to non-transmitted donor isolates (Fenton-May et al., 2013; Iyer et al., 2017). Type-I IFN half-maximal inhibitory concentrations (IC_{50}) were 8-39 fold higher in transmitted viruses than in donor isolates (Iyer et al., 2017). HIV-1 isolates from PLWH on ART showed high sensitivity to type-IFNs and rebounded viruses became highly resistant to type-I IFNs once the treatment was interrupted (Gondim et al., 2021). These findings indicate that type-I IFN resistant HIV-1 strains are selected due to the hosts innate responses during the acute phase of infection in the absence of ART. The elevation of type-I IFN levels through RIG-I agonists might assist in a more sustained viral control. We do not expect long-term adverse effects on viral control as donor isolates showed low type-I IFN resistance, indicating that resistance to type-I IFNs decreases during the chronic phase of infection on ART.

3) Once blood viremia levels are cleared and viral replication is effectively suppressed by ART, RIG-I activation might be counter-indicated. ART frequently achieves efficient viral suppression with a state of reduced chronic immune activation, the primary driver of HIV-1 pathogenesis in PLWH on ART (reviewed in Zicari et al., 2019). As outlined before, RIG-I agonists induce immune activation and the release of type-I IFNs, which could possibly reactivate latent virus and increase inflammatory processes.

6.4 Implications of this work for other RNA viruses like SARS-CoV2

At least 214 RNA virus species that infect humans have been identified, including HIV, HTLV, Zika, Dengue, Ebola, Hepatitis A/C, corona and Influenza viruses (reviewed in Woolhouse and Brierley, 2018). Some of these RNA viruses have the potential to cause epidemics or pandemics or are already renown for frequent outbreaks, imposing a high burden on public health systems (reviewed in Carrasco-Hernandez et al., 2017).

In December 2019, novel coronavirus SARS-CoV2 (severe acute respiratory syndrome coronavirus 2), causative for COVID-19 disease, was identified in Wuhan, China (reviewed in Sofi et al., 2020). SARS-CoV2 spread rapidly worldwide, infected more than 100 million people and caused nearly 2.5 million deaths (WHO, 2021).

SARS-CoV2 and HIV-1 share similarities in how they affect the immune system: Peripheral CD4 T cell loss accompanies the acute phase of HIV-1infection (Brenchley et al., 2004) and is associated with a more severe disease progression in SARS-CoV2 infected individuals (reviewed in Shrotri et al., 2021). Cytokine-induced apoptosis and T cell migration were identified to promote the peripheral CD4 T cell loss in COVID-19 disease (Adamo et al., 2020). SARS-CoV2 infected CD4 T cells but not CD8 T cells were isolated from peripheral blood of COVID-19 patients, and SARS-CoV2 infection of CD4 T cells was established *in vitro* (Davanzo et al., 2020). The same group identified significant changes in the proteome of SARS-CoV2 infected CD4 cells, affecting several

cellular pathways, including TCR signalling, cell cycle, translation initiation and apoptosis. IFNγ expression was significantly reduced in CD4 T cells derived from severe COVID-19 cases (low IFNγ expression, similar to the healthy control) when compared to CD4 T cells from moderate COVID-19 cases (up to 400-fold induction of IFNγ). It is important to note, that Davanzo et al., 2020, isolated SARS-CoV2 infected CD4 T cells from patients with severe COVID-19 disease but were unable to detect infected CD4 T cells in cases presenting with moderate COVID-19 disease. The fact that Davanzo et al., 2020 observed reduced IFNγ expression in SARS-CoV2 infected but not in uninfected CD4 T cells, hints to a possible involvement of cellular RNA sensors in modulating T cell responses during SARS-CoV2 infection. We observed similar effects in primary CD4 T cells following SeV infection, including reduced IFNγ release and decreased metabolic and proliferative activities. At the same time, SeV infected CD4 T cells were primed for a broad antiviral response as seen in transcriptomic changes, including the upregulation of antiviral genes and nucleic acid sensor pathways (among others).

Type-I IFN responses are frequently suppressed in SARS-CoV2 patients (Blanco-Melo et al., 2020; O'Brien et al., 2020). Viral membrane and nucleocapsid proteins interfered with RIG-I and MDA5 sensing of SARS-CoV2 and abrogated type-I and type-III IFN responses *in vitro* (Chen et al., 2020; Zheng et al., 2020), while chemokine levels were robust during infection as measured *in vitro* and *ex vivo* (Blanco-Melo et al., 2020). It is important to note that type-I and type-III IFNs significantly reduced SARS-CoV2 replication *in vitro* (Mantlo et al., 2020; Vanderheiden et al., 2020). Early but not late administration of recombinant IFN-α2b was associated with a reduced mortality in COVID-19 patients in a multicentre cohort study (Wang et al., 2020). Several clinical trials returned promising outcomes or are still investigating the clinical efficacies of type-I and type-III IFNs for the treatment of covid-19 disease (reviewed in Lee and Shin, 2020). We observed diminished CD4 T cell responses following IFN-α treatment in our *in vitro* T cell activation model. It is unclear if these negative effects would occur *in vivo* but they might be overcome by the positive effect of

the antiviral priming, which could possibly prevent CD4 T cell infection by SARS-CoV2 and thereby reduce immune dysregulation.

These studies highlight the importance of functional RNA signalling pathways during viral infections. Viruses evolved different innate immune evasion mechanisms to prevent antiviral responses, including the evasion of PRRs or ISGs and the degradation of adapter molecules and transcription factors (reviewed in Beachboard and Horner, 2016). Protection or restoration and activation of innate immune sensing pathways during viral infections might assist in the clearance of the virus and the prevention of severe illness.

Therapeutic RIG-I or MDA5 activation might provide a sustained type-I IFN response to prevent severe outcomes of covid-19 disease if administered early during infection. SARS-CoV2 can infect several tissue types and the upper and lower respiratory tracts are the main replication sites (reviewed in Gupta et al., 2020). Nebulised, inhaled IFNβ is currently under investigation to treat SARS-CoV2 infection and is expected to have less adverse effects than systemically administered IFNβ (Synairgen Research, 2020). RIG-I and MDA5 agonists could be delivered in a similar dosage form to act directly on the infected tissue, with possible beneficial outcomes compared to type-I IFN monotherapy.

6.5 Concluding Remarks

Functional RNA-sensing pathways are a prerequisite for efficient detection of RNA virus replication in infected cells. HIV-1 directly targets cytosolic RNA sensors RIG-I and MDA5; thereby preventing the detection of foreign and endogenous RNA species. For HIV-1, this mechanism can be inhibited by protease inhibitors, which harbours the potential for new HIV-1 cure strategies when used in combination with latency reversing agents. The activation of RNA-sensing pathways by small molecules can be exploited in other infectious and non-infectious diseases, if the activation and modulation of the immune system is considered advantageous. Targeting of innate immune pathways has broad therapeutic implications, even when infected or degenerated cells are not directly

accessible for drug delivery as bystander cells can mediate immuno-modulatory effects. The therapeutic activation of innate immune pathways is an emerging strategy which can form the basis for the precise orchestration of immune responses to achieve a better control of HIV-1 and other infectious diseases.

7. REFERENCES

Abdullah N, Atif SM. RIG-I (Retinoic Acid Inducible Gene-I). Encycl. Signal. Mol., New York, NY: Springer New York; 2017, p. 1–8.

Adamo S, Chevrier S, Cervia C, Zurbuchen Y, Raeber ME, Yang L, et al. Lymphopenia-induced T cell proliferation is a hallmark of severe COVID-19. BioRxiv 2020:2020.08.04.236521.

Agosto LM, Herring MB, Mothes W, Henderson AJ. HIV-1-Infected CD4+ T Cells Facilitate Latent Infection of Resting CD4+ T Cells through Cell-Cell Contact. Cell Rep 2018;24:2088–100.

Ahr B, Robert-Hebmann V, Devaux C, Biard-Piechaczyk M. Apoptosis of uninfected cells induced by HIV envelope glycoproteins. Retrovirology 2004;1:12.

AIDSinfo. Fact Sheet - FDA-Approved HIV Medicines 2020.

Aksoy P, Aksoy BA, Czech E, Hammerbacher J. Viable and efficient electroporation-based genetic manipulation of unstimulated human T cells. BioRxiv 2018:466243.

Alexopoulou L, Holt AC, Medzhitov R, Flavell RA. Recognition of double-stranded RNA and activation of NF-κB by Toll-like receptor 3. Nature 2001;413:732–8.

Almine JF, O'Hare CAJ, Dunphy G, Haga IR, Naik RJ, Atrih A, et al. IFI16 and cGAS cooperate in the activation of STING during DNA sensing in human keratinocytes. Nat Commun 2017;8:14392.

Amarante-Mendes GP, Adjemian S, Branco LM, Zanetti LC, Weinlich R, Bortoluci KR. Pattern Recognition Receptors and the Host Cell Death Molecular Machinery. Front Immunol 2018;9.

Amie SM, Noble E, Kim B. Intracellular nucleotide levels and the control of retroviral infections. Virology 2013;436:247–54.

Ananworanich J, Eller LA, Pinyakorn S, Kroon E, Sriplenchan S, Fletcher JL, et al. Viral kinetics in untreated versus treated acute HIV infection in prospective cohort studies in Thailand. J Int AIDS Soc 2017;20:21652.

Anderson JL, Khoury G, Fromentin R, Solomon A, Chomont N, Sinclair E, et al. Human Immunodeficiency Virus (HIV)–Infected CCR6+ Rectal CD4+ T Cells and HIV Persistence On Antiretroviral Therapy. J Infect Dis 2020;221:744–

55.

Andrejeva J, Childs KS, Young DF, Carlos TS, Stock N, Goodbourn S, et al. The V proteins of paramyxoviruses bind the IFN-inducible RNA helicase, mda-5, and inhibit its activation of the IFN- promoter. Proc Natl Acad Sci 2004;101:17264–9.

Arrigo SJ, Weitsman S, Zack JA, Chen IS. Characterization and expression of novel singly spliced RNA species of human immunodeficiency virus type 1. J Virol 1990;64:4585–8.

Aruna A, Li L. Anti-Interferon Alpha Antibodies in Patients with High-Risk BCR/ABL-Negative Myeloproliferative Neoplasms Treated with Recombinant Human Interferon-α. Med Sci Monit 2018;24:2302–9.

Asiamah EK, Ekwemalor K, Adjei-Fremah S, Osei B, Newman R, Worku M. Natural and synthetic pathogen associated molecular patterns modulate galectin expression in cow blood. J Anim Sci Technol 2019;61:245–53.

Azzoni L, Foulkes AS, Papasavvas E, Mexas AM, Lynn KM, Mounzer K, et al. Pegylated Interferon Alfa-2a Monotherapy Results in Suppression of HIV Type 1 Replication and Decreased Cell-Associated HIV DNA Integration. J Infect Dis 2013;207:213–22.

Bachmann N, von Siebenthal C, Vongrad V, Turk T, Neumann K, Beerenwinkel N, et al. Determinants of HIV-1 reservoir size and long-term dynamics during suppressive ART. Nat Commun 2019;10:3193.

Baker B, Block B, Rothchild A, Walker B. Elite control of HIV infection: implications for vaccine design. Expert Opin Biol Ther 2009;9:55–69.

Balkhi MY, Wittmann G, Xiong F, Junghans RP. YY1 Upregulates Checkpoint Receptors and Downregulates Type I Cytokines in Exhausted, Chronically Stimulated Human T Cells. IScience 2018;2:105–22.

Balyan R, Gautam N, Gascoigne NRJ. The Ups and Downs of Metabolism during the Lifespan of a T Cell. Int J Mol Sci 2020;21:7972.

Banga R, Procopio FA, Noto A, Pollakis G, Cavassini M, Ohmiti K, et al. PD-1+ and follicular helper T cells are responsible for persistent HIV-1 transcription in treated aviremic individuals. Nat Med 2016;22:754–61.

Battivelli E, Migraine J, Lecossier D, Yeni P, Clavel F, Hance AJ. Gag

Cytotoxic T Lymphocyte Escape Mutations Can Increase Sensitivity of HIV-1 to Human TRIM5 , Linking Intrinsic and Acquired Immunity. J Virol 2011;85:11846–54.

Baum A, Sachidanandam R, Garcia-Sastre A. Preference of RIG-I for short viral RNA molecules in infected cells revealed by next-generation sequencing. Proc Natl Acad Sci 2010;107:16303–8.

Bavinton BR, Rodger AJ. Undetectable viral load and HIV transmission dynamics on an individual and population level. Curr Opin Infect Dis 2020;33:20–7.

Beachboard DC, Horner SM. Innate immune evasion strategies of DNA and RNA viruses. Curr Opin Microbiol 2016;32:113–9.

Beckham SA, Brouwer J, Roth A, Wang D, Sadler AJ, John M, et al. Conformational rearrangements of RIG-I receptor on formation of a multiprotein:dsRNA assembly. Nucleic Acids Res 2013;41:3436–45.

Beignon A-S, McKenna K, Skoberne M, Manches O, DaSilva I, Kavanagh DG, et al. Endocytosis of HIV-1 activates plasmacytoid dendritic cells via Toll-like receptor-viral RNA interactions. J Clin Invest 2005;115:3265–75.

Berg RK, Melchjorsen J, Rintahaka J, Diget E, Søby S, Horan KA, et al. Genomic HIV RNA induces innate immune responses through RIG-I-dependent sensing of secondary-structured RNA. PLoS One 2012;7:1–10.

Berke IC, Modis Y. MDA5 cooperatively forms dimers and ATP-sensitive filaments upon binding double-stranded RNA. EMBO J 2012;31:1714–26.

Berkowitz RD, Ohagen A, Höglund S, Goff SP. Retroviral nucleocapsid domains mediate the specific recognition of genomic viral RNAs by chimeric Gag polyproteins during RNA packaging in vivo. J Virol 1995;69:6445–56.

Bermejo M, Martín-Serrano J, Oberlin E, Pedraza M-A, Serrano A, Santiago B, et al. Activation of blood T lymphocytes down-regulates CXCR4 expression and interferes with propagation of X4 HIV strains. Eur J Immunol 1998;28:3192–204.

Bernard JJ, Cowing-Zitron C, Nakatsuji T, Muehleisen B, Muto J, Borkowski AW, et al. Ultraviolet radiation damages self noncoding RNA and is detected by TLR3. Nat Med 2012;18:1286–90.

Blanco-Melo D, Nilsson-Payant BE, Liu W-C, Uhl S, Hoagland D, Møller R, et al. Imbalanced Host Response to SARS-CoV-2 Drives Development of COVID-19. Cell 2020;181:1036-1045.e9.

De Boer RJ, Homann D, Perelson AS. Different Dynamics of CD4 + and CD8 + T Cell Responses During and After Acute Lymphocytic Choriomeningitis Virus Infection. J Immunol 2003;171:3928–35.

Böhnlein E, Lowenthal JW, Siekevitz M, Ballard DW, Franza BR, Greene WC. The same inducible nuclear proteins regulates mitogen activation of both the interleukin-2 receptor-alpha gene and type 1 HIV. Cell 1988;53:827–36.

den Braber I, Mugwagwa T, Vrisekoop N, Westera L, Mögling R, Bregje de Boer A, et al. Maintenance of Peripheral Naive T Cells Is Sustained by Thymus Output in Mice but Not Humans. Immunity 2012;36:288–97.

Bradley LM, Dalton DK, Croft M. A direct role for IFN-gamma in regulation of Th1 cell development. J Immunol 1996;157:1350–8.

Brand SR, Kobayashi R, Mathews MB. The Tat Protein of Human Immunodeficiency Virus Type 1 Is a Substrate and Inhibitor of the Interferon-induced, Virally Activated Protein Kinase, PKR. J Biol Chem 1997;272:8388–95.

Brenchley JM, Schacker TW, Ruff LE, Price DA, Taylor JH, Beilman GJ, et al. CD4+ T Cell Depletion during all Stages of HIV Disease Occurs Predominantly in the Gastrointestinal Tract. J Exp Med 2004;200:749–59.

Brubaker SW, Gauthier AE, Mills EW, Ingolia NT, Kagan JC. A Bicistronic MAVS Transcript Highlights a Class of Truncated Variants in Antiviral Immunity. Cell 2014;156:800–11.

Bruner KM, Murray AJ, Pollack RA, Soliman MG, Laskey SB, Capoferri AA, et al. Defective proviruses rapidly accumulate during acute HIV-1 infection. Nat Med 2016;22:1043–9.

Buchbinder SP, Katz MH, Hessol NA, O'Malley PM, Holmberg SD. Long-term HIV-1 infection without immunologic progression. AIDS 1994;8:1123–8.

Bui JK, Halvas EK, Fyne E, Sobolewski MD, Koontz D, Shao W, et al. Ex vivo activation of CD4+ T-cells from donors on suppressive ART can lead to sustained production of infectious HIV-1 from a subset of infected cells. PLOS Pathog 2017;13:e1006230.

Bürckstümmer T, Baumann C, Blüml S, Dixit E, Dürnberger G, Jahn H, et al. An orthogonal proteomic-genomic screen identifies AIM2 as a cytoplasmic DNA sensor for the inflammasome. Nat Immunol 2009;10:266–72.

Burgdorf S, Kautz A, Bohnert V, Knolle PA, Kurts C. Distinct Pathways of Antigen Uptake and Intracellular Routing in CD4 and CD8 T Cell Activation. Science (80-) 2007;316:612–6.

Buzon MJ, Sun H, Li C, Shaw A, Seiss K, Ouyang Z, et al. HIV-1 persistence in CD4+ T cells with stem cell–like properties. Nat Med 2014;20:139–42.

Cai R, Carpick B, Chun RF, Jeang K-T, Williams BRG. HIV-I TAT Inhibits PKR Activity by Both RNA-Dependent and RNA-Independent Mechanisms. Arch Biochem Biophys 2000;373:361–7.

Carlson L-A, Briggs JAG, Glass B, Riches JD, Simon MN, Johnson MC, et al. Three-Dimensional Analysis of Budding Sites and Released Virus Suggests a Revised Model for HIV-1 Morphogenesis. Cell Host Microbe 2008;4:592–9.

Caron G, Duluc D, Frémaux I, Jeannin P, David C, Gascan H, et al. Direct Stimulation of Human T Cells via TLR5 and TLR7/8: Flagellin and R-848 Up-Regulate Proliferation and IFN-γ Production by Memory CD4 + T Cells. J Immunol 2005;175:1551–7.

Carrasco-Hernandez R, Jácome R, López Vidal Y, Ponce de León S. Are RNA Viruses Candidate Agents for the Next Global Pandemic? A Review. ILAR J 2017;58:343–58.

Castañeda-Delgado JE, Bastián-Hernandez Y, Macias-Segura N, Santiago-Algarra D, Castillo-Ortiz JD, Alemán-Navarro AL, et al. Type I Interferon Gene Response Is Increased in Early and Established Rheumatoid Arthritis and Correlates with Autoantibody Production. Front Immunol 2017;8.

Cavrois M, Neidleman J, Kreisberg JF, Fenard D, Callebaut C, Greene WC. Human Immunodeficiency Virus Fusion to Dendritic Cells Declines as Cells Mature. J Virol 2006;80:1992–9.

Cen S, Niu M, Saadatmand J, Guo F, Huang Y, Nabel GJ, et al. Incorporation of Pol into Human Immunodeficiency Virus Type 1 Gag Virus-Like Particles Occurs Independently of the Upstream Gag Domain in Gag-Pol. J Virol 2004;78:1042–9.

Chen K, Xiao F, Hu D, Ge W, Tian M, Wang W, et al. SARS-CoV-2 Nucleocapsid Protein Interacts with RIG-I and Represses RIG-Mediated IFN-β Production. Viruses 2020;13:47.

Chertova E, Bess JW, Crise BJ, Sowder II RC, Schaden TM, Hilburn JM, et al. Envelope Glycoprotein Incorporation, Not Shedding of Surface Envelope Glycoprotein (gp120/SU), Is the Primary Determinant of SU Content of Purified Human Immunodeficiency Virus Type 1 and Simian Immunodeficiency Virus. J Virol 2002;76:5315–25.

Chukkapalli V, Oh SJ, Ono A. Opposing mechanisms involving RNA and lipids regulate HIV-1 Gag membrane binding through the highly basic region of the matrix domain. Proc Natl Acad Sci 2010;107:1600–5.

Chun T-W, Carruth L, Finzi D, Shen X, DiGiuseppe JA, Taylor H, et al. Quantification of latent tissue reservoirs and total body viral load in HIV-1 infection. Nature 1997;387:183–8.

Chung NPY, Matthews K, Klasse PJ, Sanders RW, Moore JP. HIV-1 gp120 Impairs the Induction of B Cell Responses by TLR9-Activated Plasmacytoid Dendritic Cells. J Immunol 2012;189:5257–65.

Churchill MJ, Deeks SG, Margolis DM, Siliciano RF, Swanstrom R. HIV reservoirs: what, where and how to target them. Nat Rev Microbiol 2016;14:55–60.

Clerzius G, Gélinas J-F, Gatignol A. Multiple levels of PKR inhibition during HIV-1 replication. Rev Med Virol 2011;21:42–53.

Clever JL, Parslow TG. Mutant human immunodeficiency virus type 1 genomes with defects in RNA dimerization or encapsidation. J Virol 1997;71:3407–14.

Coch C, Stümpel JP, Lilien-Waldau V, Wohlleber D, Kümmerer BM, Bekeredjian-Ding I, et al. RIG-I Activation Protects and Rescues from Lethal Influenza Virus Infection and Bacterial Superinfection. Mol Ther 2017;25:2093–103.

Cocude C, Truong MJ, Billaut-Mulot O, Delsart V, Darcissac E, Capron A, et al. A novel cellular RNA helicase, RH116, differentially regulates cell growth, programmed cell death and human immunodeficiency virus type 1 replication. J Gen Virol 2003;84:3215–25.

Coldbeck-Shackley RC, Eyre NS, Beard MR. The Molecular Interactions of ZIKV and DENV with the Type-I IFN Response. Vaccines 2020;8:530.

Crawford A, Angelosanto JM, Kao C, Doering TA, Odorizzi PM, Barnett BE, et al. Molecular and Transcriptional Basis of CD4+ T Cell Dysfunction during Chronic Infection. Immunity 2014;40:289–302.

Cyster JG, Allen CDC. B Cell Responses: Cell Interaction Dynamics and Decisions. Cell 2019;177:524–40.

Dash PK, Kaminski R, Bella R, Su H, Mathews S, Ahooyi TM, et al. Sequential LASER ART and CRISPR Treatments Eliminate HIV-1 in a Subset of Infected Humanized Mice. Nat Commun 2019;10:2753.

Daßler-Plenker J, Paschen A, Putschli B, Rattay S, Schmitz S, Goldeck M, et al. Direct RIG-I activation in human NK cells induces TRAIL-dependent cytotoxicity toward autologous melanoma cells. Int J Cancer 2019;144:1645–56.

Davanzo GG, Codo AC, Brunetti NS, Boldrini V, Knittel TL, Monterio LB, et al. SARS-CoV-2 Uses CD4 to Infect T Helper Lymphocytes. MedRxiv 2020:2020.09.25.20200329.

Deeks SG, Lewin SR, Ross AL, Ananworanich J, Benkirane M, Cannon P, et al. International AIDS Society global scientific strategy: towards an HIV cure 2016. Nat Med 2016;22:839–50.

Deeks SG, Overbaugh J, Phillips A, Buchbinder S. HIV infection. Nat Rev Dis Prim 2015;1:15035.

Dierynck I, De Wit M, Gustin E, Keuleers I, Vandersmissen J, Hallenberger S, et al. Binding Kinetics of Darunavir to Human Immunodeficiency Virus Type 1 Protease Explain the Potent Antiviral Activity and High Genetic Barrier. J Virol 2007;81:13845–51.

Dimeloe S, Burgener A-V, Grählert J, Hess C. T-cell metabolism governing activation, proliferation and differentiation; a modular view. Immunology 2017;150:35–44.

Doitsh G, Greene WC. Dissecting How CD4 T Cells Are Lost During HIV Infection. Cell Host Microbe 2016;19:280–91.

Dominguez-Villar M, Gautron A-S, de Marcken M, Keller MJ, Hafler D a. TLR7 induces anergy in human CD4+ T cells. Nat Immunol 2015;16:118–28.

Dondi E, Rogge L, Lutfalla G, Uzé G, Pellegrini S. Down-Modulation of Responses to Type I IFN Upon T Cell Activation. J Immunol 2003;170:749–56.

Dondi E, Roué G, Yuste VJ, Susin SA, Pellegrini S. A Dual Role of IFN-α in the Balance between Proliferation and Death of Human CD4 + T Lymphocytes during Primary Response. J Immunol 2004;173:3740–7.

Douglas JL, Viswanathan K, McCarroll MN, Gustin JK, Früh K, Moses A V. Vpu Directs the Degradation of the Human Immunodeficiency Virus Restriction Factor BST-2/Tetherin via a βTrCP-Dependent Mechanism. J Virol 2009;83:7931–47.

Duewell P, Steger A, Lohr H, Bourhis H, Hoelz H, Kirchleitner S V, et al. RIG-I-like helicases induce immunogenic cell death of pancreatic cancer cells and sensitize tumors toward killing by CD8+ T cells. Cell Death Differ 2014;21:1825–37.

Dull T, Zufferey R, Kelly M, Mandel RJ, Nguyen M, Trono D, et al. A third-generation lentivirus vector with a conditional packaging system. J Virol 1998;72:8463–71.

East L, Isacke C. The mannose receptor family. Biochim Biophys Acta - Gen Subj 2002;1572:364–86.

Eisele E, Siliciano RF. Redefining the Viral Reservoirs that Prevent HIV-1 Eradication. Immunity 2012;37:377–88.

Elsner C, Ponnurangam A, Kazmierski J, Zillinger T, Jansen J, Todt D, et al. Absence of cGAS-mediated type I IFN responses in HIV-1–infected T cells. Proc Natl Acad Sci 2020;117:19475–86.

Endo-Munoz L, Warby T, Harrich D, McMillan NAJ. Phosphorylation of HIV Tat by PKR increases interaction with TAR RNA and enhances transcription. Virol J 2005;2:17.

Engelman A, Cherepanov P. The structural biology of HIV-1: mechanistic and therapeutic insights. Nat Rev Microbiol 2012;10:279–90.

Esbjörnsson J, Jansson M, Jespersen S, Månsson F, Hønge BL, Lindman J, et al. HIV-2 as a model to identify a functional HIV cure. AIDS Res Ther 2019;16:24.

Esposito D, Craigie R. HIV Integrase Structure and Function. Adv. Virus Res.,

1999, p. 319–33.

Feng Q, Langereis MA, Lork M, Nguyen M, Hato S V., Lanke K, et al. Enterovirus 2Apro Targets MDA5 and MAVS in Infected Cells. J Virol 2014;88:3369–78.

Fenton-May AE, Dibben O, Emmerich T, Ding H, Pfafferott K, Aasa-Chapman MM, et al. Relative resistance of HIV-1 founder viruses to control by interferon-alpha. Retrovirology 2013;10:146.

Ferguson MR, Rojo DR, von Lindern JJ, O'Brien WA. HIV-1 replication cycle. Clin Lab Med 2002;22:611–35.

Figueiredo A, Moore KL, Mak J, Sluis-Cremer N, de Bethune M-P, Tachedjian G. Potent Nonnucleoside Reverse Transcriptase Inhibitors Target HIV-1 Gag-Pol. PLoS Pathog 2006;2:e119.

Firpo EJ, Koff A, Solomon MJ, Roberts JM. Inactivation of a Cdk2 inhibitor during interleukin 2-induced proliferation of human T lymphocytes. Mol Cell Biol 1994;14:4889–901.

Forshey BM, von Schwedler U, Sundquist WI, Aiken C. Formation of a Human Immunodeficiency Virus Type 1 Core of Optimal Stability Is Crucial for Viral Replication. J Virol 2002;76:5667–77.

Frankel A, Young J. HIV-1: Fifteen Proteins and an RNA. Annu Rev Biochem 1998;67:1–25.

Fuertes Marraco SA, Soneson C, Cagnon L, Gannon PO, Allard M, Maillard SA, et al. Long-lasting stem cell–like memory CD8 + T cells with a naïve-like profile upon yellow fever vaccination. Sci Transl Med 2015;7:282ra48-282ra48.

Fuller SD, Wilk T, Gowen BE, Kräusslich H-G, Vogt VM. Cryo-electron microscopy reveals ordered domains in the immature HIV-1 particle. Curr Biol 1997;7:729–38.

Gack MU, Albrecht RA, Urano T, Inn K-S, Huang I-C, Carnero E, et al. Influenza A Virus NS1 Targets the Ubiquitin Ligase TRIM25 to Evade Recognition by the Host Viral RNA Sensor RIG-I. Cell Host Microbe 2009;5:439–49.

Garcia-Vidal E, Castellví M, Pujantell M, Badia R, Jou A, Gomez L, et al. Evaluation of the innate immune modulator acitretin as a strategy to clear the HIV reservoir. Antimicrob Agents Chemother 2017;61:1–11.

Garcia S, DiSanto J, Stockinger B. Following the Development of a CD4 T Cell Response In Vivo. Immunity 1999;11:163–71.

Gardner JM, Abrams CF. Energetics of Flap Opening in HIV-1 Protease: String Method Calculations. J Phys Chem B 2019;123:9584–91.

Gargan S, Ahmed S, Mahony R, Bannan C, Napoletano S, O'Farrelly C, et al. HIV-1 Promotes the Degradation of Components of the Type 1 IFN JAK/STAT Pathway and Blocks Anti-viral ISG Induction. EBioMedicine 2018;30:203–16.

Garrus JE, von Schwedler UK, Pornillos OW, Morham SG, Zavitz KH, Wang HE, et al. Tsg101 and the Vacuolar Protein Sorting Pathway Are Essential for HIV-1 Budding. Cell 2001;107:55–65.

Gasper DJ, Tejera MM, Suresh M. CD4 T-Cell Memory Generation and Maintenance. Crit Rev Immunol 2014;34(2): 121.

Gasteiger G, D'Osualdo A, Schubert DA, Weber A, Bruscia EM, Hartl D. Cellular Innate Immunity: An Old Game with New Players. J Innate Immun 2017;9:111–25.

Geijtenbeek TB., Kwon DS, Torensma R, van Vliet SJ, van Duijnhoven GC., Middel J, et al. DC-SIGN, a Dendritic Cell–Specific HIV-1-Binding Protein that Enhances trans-Infection of T Cells. Cell 2000;100:587–97.

Gelman AE, Zhang J, Choi Y, Turka LA. Toll-Like Receptor Ligands Directly Promote Activated CD4 + T Cell Survival. J Immunol 2004;172:6065–73.

Giron LB, Colomb F, Papasavvas E, Azzoni L, Yin X, Fair M, et al. Interferon-α alters host glycosylation machinery during treated HIV infection. EBioMedicine 2020;59:102945.

Golubovskaya V, Wu L. Different Subsets of T Cells, Memory, Effector Functions, and CAR-T Immunotherapy. Cancers (Basel) 2016;8:36.

Gondim MVP, Sherrill-Mix S, Bibollet-Ruche F, Russell RM, Trimboli S, Smith AG, et al. Heightened resistance to host type 1 interferons characterizes HIV-1 at transmission and after antiretroviral therapy interruption. Sci Transl Med 2021;13.

Goubau D, Schlee M, Deddouche S, Pruijssers AJ, Zillinger T, Goldeck M, et al. Antiviral immunity via RIG-I-mediated recognition of RNA bearing 5′-diphosphates. Nature 2014;514:372–5.

Grossman Z, Meier-Schellersheim M, Paul WE, Picker LJ. Pathogenesis of HIV infection: What the virus spares is as important as what it destroys. Nat Med 2006;12:289–95.

Gunnery S, Rice AP, Robertson HD, Mathews MB. Tat-responsive region RNA of human immunodeficiency virus 1 can prevent activation of the double-stranded-RNA-activated protein kinase. Proc Natl Acad Sci 1990;87:8687–91.

Gupta A, Madhavan M V., Sehgal K, Nair N, Mahajan S, Sehrawat TS, et al. Extrapulmonary manifestations of COVID-19. Nat Med 2020;26:1017–32.

Gupta RK, Peppa D, Hill AL, Gálvez C, Salgado M, Pace M, et al. Evidence for HIV-1 cure after CCR5Δ32/Δ32 allogeneic haemopoietic stem-cell transplantation 30 months post analytical treatment interruption: a case report. Lancet HIV 2020.

Hadzopoulou-Cladaras M, Felber BK, Cladaras C, Athanassopoulos A, Tse A, Pavlakis GN. The rev (trs/art) protein of human immunodeficiency virus type 1 affects viral mRNA and protein expression via a cis-acting sequence in the env region. J Virol 1989;63:1265–74.

Haftmann C, Riedel R, Porstner M, Wittmann J, Chang H, Radbruch A, et al. Direct uptake of Antagomirs and efficient knockdown of miRNA in primary B and T lymphocytes. J Immunol Methods 2015;426:128–33.

Hakre S, Chavez L, Shirakawa K, Verdin E. HIV latency: experimental systems and molecular models. FEMS Microbiol Rev 2012;36:706–16.

Hakre S, Chavez L, Shirakawa K, Verdin E. Epigenetic regulation of HIV latency. Curr Opin HIV AIDS 2011;6:19–24.

Hallenberger S, Bosch V, Angliker H, Shaw E, Klenk H-D, Garten W. Inhibition of furin-mediated cleavage activation of HIV-1 glycoprotein gpl60. Nature 1992;360:358–61.

Hamilos DL. Antigen presenting cells. Immunol Res 1989;8:98–117.

Hardy GAD, Sieg S, Rodriguez B, Anthony D, Asaad R, Jiang W, et al. Interferon-α Is the Primary Plasma Type-I IFN in HIV-1 Infection and Correlates with Immune Activation and Disease Markers. PLoS One 2013;8:e56527.

Havenar-Daughton C, Kolumam GA, Murali-Krishna K. Cutting Edge: The Direct Action of Type I IFN on CD4 T Cells Is Critical for Sustaining Clonal

Expansion in Response to a Viral but Not a Bacterial Infection. J Immunol 2006;176:3315–9.

He N, Liu M, Hsu J, Xue Y, Chou S, Burlingame A, et al. HIV-1 Tat and host AFF4 recruit two transcription elongation factors into a bifunctional complex for coordinated activation of HIV-1 transcription. Mol Cell 2010;38:428–38.

Helgeland H, Gabrielsen I, Akselsen H, Sundaram AYM, Flåm ST, Lie BA. Transcriptome profiling of human thymic CD4+ and CD8+ T cells compared to primary peripheral T cells. BMC Genomics 2020;21:350.

Hernandez-Pando R, Rook GA. The role of TNF-alpha in T-cell-mediated inflammation depends on the Th1/Th2 cytokine balance. Immunology 1994;82:591–5.

Ho V, Yong HY, Chevrier M, Narang V, Lum J, Toh Y-X, et al. RIG-I Activation by a Designer Short RNA Ligand Protects Human Immune Cells against Dengue Virus Infection without Causing Cytotoxicity. J Virol 2019;93.

Hoenigl M, Chaillon A, Moore DJ, Morris SR, Mehta SR, Gianella S, et al. Rapid HIV Viral Load Suppression in those Initiating Antiretroviral Therapy at First Visit after HIV Diagnosis. Sci Rep 2016;6:32947.

Hornung V, Ablasser A, Charrel-Dennis M, Bauernfeind F, Horvath G, Caffrey DR, et al. AIM2 recognizes cytosolic dsDNA and forms a caspase-1-activating inflammasome with ASC. Nature 2009;458:514–8.

Hornung V, Ellegast J, Kim S, Brzozka K, Jung A, Kato H, et al. 5'-Triphosphate RNA Is the Ligand for RIG-I. Science (80-) 2006;314:994–7.

Hornung V, Rothenfusser S, Britsch S, Krug A, Jahrsdörfer B, Giese T, et al. Quantitative Expression of Toll-Like Receptor 1–10 mRNA in Cellular Subsets of Human Peripheral Blood Mononuclear Cells and Sensitivity to CpG Oligodeoxynucleotides. J Immunol 2002;168:4531–7.

Hou F, Sun L, Zheng H, Skaug B, Jiang Q-X, Chen ZJ. MAVS Forms Functional Prion-like Aggregates to Activate and Propagate Antiviral Innate Immune Response. Cell 2011;146:448–61.

Hu W-S, Hughes SH. HIV-1 Reverse Transcription. Cold Spring Harb Perspect Med 2012;2:a006882–a006882.

Huang L, Li L, Tien C, LaBarbera D V., Chen C. Targeting HIV-1 Protease

Autoprocessing for High-throughput Drug Discovery and Drug Resistance Assessment. Sci Rep 2019;9:301.

Huang L, Li Y, Chen C. Flexible catalytic site conformations implicated in modulation of HIV-1 protease autoprocessing reactions. Retrovirology 2011;8:79.

Hütter G, Nowak D, Mossner M, Ganepola S, Müßig A, Allers K, et al. Long-Term Control of HIV by CCR5 Delta32/Delta32 Stem-Cell Transplantation. N Engl J Med 2009;360:692–8.

Ido E, Han -p. H, Kezdy FJ, Tang J. Kinetic studies of human immunodeficiency virus type 1 protease and its active-site hydrogen bond mutant A28S. J Biol Chem 1991;266:24359–66.

Imamichi H, Natarajan V, Adelsberger JW, Rehm CA, Lempicki RA, Das B, et al. Lifespan of effector memory CD4+ T cells determined by replication-incompetent integrated HIV-1 provirus. AIDS 2014;28:1091–9.

Impens F, Timmerman E, Staes A, Moens K, Ariën KK, Verhasselt B, et al. A catalogue of putative HIV-1 protease host cell substrates. Biol Chem 2012;393:915–31.

Isel C, Lanchy JM, Le Grice SF, Ehresmann C, Ehresmann B, Marquet R. Specific initiation and switch to elongation of human immunodeficiency virus type 1 reverse transcription require the post-transcriptional modifications of primer tRNA3Lys. EMBO J 1996;15:917–24.

Iurescia S, Fioretti D, Rinaldi M. The Innate Immune Signalling Pathways: Turning RIG-I Sensor Activation against Cancer. Cancers (Basel) 2020;12:3158.

Iwabu Y, Fujita H, Kinomoto M, Kaneko K, Ishizaka Y, Tanaka Y, et al. HIV-1 Accessory Protein Vpu Internalizes Cell-surface BST-2/Tetherin through Transmembrane Interactions Leading to Lysosomes. J Biol Chem 2009;284:35060–72.

Iwasaki A, Medzhitov R. Control of adaptive immunity by the innate immune system. Nat Immunol 2015;16:343–53.

Iyer SS, Bibollet-Ruche F, Sherrill-Mix S, Learn GH, Plenderleith L, Smith AG, et al. Resistance to type 1 interferons is a major determinant of HIV-1 transmission fitness. Proc Natl Acad Sci 2017;114:E590–9.

Jacks T, Power MD, Masiarz FR, Luciw PA, Barr PJ, Varmus HE.

Characterization of ribosomal frameshifting in HIV-1 gag-pol expression. Nature 1988;331:280–3.

Jasenosky LD, Cadena C, Mire CE, Borisevich V, Haridas V, Ranjbar S, et al. The FDA-Approved Oral Drug Nitazoxanide Amplifies Host Antiviral Responses and Inhibits Ebola Virus. IScience 2019;19:1279–90.

Jiang G, Mendes EA, Kaiser P, Wong DP, Tang Y, Cai I, et al. Synergistic Reactivation of Latent HIV Expression by Ingenol-3-Angelate, PEP005, Targeted NF-kB Signaling in Combination with JQ1 Induced p-TEFb Activation. PLOS Pathog 2015;11:e1005066.

Jinek M, Chylinski K, Fonfara I, Hauer M, Doudna JA, Charpentier E. A programmable dual-RNA-guided DNA endonuclease in adaptive bacterial immunity. Science (80-) 2012;337:816–21.

Juno JA, van Bockel D, Kent SJ, Kelleher AD, Zaunders JJ, Munier CML. Cytotoxic CD4 T Cells—Friend or Foe during Viral Infection? Front Immunol 2017;8.

Kaartinen T, Luostarinen A, Maliniemi P, Keto J, Arvas M, Belt H, et al. Low interleukin-2 concentration favors generation of early memory T cells over effector phenotypes during chimeric antigen receptor T-cell expansion. Cytotherapy 2017;19:689–702.

Kandasamy M, Suryawanshi A, Tundup S, Perez JT, Schmolke M, Manicassamy S, et al. RIG-I Signaling Is Critical for Efficient Polyfunctional T Cell Responses during Influenza Virus Infection. PLOS Pathog 2016;12:e1005754.

Kang D -c., Gopalkrishnan R V., Wu Q, Jankowsky E, Pyle AM, Fisher PB. mda-5: An interferon-inducible putative RNA helicase with double-stranded RNA-dependent ATPase activity and melanoma growth-suppressive properties. Proc Natl Acad Sci 2002;99:637–42.

Kao SY, Calman AF, Luciw PA, Peterlin BM. Anti-termination of transcription within the long terminal repeat of HIV-1 by tat gene product. Nature 1987;330:489–93.

Kazer SW, Walker BD, Shalek AK. Evolution and Diversity of Immune Responses during Acute HIV Infection. Immunity 2020;53:908–24.

Kedzierska K, Crowe S. The Role of Monocytes and Macrophages in the Pathogenesis of HIV-1 Infection. Curr Med Chem 2002;9:1893–903.

Kedzierska K, Koutsakos M. The ABC of Major Histocompatibility Complexes and T Cell Receptors in Health and Disease. Viral Immunol 2020;33:160–78.

Kemnic TR, Gulick PG. HIV Antiretroviral Therapy. StatPearls, Treasure Island (FL): 2020.

Khan E, Mack JPG, Katz RA, Kulkosky J, Skalka AM. Retroviral integrase domains: DNA binding and the recognition of LTR sequences. Nucleic Acids Res 1991;19:851–60.

Kim SY, Byrn R, Groopman J, Baltimore D. Temporal aspects of DNA and RNA synthesis during human immunodeficiency virus infection: evidence for differential gene expression. J Virol 1989;63:3708–13.

Kim Y, Anderson JL, Lewin SR. Getting the “Kill” into “Shock and Kill”: Strategies to Eliminate Latent HIV. Cell Host Microbe 2018;23:14–26.

Kitagawa Y, Yamaguchi M, Kohno M, Sakai M, Itoh M, Gotoh B. Respirovirus C protein inhibits activation of type I interferon receptor-associated kinases to block JAK-STAT signaling. FEBS Lett 2020;594:864–77.

Klotman ME, Kim S, Buchbinder A, DeRossi A, Baltimore D, Wong-Staal F. Kinetics of expression of multiply spliced RNA in early human immunodeficiency virus type 1 infection of lymphocytes and monocytes. Proc Natl Acad Sci 1991;88:5011–5.

Könnyű B, Sadiq SK, Turányi T, Hírmondó R, Müller B, Kräusslich H-G, et al. Gag-Pol Processing during HIV-1 Virion Maturation: A Systems Biology Approach. PLoS Comput Biol 2013;9:e1003103.

Korolowicz KE, Iyer RP, Czerwinski S, Suresh M, Yang J, Padmanabhan S, et al. Antiviral Efficacy and Host Innate Immunity Associated with SB 9200 Treatment in the Woodchuck Model of Chronic Hepatitis B. PLoS One 2016;11:e0161313.

Kovacsovics M, Martinon F, Micheau O, Bodmer JL, Hofmann K, Tschopp J. Overexpression of Helicard, a CARD-containing helicase cleaved during apoptosis, accelerates DNA degradation. Curr Biol 2002;12:838–43.

Kowalinski E, Lunardi T, McCarthy AA, Louber J, Brunel J, Grigorov B, et

al. Structural Basis for the Activation of Innate Immune Pattern-Recognition Receptor RIG-I by Viral RNA. Cell 2011;147:423–35.

Krawczyk CM, Shen H, Pearce EJ. Functional Plasticity in Memory T Helper Cell Responses. J Immunol 2007;178:4080–8.

Kroupa T, Datta SAK, Rein A. Distinct Contributions of Different Domains within the HIV-1 Gag Polyprotein to Specific and Nonspecific Interactions with RNA. Viruses 2020;12:394.

Kuhn L, Paximadis M, Da Costa Dias B, Loubser S, Strehlau R, Patel F, et al. Age at antiretroviral therapy initiation and cell-associated HIV-1 DNA levels in HIV-1-infected children. PLoS One 2018;13:e0195514.

Kulpa DA, Chomont N. HIV persistence in the setting of antiretroviral therapy: when, where and how does HIV hide? J Virus Erad 2015;1:59–66.

Kumar A, Darcis G, Van Lint C, Herbein G. Epigenetic control of HIV-1 post integration latency: implications for therapy. Clin Epigenetics 2015;7:103.

Kumar B V., Connors TJ, Farber DL. Human T Cell Development, Localization, and Function throughout Life. Immunity 2018;48:202–13.

Kutluay SB, Bieniasz PD. Analysis of the Initiating Events in HIV-1 Particle Assembly and Genome Packaging. PLoS Pathog 2010;6:e1001200.

Kwong PD, Wyatt R, Robinson J, Sweet RW, Sodroski J, Hendrickson WA. Structure of an HIV gp120 envelope glycoprotein in complex with the CD4 receptor and a neutralizing human antibody. Nature 1998;393:648–59.

Lad SP, Yang G, Scott DA, Chao TH, Correia J da S, de la Torre JC, et al. Identification of MAVS splicing variants that interfere with RIGI/MAVS pathway signaling. Mol Immunol 2008;45:2277–87.

Lai AL, Freed JH. HIV gp41 Fusion Peptide Increases Membrane Ordering in a Cholesterol-Dependent Fashion. Biophys J 2014;106:172–81.

Lanchy J-M, Keith G, Le Grice SFJ, Ehresmann B, Ehresmann C, Marquet R. Contacts between Reverse Transcriptase and the Primer Strand Govern the Transition from Initiation to Elongation of HIV-1 Reverse Transcription. J Biol Chem 1998;273:24425–32.

Larange A, Antonios D, Pallardy M, Kerdine-Romer S. TLR7 and TLR8 agonists trigger different signaling pathways for human dendritic cell maturation.

J Leukoc Biol 2009;85:673–83.

Larkin B, Ilyukha V, Sorokin M, Buzdin A, Vannier E, Poltorak A. Cutting Edge: Activation of STING in T Cells Induces Type I IFN Responses and Cell Death. J Immunol 2017;199:397–402.

Lavender KJ, Gibbert K, Peterson KE, Van Dis E, Francois S, Woods T, et al. Interferon Alpha Subtype-Specific Suppression of HIV-1 Infection In Vivo. J Virol 2016;90:6001–13.

Lazear HM, Schoggins JW, Diamond MS. Shared and Distinct Functions of Type I and Type III Interferons. Immunity 2019;50:907–23.

Lee JS, Shin E-C. The type I interferon response in COVID-19: implications for treatment. Nat Rev Immunol 2020;20:585–6.

Lee YK, Turner H, Maynard CL, Oliver JR, Chen D, Elson CO, et al. Late Developmental Plasticity in the T Helper 17 Lineage. Immunity 2009;30:92–107.

Lepelley A, Louis S, Sourisseau M, Law HKW, Pothlichet J, Schilte C, et al. Innate Sensing of HIV-Infected Cells. PLoS Pathog 2011;7:e1001284.

Leuthardt A, Roesel JL. Cloning , expression and purification of a recombinant poly-histidine-linked HIV-1 protease 1993;326:275–80.

Levy JA. Pathogenesis of human immunodeficiency virus infection. Microbiol Rev 1993;57:183–289.

Lewin SR, Vesanen M, Kostrikis L, Hurley A, Duran M, Zhang L, et al. Use of Real-Time PCR and Molecular Beacons To Detect Virus Replication in Human Immunodeficiency Virus Type 1-Infected Individuals on Prolonged Effective Antiretroviral Therapy. J Virol 1999;73:6099–103.

Li G, Cheng M, Nunoya J, Cheng L, Guo H, Yu H, et al. Plasmacytoid Dendritic Cells Suppress HIV-1 Replication but Contribute to HIV-1 Induced Immunopathogenesis in Humanized Mice. PLoS Pathog 2014;10:e1004291.

Li P, Kaiser P, Lampiris HW, Kim P, Yukl SA, Havlir D V, et al. Stimulating the RIG-I pathway to kill cells in the latent HIV reservoir following viral reactivation. Nat Med 2016;22:807–11.

Li X-D, Sun L, Seth RB, Pineda G, Chen ZJ. Hepatitis C virus protease NS3/4A cleaves mitochondrial antiviral signaling protein off the mitochondria to evade innate immunity. Proc Natl Acad Sci 2005;102:17717–22.

Li X, Shu C, Yi G, Chaton CT, Shelton CL, Diao J, et al. Cyclic GMP-AMP synthase is activated by double-stranded DNA-induced oligomerization. Immunity 2013;39:1019–31.

Lim S-Y, Osuna CE, Hraber PT, Hesselgesser J, Gerold JM, Barnes TL, et al. TLR7 agonists induce transient viremia and reduce the viral reservoir in SIV-infected rhesus macaques on antiretroviral therapy. Sci Transl Med 2018;10:eaao4521.

Lindwasser W, Chaudhuri R, Bonifacino J. Mechanisms of CD4 Downregulation by the Nef and Vpu Proteins of Primate Immunodeficiency Viruses. Curr Mol Med 2007;7:171–84.

Linehan MM, Dickey TH, Molinari ES, Fitzgerald ME, Potapova O, Iwasaki A, et al. A minimal RNA ligand for potent RIG-I activation in living mice. BioRxiv 2017:1–11.

Liu R, Simonetti FR, Ho Y-C. The forces driving clonal expansion of the HIV-1 latent reservoir. Virol J 2020;17:4.

Liu X, Ye J, Wang Y, Zhong X, Li L, Opejin A, et al. Controlling T cell development and function via innate Toll-like receptor signaling for autoimmune therapy. J Immunol 2017;198:80.4 LP-80.4.

Louis JM, Ishima R, Nesheiwat I, Pannell LK, Lynch SM, Torchia DA, et al. Revisiting Monomeric HIV-1 Protease. J Biol Chem 2003;278:6085–92.

Luengo A, Li Z, Gui DY, Sullivan LB, Zagorulya M, Do BT, et al. Increased demand for NAD+ relative to ATP drives aerobic glycolysis. Mol Cell 2020.

Maccarrone M, Navarra M, Corasaniti MT, Nisticò G, Finazzi Agrò A. Cytotoxic effect of HIV-1 coat glycoprotein gp120 on human neuroblastoma CHP100 cells involves activation of the arachidonate cascade. Biochem J 1998;333:45–9.

Macedo AB, Novis CL, De Assis CM, Sorensen ES, Moszczynski P, Huang S, et al. Dual TLR2 and TLR7 agonists as HIV latency-reversing agents. JCI Insight 2018;3.

MacIver NJ, Michalek RD, Rathmell JC. Metabolic Regulation of T Lymphocytes. Annu Rev Immunol 2013;31:259–83.

Maddon PJ, Dalgleish AG, McDougal JSS, Clapham PR, Weiss RA, Axel R.

The T4 gene encodes the AIDS virus receptor and is expressed in the immune system and the brain. Cell 1986;47:333–48.

Magadán JG, Pérez-Victoria FJ, Sougrat R, Ye Y, Strebel K, Bonifacino JS. Multilayered Mechanism of CD4 Downregulation by HIV-1 Vpu Involving Distinct ER Retention and ERAD Targeting Steps. PLoS Pathog 2010;6:e1000869.

Maitra RK, McMillan NAJ, Desai S, McSwiggen J, Hovanessian AG, Sen G, et al. HIV-1 TAR RNA Has an Intrinsic Ability to Activate Interferon-Inducible Enzymes. Virology 1994;204:823–7.

Mak J, Jiang M, Wainberg MA, Hammarskjöld ML, Rekosh D, Kleiman L. Role of Pr160gag-pol in mediating the selective incorporation of tRNA(Lys) into human immunodeficiency virus type 1 particles. J Virol 1994;68:2065–72.

Malim MH, Emerman M. HIV-1 Accessory Proteins—Ensuring Viral Survival in a Hostile Environment. Cell Host Microbe 2008;3:388–98.

Mandac JC, Chaudhry S, Sherman KE, Tomer Y. The clinical and physiological spectrum of interferon-alpha induced thyroiditis: Toward a new classification. Hepatology 2006;43:661–72.

Mandhana R, Horvath CM. Sendai Virus Infection Induces Expression of Novel RNAs in Human Cells. Sci Rep 2018;8:16815.

Mangeat B, Turelli P, Caron G, Friedli M, Perrin L, Trono D. Broad antiretroviral defence by human APOBEC3G through lethal editing of nascent reverse transcripts. Nature 2003;424:99–103.

Mantlo E, Bukreyeva N, Maruyama J, Paessler S, Huang C. Antiviral activities of type I interferons to SARS-CoV-2 infection. Antiviral Res 2020;179:104811.

Marciniak RA, Sharp PA. HIV-1 Tat protein promotes formation of more-processive elongation complexes. EMBO J 1991;10:4189–96.

de Marcken M, Dhaliwal K, Danielsen AC, Gautron AS, Dominguez-Villar M. TLR7 and TLR8 activate distinct pathways in monocytes during RNA virus infection. Sci Signal 2019;12:eaaw1347.

Mariani C, Desdouits M, Favard C, Benaroch P, Muriaux DM. Role of Gag and lipids during HIV-1 assembly in CD4+ T cells and macrophages. Front Microbiol 2014;5.

Marrero-Hernández S, Márquez-Arce D, Cabrera-Rodríguez R, Estévez-

Herrera J, Pérez-Yanes S, Barroso-González J, et al. HIV-1 Nef Targets HDAC6 to Assure Viral Production and Virus Infection. Front Microbiol 2019;10.

Marsden MD. Benefits and limitations of humanized mice in HIV persistence studies. Retrovirology 2020;17:7.

Marsden MD, Zack JA. Humanized Mouse Models for Human Immunodeficiency Virus Infection. Annu Rev Virol 2017;4:393–412.

Marshall JS, Warrington R, Watson W, Kim HL. An introduction to immunology and immunopathology. Allergy, Asthma Clin Immunol 2018;14:49.

Martinelli E, Cicala C, Van Ryk D, Goode DJ, Macleod K, Arthos J, et al. HIV-1 gp120 inhibits TLR9-mediated activation and IFN- secretion in plasmacytoid dendritic cells. Proc Natl Acad Sci 2007;104:3396–401.

Maximova K, Wojtczak J, Trylska J. Enzymatic activity of human immunodeficiency virus type 1 protease in crowded solutions. Eur Biophys J 2019;48:685–9.

McDougal J, Kennedy M, Sligh J, Cort S, Mawle A, Nicholson J. Binding of HTLV-III/LAV to T4+ T cells by a complex of the 110K viral protein and the T4 molecule. Science (80-) 1986;231:382–5.

Meås HZ, Haug M, Beckwith MS, Louet C, Ryan L, Hu Z, et al. Sensing of HIV-1 by TLR8 activates human T cells and reverses latency. Nat Commun 2020;11:1–16.

Miller MD, Farnet CM, Bushman FD. Human immunodeficiency virus type 1 preintegration complexes: studies of organization and composition. J Virol 1997;71:5382–90.

Mogensen TH, Melchjorsen J, Larsen CS, Paludan SR. Innate immune recognition and activation during HIV infection. Retrovirology 2010;7:1–19.

Monroe KM, Yang Z, Johnson JR, Geng X, Doitsh G, Krogan NJ, et al. IFI16 DNA Sensor Is Required for Death of Lymphoid CD4 T Cells Abortively Infected with HIV. Science (80-) 2014;343:428–32.

Montealegre S, van Endert PM. Endocytic Recycling of MHC Class I Molecules in Non-professional Antigen Presenting and Dendritic Cells. Front Immunol 2019;9.

Morou A, Brunet-Ratnasingham E, Dubé M, Charlebois R, Mercier E, Darko

S, et al. Altered differentiation is central to HIV-specific CD4+ T cell dysfunction in progressive disease. Nat Immunol 2019;20:1059–70.

Motwani M, Pesiridis S, Fitzgerald KA. DNA sensing by the cGAS–STING pathway in health and disease. Nat Rev Genet 2019;20:657–74.

Mullen AC. Role of T-bet in Commitment of TH1 Cells Before IL-12-Dependent Selection. Science (80-) 2001;292:1907–10.

Muzio M, Bosisio D, Polentarutti N, D'amico G, Stoppacciaro A, Mancinelli R, et al. Differential Expression and Regulation of Toll-Like Receptors (TLR) in Human Leukocytes: Selective Expression of TLR3 in Dendritic Cells. J Immunol 2000;164:5998–6004.

Nabel G, Baltimore D. An inducible transcription factor activates expression of human immunodeficiency virus in T cells. Nature 1987;326:711–3.

Nagai K, Wong AH, Li S, Tam WN, Cuddihy AR, Sonenberg N, et al. Induction of CD4 expression and human immunodeficiency virus type 1 replication by mutants of the interferon-inducible protein kinase PKR. J Virol 1997;71:1718–25.

Nakayama EE, Shioda T. TRIM5α and Species Tropism of HIV/SIV. Front Microbiol 2012;3.

Naseri Z, Kazemi Oskuee R, Jaafari MR, Forouzandeh M. Exosome-mediated delivery of functionally active miRNA-142-3p inhibitor reduces tumorigenicity of breast cancer in vitro and in vivo. Int J Nanomedicine 2018;Volume 13:7727–47.

Nasr N, Alshehri AA, Wright TK, Shahid M, Heiner BM, Harman AN, et al. Mechanism of Interferon-Stimulated Gene Induction in HIV-1-Infected Macrophages. J Virol 2017;91:1–19.

NCT03493698. A Fixed-Sequence, Drug-Drug Interaction Study Between Multiple Oral Doses of Inarigivir Soproxil and a Single Oral Dose of Midazolam in Healthy Subjects. ClinicalTrials.gov [Internet]. Bethesda (MD): National Library of Medicine (US). n.d.

NCT04059198. Evaluating the Safety and Efficacy of Inarigivir in Non-cirrhotic Treatment Naive Subjects Infected With Hepatitis B Virus. ClinicalTrials.gov [Internet]. Bethesda (MD): National Library of Medicine (US). n.d.

Ndung'u T, McCune JM, Deeks SG. Why and where an HIV cure is needed and how it might be achieved. Nature 2019;576:397–405.

Neil SJD, Sandrin V, Sundquist WI, Bieniasz PD. An Interferon-α-Induced Tethering Mechanism Inhibits HIV-1 and Ebola Virus Particle Release but Is Counteracted by the HIV-1 Vpu Protein. Cell Host Microbe 2007;2:193–203.

Nguyen N V, Tran JT, Sanchez DJ. HIV blocks Type I IFN signaling through disruption of STAT1 phosphorylation. Innate Immun 2018;24:490–500.

Niu B, Zhou F, Su Y, Wang L, Xu Y, Yi Z, et al. Different Expression Characteristics of LAG3 and PD-1 in Sepsis and Their Synergistic Effect on T Cell Exhaustion: A New Strategy for Immune Checkpoint Blockade. Front Immunol 2019;10.

Nolte-'t Hoen ENM, Buschow SI, Anderton SM, Stoorvogel W, Wauben MHM. Activated T cells recruit exosomes secreted by dendritic cells via LFA-1. Blood 2009;113:1977–81.

Novis CL, Archin NM, Buzon MJ, Verdin E, Round JL, Lichterfeld M, et al. Reactivation of latent HIV-1 in central memory CD4+ T cells through TLR-1/2 stimulation. Retrovirology 2013;10:119.

O'Brien TR, Thomas DL, Jackson SS, Prokunina-Olsson L, Donnelly RP, Hartmann R. Weak Induction of Interferon Expression by Severe Acute Respiratory Syndrome Coronavirus 2 Supports Clinical Trials of Interferon-λ to Treat Early Coronavirus Disease 2019. Clin Infect Dis 2020;71:1410–2.

Oda K, Matoba Y, Irie T, Kawabata R, Fukushi M, Sugiyama M, et al. Structural Basis of the Inhibition of STAT1 Activity by Sendai Virus C Protein. J Virol 2015;89:11487–99.

Okoye IS, Coomes SM, Pelly VS, Czieso S, Papayannopoulos V, Tolmachova T, et al. MicroRNA-Containing T-Regulatory-Cell-Derived Exosomes Suppress Pathogenic T Helper 1 Cells. Immunity 2014;41:89–103.

Ota T, Suzuki Y, Nishikawa T, Otsuki T, Sugiyama T, Irie R, et al. Complete sequencing and characterization of 21,243 full-length human cDNAs. Nat Genet 2004;36:40–5.

Palesch D, Bosinger SE, Mavigner M, Billingsley JM, Mattingly C, Carnathan DG, et al. Short-Term Pegylated Interferon α2a Treatment Does Not Significantly Reduce the Viral Reservoir of Simian Immunodeficiency Virus-Infected, Antiretroviral Therapy-Treated Rhesus Macaques. J Virol 2018;92.

Palmer CS, Palchaudhuri R, Albargy H, Abdel-Mohsen M, Crowe SM. Exploiting immune cell metabolic machinery for functional HIV cure and the prevention of inflammaging. F1000Research 2018;7:125.

Palmer S, Maldarelli F, Wiegand A, Bernstein B, Hanna GJ, Brun SC, et al. Low-level viremia persists for at least 7 years in patients on suppressive antiretroviral therapy. Proc Natl Acad Sci 2008;105:3879–84.

Pan X, Baldauf H-M, Keppler OT, Fackler OT. Restrictions to HIV-1 replication in resting CD4+ T lymphocytes. Cell Res 2013;23:876–85.

Pannus P, Rutsaert S, De Wit S, Allard SD, Vanham G, Cole B, et al. Rapid viral rebound after analytical treatment interruption in patients with very small HIV reservoir and minimal on-going viral transcription. J Int AIDS Soc 2020;23.

Papon L, Oteiza A, Imaizumi T, Kato H, Brocchi E, Lawson TG, et al. The viral RNA recognition sensor RIG-I is degraded during encephalomyocarditis virus (EMCV) infection. Virology 2009;393:311–8.

Parada CA, Roeder RG. Enhanced processivity of RNA polymerase II triggered by Tat-induced phosphorylation of its carboxy-terminal domain. Nature 1996;384:375–8.

Park J, Morrow CD. Overexpression of the gag-pol precursor from human immunodeficiency virus type 1 proviral genomes results in efficient proteolytic processing in the absence of virion production. J Virol 1991;65:5111–7.

Pasquereau S, Kumar A, Abbas W, Herbein G. Counteracting Akt Activation by HIV Protease Inhibitors in Monocytes/Macrophages. Viruses 2018;10:190.

Patsoukis N, Bardhan K, Chatterjee P, Sari D, Liu B, Bell LN, et al. PD-1 alters T-cell metabolic reprogramming by inhibiting glycolysis and promoting lipolysis and fatty acid oxidation. Nat Commun 2015;6:6692.

Pearce EL, Poffenberger MC, Chang C-H, Jones RG. Fueling Immunity: Insights into Metabolism and Lymphocyte Function. Science (80-) 2013;342:1242454–1242454.

Pennock ND, White JT, Cross EW, Cheney EE, Tamburini BA, Kedl RM. T cell responses: naïve to memory and everything in between. Adv Physiol Educ 2013;37:273–83.

Perelson AS, Neumann AU, Markowitz M, Leonard JM, Ho DD. HIV-1

Dynamics in Vivo: Virion Clearance Rate, Infected Cell Life-Span, and Viral Generation Time. Science (80-) 1996;271:1582–6.

Perkins ND, Edwards NL, Duckett CS, Agranoff AB, Schmid RM, Nabel GJ. A cooperative interaction between NF-kappa B and Sp1 is required for HIV-1 enhancer activation. EMBO J 1993;12:3551–8.

Pernas M, Tarancón-Diez L, Rodríguez-Gallego E, Gómez J, Prado JG, Casado C, et al. Factors Leading to the Loss of Natural Elite Control of HIV-1 Infection. J Virol 2017;92.

Peterlin BM, Trono D. Hide, shield and strike back: How HIV-infected cells avoid immune eradication. Nat Rev Immunol 2003;3:97–107.

Pettit SC, Gulnik S, Everitt L, Kaplan AH. The Dimer Interfaces of Protease and Extra-Protease Domains Influence the Activation of Protease and the Specificity of GagPol Cleavage. J Virol 2003;77:366–74.

Phanuphak N, Gulick RM. HIV treatment and prevention 2019. Curr Opin HIV AIDS 2020;15:4–12.

Pion M, Granelli-Piperno A, Mangeat B, Stalder R, Correa R, Steinman RM, et al. APOBEC3G/3F mediates intrinsic resistance of monocyte-derived dendritic cells to HIV-1 infection. J Exp Med 2006;203:2887–93.

Pitman MC, Lau JSY, McMahon JH, Lewin SR. Barriers and strategies to achieve a cure for HIV. Lancet HIV 2018;5:e317–28.

Podkalicka J, Bassereau P. How membrane physics rules the HIV envelope. Nat Cell Biol 2019;21:413–5.

Popov S. Viral protein R regulates nuclear import of the HIV-1 pre-integration complex. EMBO J 1998;17:909–17.

Price DA, Goulder PJR, Klenerman P, Sewell AK, Easterbrook PJ, Troop M, et al. Positive selection of HIV-1 cytotoxic T lymphocyte escape variants during primary infection. Proc Natl Acad Sci 1997;94:1890–5.

Proteinatlas. The Human Protein Atlas 2020.

Qi N, Shi Y, Zhang R, Zhu W, Yuan B, Li X, et al. Multiple truncated isoforms of MAVS prevent its spontaneous aggregation in antiviral innate immune signalling. Nat Commun 2017;8:1–16.

Qi Q, Liu Y, Cheng Y, Glanville J, Zhang D, Lee J-Y, et al. Diversity and clonal

selection in the human T-cell repertoire. Proc Natl Acad Sci 2014;111:13139–44.

Rahimi H, Rezaee SA, Valizade N, Vakili R, Rafatpanah H. Assessment of HTLV-I proviral load, HIV viral load and CD4 T cell count in infected subjects; with an emphasis on viral replication in co-infection. Iran J Basic Med Sci 2014;17:49–54.

Raja A, Venturi M, Kwong P, Sodroski J. CD4 Binding Site Antibodies Inhibit Human Immunodeficiency Virus gp120 Envelope Glycoprotein Interaction with CCR5. J Virol 2003;77:713–8.

Raphael I, Joern RR, Forsthuber TG. Memory CD4+ T Cells in Immunity and Autoimmune Diseases. Cells 2020;9:531.

Rasmussen TA, Tolstrup M, Brinkmann CR, Olesen R, Erikstrup C, Solomon A, et al. Panobinostat, a histone deacetylase inhibitor, for latent-virus reactivation in HIV-infected patients on suppressive antiretroviral therapy: a phase 1/2, single group, clinical trial. Lancet HIV 2014;1:e13–21.

Raudvere U, Kolberg L, Kuzmin I, Arak T, Adler P, Peterson H, et al. g:Profiler: a web server for functional enrichment analysis and conversions of gene lists (2019 update). Nucleic Acids Res 2019;47:W191–8.

Rausell A, Muñoz M, Martinez R, Roger T, Telenti A, Ciuffi A. Innate immune defects in HIV permissive cell lines. Retrovirology 2016;13:43.

Rawling DC, Pyle AM. Parts, assembly and operation of the RIG-I family of motors. Curr Opin Struct Biol 2014;25:25–33.

Reed LJ, Muench H. A Simple Method of Estimating Fifty Percent Endpoints. Am J Epidemiol 1938;27:493–7.

Reynolds JM, Pappu BP, Peng J, Martinez GJ, Zhang Y, Chung Y, et al. Toll-like Receptor 2 Signaling in CD4+ T Lymphocytes Promotes T Helper 17 Responses and Regulates the Pathogenesis of Autoimmune Disease. Immunity 2010;32:692–702.

Rezaei SD. The Pathway To Establishing HIV Latency Is Critical to How Latency Is Maintained and Reversed 2018;92:1–20.

Ricciardi S, Manfrini N, Alfieri R, Calamita P, Crosti MC, Gallo S, et al. The Translational Machinery of Human CD4+ T Cells Is Poised for Activation and Controls the Switch from Quiescence to Metabolic Remodeling (Cell Metabolism

(2018) 28(6) (895–906.e5), (S1550413118305102), (10.1016/j.cmet.2018.08.009)). Cell Metab 2018;28:961.

Riddell J, Amico KR, Mayer KH. HIV Preexposure Prophylaxis. JAMA 2018;319:1261.

Ringeard M, Marchand V, Decroly E, Motorin Y, Bennasser Y. FTSJ3 is an RNA 2′-O-methyltransferase recruited by HIV to avoid innate immune sensing. Nature 2019;565:500–4. http://dx.doi.org/10.1038/s41586-018-0841-4.

Rivero J, Fraga M, Cancio I, Cuervo J, López-Saura P. Long-term treatment with recombinant interferon alpha-2b prolongs survival of asymptomatic HIV-infected individuals. Biotherapy 1997;10:107–13.

Rivero J, Limonta M, Aguilera A, Fraga M, Saura PL. Use of recombinant interferon-α in Human Immunodeficiency Virus (HIV)-infected individuals. Biotherapy 1994;8:23–31.

Roberts J, Bebenek K, Kunkel T. The accuracy of reverse transcriptase from HIV-1. Science (80-) 1988;242:1171–3.

Roberts N, Martin J, Kinchington D, Broadhurst A, Craig J, Duncan I, et al. Rational design of peptide-based HIV proteinase inhibitors. Science (80-) 1990;248:358–61.

Rögnvaldsson T, You L, Garwicz D. State of the art prediction of HIV-1 protease cleavage sites. Bioinformatics 2015;31:1204–10.

Román E, Miller E, Harmsen A, Wiley J, von Andrian UH, Huston G, et al. CD4 Effector T Cell Subsets in the Response to Influenza. J Exp Med 2002;196:957–68.

Ruzicka M, Koenig LM, Formisano S, Boehmer DFR, Vick B, Heuer E-M, et al. RIG-I-based immunotherapy enhances survival in preclinical AML models and sensitizes AML cells to checkpoint blockade. Leukemia 2020;34:1017–26.

Sánchez-Aparicio MT, Feinman LJ, García-Sastre A, Shaw ML. Paramyxovirus V Proteins Interact with the RIG-I/TRIM25 Regulatory Complex and Inhibit RIG-I Signaling. J Virol 2018;92.

Sánchez-Aparicio MT, Garcin D, Rice CM, Kolakofsky D, García-Sastre A, Baum A. Loss of Sendai virus C protein leads to accumulation of RIG-I immunostimulatory defective interfering RNA. J Gen Virol 2017;98:1282–93.

Sanchez JL, Hunt PW, Reilly CS, Hatano H, Beilman GJ, Khoruts A, et al. Lymphoid Fibrosis Occurs in Long-Term Nonprogressors and Persists With Antiretroviral Therapy but May Be Reversible With Curative Interventions. J Infect Dis 2015;211:1068–75.

Sandler NG, Bosinger SE, Estes JD, Zhu RTR, Tharp GK, Boritz E, et al. Type I interferon responses in rhesus macaques prevent SIV infection and slow disease progression. Nature 2014;511:601–5.

Sawyer SL, Wu LI, Emerman M, Malik HS. Positive selection of primate TRIM5alpha identifies a critical species-specific retroviral restriction domain. Proc Natl Acad Sci U S A 2005;102:2832–7.

Scagnolari C, Trombetti S, Soldà A, Milella M, Gaeta GB, Angarano G, et al. Development and specificities of anti-interferon neutralizing antibodies in patients with chronic hepatitis C treated with pegylated interferon-α. Clin Microbiol Infect 2012;18:1033–9.

Schaefer MR, Wonderlich ER, Roeth JF, Leonard JA, Collins KL. HIV-1 Nef Targets MHC-I and CD4 for Degradation Via a Final Common β-COP–Dependent Pathway in T Cells. PLoS Pathog 2008;4:e1000131.

Schlee M, Hartmann G. Discriminating self from non-self in nucleic acid sensing. Nat Rev Immunol 2016;16:566–80.

Schlee M, Roth A, Hornung V, Hagmann CA, Wimmenauer V, Barchet W, et al. Recognition of 5′ Triphosphate by RIG-I Helicase Requires Short Blunt Double-Stranded RNA as Contained in Panhandle of Negative-Strand Virus. Immunity 2009;31:25–34.

Schmidt A, Schwerd T, Hamm W, Hellmuth JC, Cui S, Wenzel M, et al. 5'-triphosphate RNA requires base-paired structures to activate antiviral signaling via RIG-I. Proc Natl Acad Sci 2009;106:12067–72.

Seth RB, Sun L, Ea C-K, Chen ZJ. Identification and Characterization of MAVS, a Mitochondrial Antiviral Signaling Protein that Activates NF-κB and IRF3. Cell 2005;122:669–82.

Shah S, Alexaki A, Pirrone V, Dahiya S, Nonnemacher MR, Wigdahl B. Functional properties of the HIV-1 long terminal repeat containing single-nucleotide polymorphisms in Sp site III and CCAAT/enhancer binding protein site

I. Virol J 2014;11:92.

Shao W-H, Shu DH, Zhen Y, Hilliard B, Priest SO, Cesaroni M, et al. Prion-like Aggregation of Mitochondrial Antiviral Signaling Protein in Lupus Patients Is Associated With Increased Levels of Type I Interferon. Arthritis Rheumatol 2016;68:2697–707.

Sharp PM, Hahn BH. Origins of HIV and the AIDS Pandemic. Cold Spring Harb Perspect Med 2011;1:a006841–a006841.

Sheehy AM, Gaddis NC, Malim MH. The antiretroviral enzyme APOBEC3G is degraded by the proteasome in response to HIV-1 Vif. Nat Med 2003;9:1404–7.

Shehu-Xhilaga M, Crowe SM, Mak J. Maintenance of the Gag/Gag-Pol Ratio Is Important for Human Immunodeficiency Virus Type 1 RNA Dimerization and Viral Infectivity. J Virol 2001;75:1834–41.

Shi R-Z, Pan Y-Q, Xing L. RNA Helicase A Regulates the Replication of RNA Viruses. Viruses 2021;13:361.

Shrotri M, van Schalkwyk MCI, Post N, Eddy D, Huntley C, Leeman D, et al. T cell response to SARS-CoV-2 infection in humans: A systematic review. PLoS One 2021;16:e0245532.

Shyer JA, Flavell RA, Bailis W. Metabolic signaling in T cells. Cell Res 2020;30:649–59.

Silicano R. What do we need to do to cure HIV infection? TOP HIV Med 2010;18(3):104–8.

Siliciano RF, Greene WC. HIV latency. Cold Spring Harb Perspect Med 2011;1:a007096.

van der Sluis RM, Zerbato JM, Rhodes JW, Pascoe RD, Solomon A, Kumar NA, et al. Diverse effects of interferon alpha on the establishment and reversal of HIV latency. PLoS Pathog 2020;16:1–27.

Sobhian B, Laguette N, Yatim A, Nakamura M, Levy Y, Kiernan R, et al. HIV-1 Tat assembles a multifunctional transcription elongation complex and stably associates with the 7SK snRNP. Mol Cell 2010;38:439–51.

Sofi MS, Hamid A, Bhat SU. SARS-CoV-2: A critical review of its history, pathogenesis, transmission, diagnosis and treatment. Biosaf Heal 2020;2:217–25.

Solis M, Nakhaei P, Jalalirad M, Lacoste J, Douville R, Arguello M, et al. RIG-I-mediated antiviral signaling is inhibited in HIV-1 infection by a protease-mediated sequestration of RIG-I. J Virol 2011;85:1224–36.

Sork H, Corso G, Krjutskov K, Johansson HJ, Nordin JZ, Wiklander OPB, et al. Heterogeneity and interplay of the extracellular vesicle small RNA transcriptome and proteome. Sci Rep 2018;8:10813.

Sousa IG, Simi KCR, do Almo MM, Bezerra MAG, Doose G, Raiol T, et al. Gene expression profile of human T cells following a single stimulation of peripheral blood mononuclear cells with anti-CD3 antibodies. BMC Genomics 2019;20:593.

Spina CA, Anderson J, Archin NM, Bosque A, Chan J, Famiglietti M, et al. An In-Depth Comparison of Latent HIV-1 Reactivation in Multiple Cell Model Systems and Resting CD4+ T Cells from Aviremic Patients. PLoS Pathog 2013;9:e1003834.

Steckbeck JD, Kuhlmann A-S, Montelaro RC. C-terminal tail of human immunodeficiency virus gp41: functionally rich and structurally enigmatic. J Gen Virol 2013;94:1–19.

Stein BS, Engleman EG. Intracellular processing of the gp160 HIV-1 envelope precursor. Endoproteolytic cleavage occurs in a cis or medial compartment of the Golgi complex. J Biol Chem 1990;265:2640–9.

Stevenson M, Stanwick TL, Dempsey MP, Lamonica CA. HIV-1 replication is controlled at the level of T cell activation and proviral integration. EMBO J 1990;9:1551–60.

Stögerer T, Stäger S. Innate Immune Sensing by Cells of the Adaptive Immune System. Front Immunol 2020;11.

Stoltzfus MC. Chapter 1 Regulation of HIV-1 Alternative RNA Splicing and Its Role in Virus Replication. vol. 74. 1st ed. Elsevier Inc.; 2009.

Strähle L, Marq J-B, Brini A, Hausmann S, Kolakofsky D, Garcin D. Activation of the Beta Interferon Promoter by Unnatural Sendai Virus Infection Requires RIG-I and Is Inhibited by Viral C Proteins. J Virol 2007;81:12227–37.

Sundquist WI, Krausslich H-G. HIV-1 Assembly, Budding, and Maturation. Cold Spring Harb Perspect Med 2012;2:a006924–a006924.

Synairgen Research. Trial of Inhaled Anti-viral (SNG001) for SARS-CoV-2 (COVID-19) Infection. ClinicalTrials.gov [Internet]. Bethesda (MD): National Library of Medicine (US) Identifier: NCT04385095 2020.

Takeuchi A, Saito T. CD4 CTL, a Cytotoxic Subset of CD4+ T Cells, Their Differentiation and Function. Front Immunol 2017;8.

Takeuchi K, Komatsu T, Kitagawa Y, Sada K, Gotoh B. Sendai Virus C Protein Plays a Role in Restricting PKR Activation by Limiting the Generation of Intracellular Double-Stranded RNA. J Virol 2008;82:10102–10.

Tanabe Y, Nishibori T, Su L, Arduini RM, Baker DP, David M. Cutting Edge: Role of STAT1, STAT3, and STAT5 in IFN-αβ Responses in T Lymphocytes. J Immunol 2005;174:609–13.

Tazi J, Bakkour N, Marchand V, Ayadi L, Aboufirassi A, Branlant C. Alternative splicing: regulation of HIV-1 multiplication as a target for therapeutic action. FEBS J 2010;277:867–76.

Telwatte S, Morón-López S, Aran D, Kim P, Hsieh C, Joshi S, et al. Heterogeneity in HIV and cellular transcription profiles in cell line models of latent and productive infection: implications for HIV latency. Retrovirology 2019;16:32.

Thomas JA, Gorelick RJ. Nucleocapsid protein function in early infection processes. Virus Res 2008;134:39–63.

Tong-Starksen SE, Luciw PA, Peterlin BM. Human immunodeficiency virus long terminal repeat responds to T-cell activation signals. Proc Natl Acad Sci 1987;84:6845–9.

Tong D, Zhang L, Ning F, Xu Y, Hu X, Shi Y. Contact-dependent delivery of IL-2 by dendritic cells to CD4 T cells in the contraction phase promotes their long-term survival. Protein Cell 2020;11:108–23.

Torrecilla E, Llácer Delicado T, Holguín Á. New Findings in Cleavage Sites Variability across Groups, Subtypes and Recombinants of Human Immunodeficiency Virus Type 1. PLoS One 2014;9:e88099.

Tóth G, Borics A. Flap opening mechanism of HIV-1 protease. J Mol Graph Model 2006;24:465–74.

Tran BX, Phan HT, Latkin CA, Nguyen HLT, Hoang CL, Ho CSH, et al. Understanding Global HIV Stigma and Discrimination: Are Contextual Factors

Sufficiently Studied? (GAPRESEARCH). Int J Environ Res Public Health 2019;16:1899.

Tsai A, Irrinki A, Kaur J, Cihlar T, Kukolj G, Sloan DD, et al. Toll-Like Receptor 7 Agonist GS-9620 Induces HIV Expression and HIV-Specific Immunity in Cells from HIV-Infected Individuals on Suppressive Antiretroviral Therapy. J Virol 2017;91:e02166-16.

Tsai M-H, Pai L-M, Lee C-K. Fine-Tuning of Type I Interferon Response by STAT3. Front Immunol 2019;10.

Uchikawa E, Lethier M, Malet H, Brunel J, Gerlier D, Cusack S. Structural Analysis of dsRNA Binding to Anti-viral Pattern Recognition Receptors LGP2 and MDA5. Mol Cell 2016;62:586–602.

Uhlen M, Zhang C, Lee S, Sjöstedt E, Fagerberg L, Bidkhori G, et al. A pathology atlas of the human cancer transcriptome. Science (80-) 2017;357:eaan2507.

UNAIDS. UNAIDS 2019 Fact Sheet. vol. 1. 2019.

Vabret N, Najburg V, Solovyov A, Šulc P, Balan S, Beauclair G, et al. Y-RNAs Lead an Endogenous Program of RIG-I Agonism Mobilized upon RNA Virus Infection and Targeted by HIV 2019.

Valle-Casuso JC, Angin M, Volant S, Passaes C, Monceaux V, Mikhailova A, et al. Cellular Metabolism Is a Major Determinant of HIV-1 Reservoir Seeding in CD4+ T Cells and Offers an Opportunity to Tackle Infection. Cell Metab 2019;29:611-626.e5.

Vanderheiden A, Ralfs P, Chirkova T, Upadhyay AA, Zimmerman MG, Bedoya S, et al. Type I and Type III Interferons Restrict SARS-CoV-2 Infection of Human Airway Epithelial Cultures. J Virol 2020;94.

Venkatesh S, Bieniasz PD. Mechanism of HIV-1 Virion Entrapment by Tetherin. PLoS Pathog 2013;9:e1003483.

Venter WDF, Moorhouse M, Sokhela S, Fairlie L, Mashabane N, Masenya M, et al. Dolutegravir plus Two Different Prodrugs of Tenofovir to Treat HIV. N Engl J Med 2019;381:803–15.

Vermeire J, Roesch F, Sauter D, Rua R, Hotter D, Van Nuffel A, et al. HIV Triggers a cGAS-Dependent, Vpu- and Vpr-Regulated Type I Interferon

Response in CD4 + T Cells. Cell Rep 2016;17:413–24.

Verstak B, Arnot CJ, Gay NJ. An Alanine-to-Proline Mutation in the BB-Loop of TLR3 Toll/IL-1R Domain Switches Signalling Adaptor Specificity from TRIF to MyD88. J Immunol 2013;191:6101–9.

Vibholm L, Schleimann MH, Højen JF, Benfield T, Offersen R, Rasmussen K, et al. Short-Course Toll-Like Receptor 9 Agonist Treatment Impacts Innate Immunity and Plasma Viremia in Individuals With Human Immunodeficiency Virus Infection. Clin Infect Dis 2017;64:1686–95.

Wang B, Norbury CC, Greenwood R, Bennink JR, Yewdell JW, Frelinger JA. Multiple Paths for Activation of Naive CD8 + T Cells: CD4-Independent Help. J Immunol 2001;167:1283–9.

Wang J, Smerdon SJ, Jager J, Kohlstaedt LA, Rice PA, Friedman JM, et al. Structural basis of asymmetry in the human immunodeficiency virus type 1 reverse transcriptase heterodimer. Proc Natl Acad Sci 1994;91:7242–6.

Wang MQ, Huang YL, Huang J, Zheng JL, Qian GX. RIG-I detects HIV-1 infection and mediates type i interferon response in human macrophages from patients with HIV-1-associated neurocognitive disorders. Genet Mol Res 2015;14:13799–811.

Wang N, Zhan Y, Zhu L, Hou Z, Liu F, Song P, et al. Retrospective Multicenter Cohort Study Shows Early Interferon Therapy Is Associated with Favorable Clinical Responses in COVID-19 Patients. Cell Host Microbe 2020;28:455-464.e2.

Wang Q, Gao H, Clark KM, Mugisha CS, Davis K, Tang JP, et al. CARD8 is an inflammasome sensor for HIV-1 protease activity. Science (80-) 2021;1707:eabe1707.

Wang T, Green LA, Gupta SK, Amet T, Byrd DJ, Yu Q, et al. Intracellular Nef Detected in Peripheral Blood Mononuclear Cells from HIV Patients. AIDS Res Hum Retroviruses 2015;31:217–20.

Wang Y, Lv Z, Chu Y. HIV protease inhibitors: a review of molecular selectivity and toxicity. HIV/AIDS - Res Palliat Care 2015;7:95.

Wang Y, Zhang H-X, Sun Y-P, Liu Z-X, Liu X-S, Wang L, et al. Rig-I−/− mice develop colitis associated with downregulation of Gαi2. Cell Res 2007;17:858–

68.

Wei X, Ghosh SK, Taylor ME, Johnson VA, Emini EA, Deutsch P, et al. Viral dynamics in human immunodeficiency virus type 1 infection. Nature 1995;373:117–22.

WHO. WHO Health Emergency Dashboard. Covid19.who.int [Internet]. 2021.

Wiegers K, Rutter G, Kottler H, Tessmer U, Hohenberg H, Kräusslich H-G. Sequential Steps in Human Immunodeficiency Virus Particle Maturation Revealed by Alterations of Individual Gag Polyprotein Cleavage Sites. J Virol 1998;72:2846 LP – 2854.

Wilen CB, Tilton JC, Doms RW. HIV: Cell Binding and Entry. Cold Spring Harb Perspect Med 2012;2:a006866–a006866.

Willey RL, Bonifacino JS, Potts BJ, Martin MA, Klausner RD. Biosynthesis, cleavage, and degradation of the human immunodeficiency virus 1 envelope glycoprotein gp160. Proc Natl Acad Sci 1988;85:9580–4.

Williams T, Ngo LH, Wickramasinghe VO. Nuclear export of RNA: Different sizes, shapes and functions. Semin Cell Dev Biol 2018;75:70–7.

Wilson W, Braddock M, Adams SE, Rathjen PD, Kingsman SM, Kingsman AJ. HIV expression strategies: Ribosomal frameshifting is directed by a short sequence in both mammalian and yeast systems. Cell 1988;55:1159–69.

Woolhouse MEJ, Brierley L. Epidemiological characteristics of human-infective RNA viruses. Sci Data 2018;5:1–6.

Wu B, Peisley A, Richards C, Yao H, Zeng X, Lin C, et al. Structural Basis for dsRNA Recognition, Filament Formation, and Antiviral Signal Activation by MDA5. Cell 2013;152:276–89.

Xiao Q, Guo D, Chen S. Application of CRISPR/Cas9-Based Gene Editing in HIV-1/AIDS Therapy. Front Cell Infect Microbiol 2019;9.

Xu L, Wang J, Liu Y, Xie L, Su B, Mou D, et al. CRISPR-Edited Stem Cells in a Patient with HIV and Acute Lymphocytic Leukemia. N Engl J Med 2019;381:1240–7.

Xu L, Wang W, Li Y, Zhou X, Yin Y, Wang Y, et al. RIG-I is a key antiviral interferon-stimulated gene against hepatitis E virus regardless of interferon production. Hepatology 2017;65:1823–39.

Xu W, Li H, Wang Q, Hua C, Zhang H, Li W, et al. Advancements in Developing Strategies for Sterilizing and Functional HIV Cures. Biomed Res Int 2017;2017:1–12.

Yamamoto T, Tsunetsugu-Yokota Y, Mitsuki Y, Mizukoshi F, Tsuchiya T, Terahara K, et al. Selective Transmission of R5 HIV-1 over X4 HIV-1 at the Dendritic Cell–T Cell Infectious Synapse Is Determined by the T Cell Activation State. PLoS Pathog 2009;5:e1000279.

Yang H, Guo H-Z, Li X-Y, Lin J, Zhang W, Zhao J-M, et al. Viral RNA–Unprimed Rig-I Restrains Stat3 Activation in the Modulation of Regulatory T Cell/Th17 Cell Balance. J Immunol 2017;199:119–28.

Yoh SM, Schneider M, Seifried J, Soonthornvacharin S, Akleh RE, Olivieri KC, et al. PQBP1 Is a Proximal Sensor of the cGAS-Dependent Innate Response to HIV-1. Cell 2015;161:1293–305.

Yoneyama M, Kikuchi M, Natsukawa T, Shinobu N, Imaizumi T, Miyagishi M, et al. The RNA helicase RIG-I has an essential function in double-stranded RNA-induced innate antiviral responses. Nat Immunol 2004;5:730–7.

Yong HY, Luo D. RIG-I-Like Receptors as Novel Targets for Pan-Antivirals and Vaccine Adjuvants Against Emerging and Re-Emerging Viral Infections. Front Immunol 2018;9.

Yu HJ, Reuter MA, McDonald D. HIV Traffics through a Specialized, Surface-Accessible Intracellular Compartment during trans-Infection of T Cells by Mature Dendritic Cells. PLoS Pathog 2008;4:e1000134.

Yu Y, Wang J, Chen Z, Wang G, Shao Q, Shi J, et al. Structural insights into HIV-1 protease flap opening processes and key intermediates. RSC Adv 2017;7:45121–8.

Yukl SA, Boritz E, Busch M, Bentsen C, Chun T-W, Douek D, et al. Challenges in Detecting HIV Persistence during Potentially Curative Interventions: A Study of the Berlin Patient. PLoS Pathog 2013;9:e1003347.

Yukl SA, Kaiser P, Kim P, Telwatte S, Joshi SK, Vu M, et al. HIV latency in isolated patient CD4 + T cells may be due to blocks in HIV transcriptional elongation, completion, and splicing. Sci Transl Med 2018;10:eaap9927.

Zerbato JM, Purves H V, Lewin SR, Rasmussen TA. Between a shock and a

hard place: challenges and developments in HIV latency reversal. Curr Opin Virol 2019;38:1–9.

Zhan Y, Carrington EM, Zhang Y, Heinzel S, Lew AM. Life and Death of Activated T Cells: How Are They Different from Naïve T Cells? Front Immunol 2017;8.

Zhang G, Luk BT, Wei X, Campbell GR, Fang RH, Zhang L, et al. Selective cell death of latently HIV-infected CD4+ T cells mediated by autosis inducing nanopeptides. Cell Death Dis 2019;10:419.

Zhang L, Xia Q, Li W, Peng Q, Yang H, Lu X, et al. The RIG-I pathway is involved in peripheral T cell lymphopenia in patients with dermatomyositis. Arthritis Res Ther 2019;21:1–12.

Zhang N-N, Shen S-H, Jiang L-J, Zhang W, Zhang H-X, Sun Y-P, et al. RIG-I plays a critical role in negatively regulating granulocytic proliferation. Proc Natl Acad Sci 2008;105:10553–8.

Zhang Y, Barklis E. Nucleocapsid protein effects on the specificity of retrovirus RNA encapsidation. J Virol 1995;69:5716–22.

Zhao Y, Zheng Z, Cohen CJ, Gattinoni L, Palmer DC, Restifo NP, et al. High-Efficiency Transfection of Primary Human and Mouse T Lymphocytes Using RNA Electroporation. Mol Ther 2006;13:151–9.

Zheng J, Yong HY, Panutdaporn N, Liu C, Tang K, Luo D. High-resolution HDX-MS reveals distinct mechanisms of RNA recognition and activation by RIG-I and MDA5. Nucleic Acids Res 2015;43:1216–30.

Zheng Y-H, Irwin D, Kurosu T, Tokunaga K, Sata T, Peterlin BM. Human APOBEC3F Is Another Host Factor That Blocks Human Immunodeficiency Virus Type 1 Replication. J Virol 2004;78:6073–6.

Zheng Y, Zhuang M-WW, Han L, Zhang J, Nan M-LL, Zhan P, et al. Severe acute respiratory syndrome coronavirus 2 (SARS-CoV-2) membrane (M) protein inhibits type I and III interferon production by targeting RIG-I/MDA-5 signaling. Signal Transduct Target Ther 2020;5:299.

Zhu X, Zhu J. CD4 T Helper Cell Subsets and Related Human Immunological Disorders. Int J Mol Sci 2020;21:8011.

Zhu Y, Pe'ery T, Peng J, Ramanathan Y, Marshall N, Marshall T, et al.

Transcription elongation factor P-TEFb is required for HIV-1 tat transactivation in vitro. Genes Dev 1997;11:2622–32.

Zicari S, Sessa L, Cotugno N, Ruggiero A, Morrocchi E, Concato C, et al. Immune Activation, Inflammation, and Non-AIDS Co-Morbidities in HIV-Infected Patients under Long-Term ART. Viruses 2019;11:200.

Zinkernagel RM, Doherty PC. Restriction of in vitro T cell-mediated cytotoxicity in lymphocytic choriomeningitis within a syngeneic or semiallogeneic system. Nature 1974;248:701–2.

Zou S, Glynn S, Kuritzkes D, Shah M, Cook N, Berliner N. Hematopoietic cell transplantation and HIV cure: where we are and what next? Blood 2013;122:3111–5.

8. Appendix

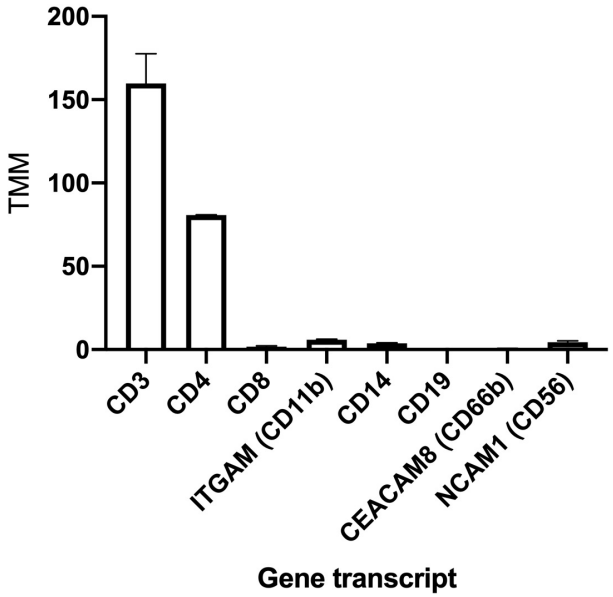

Figure 8.1: Gene expression profile of enriched, primary CD4 T cells. CD4 T cells were enriched from PBMCs and analysed using RNA deep sequencing. The representative data (1 Donor, naïve CD4 T cells) shows an enrichment of T cell specific markers (CD3, CD4), while transcripts for markers indicative for other cell types were less abundant: CD8 T cells (CD8), monocytes (CD11b, CD14), macrophages (CD14), granulocytes (CD66b), NK cells (CD56), B cells (CD19). N = 3, mean + SD.

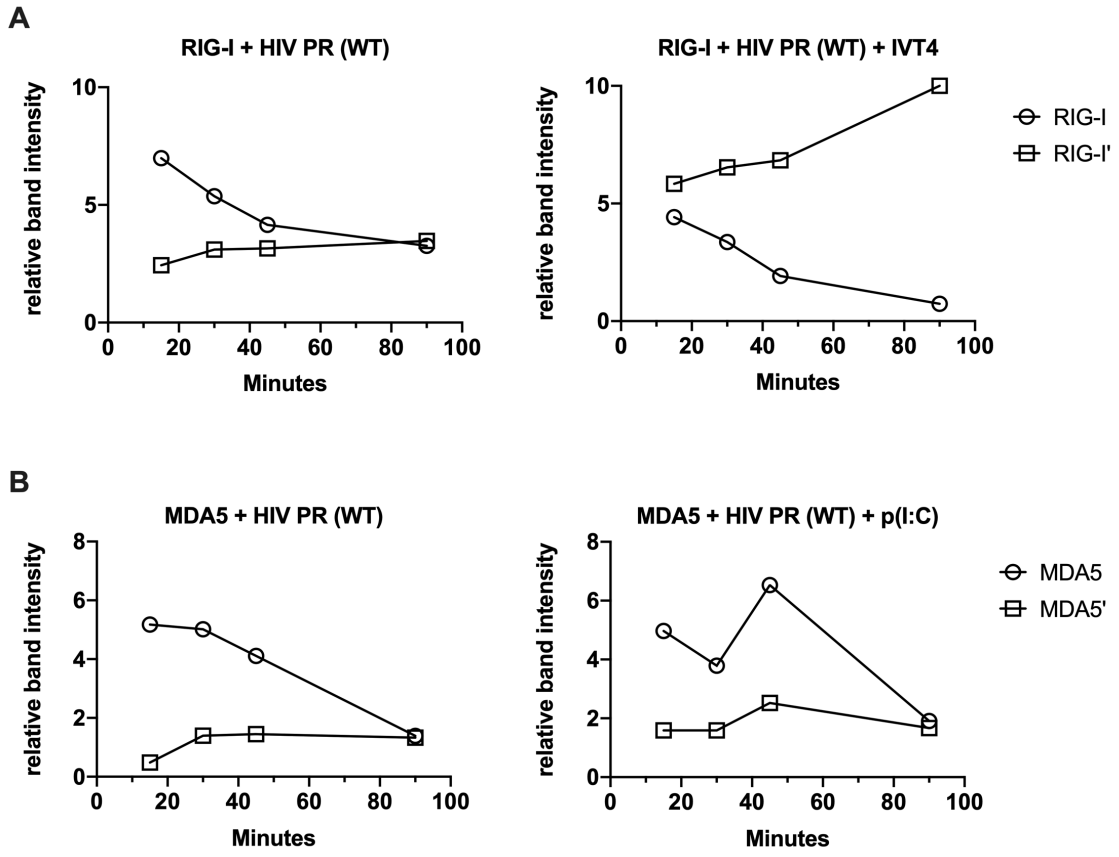

Figure 8.2: Quantification of RIG-I and MDA5 band intensities in the HIV protease degradation assay. Band intensities of full-length proteins (RIG or MDA5) and degradation products (RIG-I' and MDA5') shown in western blots detected with anti-RIG-I and anti-MDA5 antibodies (Figure 4.10) were quantified using ImageStudioLite software. Intensities are shown in relative units. RIG-I (retinoic-inducible gene 1), MDA5 (melanoma differentiation-associated protein 5), HIV PR (Human Immunodeficiency virus protease), WT (wildtype), IVT4 (in vitro transcript 4), p(I:C) (polyinosinic-polycytidylic acid).

Table 8.1: Top 50 differentially-regulated genes in Sendai virus infected resting CD4 T cells. Transcriptomic changes in resting CD4 T cells following Sendai virus infection. The top 50 up- and down-regulated genes are listed from a total of approx. 2000 differentially expressed genes in this data set. Samples and data were processed as described in 2.2.2.9. Pooled data from two different donors, n = 6 (3 samples per donor).

Gene Symbol (Up-regulated)	**Fold change (infected vs. control)**	**Gene Symbol (Down-regulated)**	**Fold change (infected vs. control)**
SLC28A3	1424.3	LOC100507564	-26.5
IFNB1	170.4	GNB3	-12.3
SOBP	102.4	PHKG1	-12.0
IFIT1	74.8	CAPN12	-10.6
LINC01671	71.5	VSIG1	-9.9
IFIT2	55.9	KISS1R	-8.6
B3GNT9	41.2	MSX2P1	-8.5
RSAD2	40.9	NOG	-8.3
CXCL10	38.4	LOC100129148	-8.0
SPAG6	35.5	PTCH1	-6.5
AMOTL2	34.1	HPCAL4	-6.3
ANKRD37	33.3	PLLP	-6.1
USP18	31.6	CROCCP3	-6.0
PPM1K-DT	30.2	IL23A	-6.0
CMPK2	29.9	FBXL16	-5.8
MX1	28.2	THRA	-5.6
HERC5	24.9	WNT10A	-5.6
CH25H	24.6	EEPD1	-5.6
IFIT3	24.6	LINC00092	-5.5
IFI6	23.6	PDGFB	-5.1
LAMP3	23.3	PALD1	-5.0
NEXN	23.2	SMIM10L2A	-4.8
OAS1	21.6	PI16	-4.7

Gene Symbol (Up-regulated)	Fold change (infected vs. control)	Gene Symbol (Down-regulated)	Fold change (infected vs. control)
CHRNA6	21.1	PCF11-AS1	-4.7
OASL	21.1	ASDURF	-4.6
CXCL11	19.6	RIMBP3	-4.6
LOC102723534	19.6	GTF2IRD1P1	-4.6
OAS3	18.7	TSPAN18	-4.3
MX2	17.8	RAB4B-EGLN2	-4.3
CYP2J2	17.7	ANKRD44-AS1	-4.3
ISG15	17.4	EPHA4	-4.3
IFI44L	17.0	SULT1B1	-4.2
LGALS17A	16.0	PLD6	-4.2
HELZ2	16.0	SEMA4C	-4.2
BCL2L14	15.7	VSIR	-4.2
IFI44	15.6	PITPNM2	-4.1
LGALS9C	15.5	GRASP	-4.1
TTC21A	15.4	SNAI3	-4.1
PLSCR1	14.6	LOC100134868	-4.0
CSAG3	14.4	MIR4697HG	-4.0
ZBP1	13.5	MAP1A	-4.0
PRR5	12.8	HKDC1	-4.0
DDX58	12.2	GALNT18	-4.0
NT5C3A	12.2	CP	-3.9
DDX60L	11.9	LZTS1	-3.9
RNF152	11.7	CCDC74A	-3.9
HERC6	11.4	VPS9D1-AS1	-3.9
IRF7	11.4	CD27	-3.8
LRRC3	11.2	CAMKK1	-3.8
FRMD3	10.9	PEG13	-3.8